

Title of thesis

**Spatio-Temporal processing for Optimum Uplink-Downlink
WCDMA Systems**

I. AHMED MOHAMMED AHMED JAD ELRAB

Here by allow my thesis to be placed at the Information Resource Center (IRC) of Universiti Teknologi PETRONAS (UTP) with the following conditions:

1. The thesis becomes the property of UTP.
2. The IRC of UTP may make copies of the thesis for academic purposes only.
3. This thesis is classified as

☐

Confidential

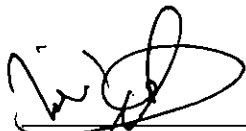
☒

Non-confidential

If this thesis is confidential, please state the reason:

The contents of the thesis will remain confidential for _____ years.

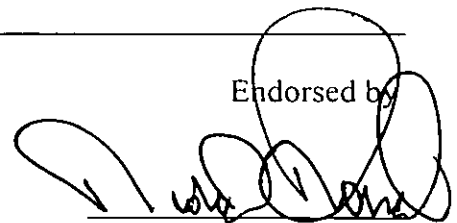
Remarks on disclosure:



Signature of Author

Permanent: *Faculty of Engineering and Architecture*
Address *Juba University*
Khartoum, Sudan

Date: 11/02/2008



Endorsed by

Signature of Supervisor

Name of Supervisor
Dr. Nidal S.Kamel

Date: 11/02/2008

UNIVERSITI TEKNOLOGI PETRONAS

Approval by Supervisor

The undersigned certify that they have read, and recommend to The Postgraduate Studies

Programme for acceptance, a thesis entitled

**Spatio-Temporal processing for Optimum Uplink-Downlink
WCDMA Systems**

submitted by

Ahmed Mohammed Ahmed Jad Elrab

for the fulfilment of the requirements for the degree of

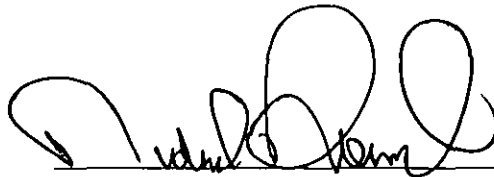
Masters of Science in Electrical and Electronics Engineering

11/02/2008

Date

Signature

:



Main Supervisor

:

Dr. Nidal S.Kamel

Date

:

11/02/2008

Co-Supervisor

:

UNIVERSITI TEKNOLOGI PETRONAS

**Spatio-Temporal processing for Optimum Uplink-Downlink
WCDMA Systems**

By

Ahmed Mohammed Ahmed Jad Elrab

A THESIS

SUBMITTED TO THE POSTGRADUATE STUDIES PROGRAMME

AS A REQUIREMENT FOR THE

DEGREE OF MASTERS OF SCIENCE IN ELECTRICAL AND ELECTRONICS
ENGINEERING

Electrical and Electronics Engineering

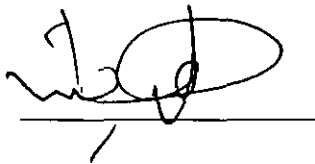
BANDAR SERI ISKANDAR,
PERAK

FEBRUARY, 2008

DECLARATION

I hereby declare that the thesis is based on my original work except for quotations and citations which have been duly acknowledged. I also declare that it has not been previously or concurrently submitted for any other degree at UTP or other institutions.

Signature:

A handwritten signature in black ink, appearing to be 'Ahmed', written over a horizontal line.

Name : Ahmed Mohammed Ahmed Jad Elrab

Date : 11/02/2008

ACKNOWLEDGEMENT

- ✦ To my parents and family for their love, support and encouragement.
- ✦ To my supervisor Dr. Nidal S.Kamel for his support and guidance that helped accomplish this work.
- ✦ To Dr. Mahamod Ismail for his valuable time and advice.
- ✦ To the Electrical and Electronics Engineering Department, especially Dr. Varoun for his support.
- ✦ To all members of the Post Graduate Studies Office for help and advice.
- ✦ To all my friends and colleagues for the joy they brought into my life.

ABSTRACT

The capacity of a cellular system is limited by two different phenomena, namely multipath fading and multiple access interference (MAI). A Two Dimensional (2-D) receiver combats both of these by processing the signal both in the spatial and temporal domain. An ideal 2-D receiver would perform joint space-time processing, but at the price of high computational complexity. In this research we investigate computationally simpler technique termed as a Beamformer-Rake. In a Beamformer-Rake, the output of a beamformer is fed into a succeeding temporal processor to take advantage of both the beamformer and Rake receiver. Wireless service providers throughout the world are working to introduce the third generation (3G) and beyond (3G) cellular service that will provide higher data rates and better spectral efficiency. Wideband CDMA (WCDMA) has been widely accepted as one of the air interfaces for 3G. A Beamformer-Rake receiver can be an effective solution to provide the receivers enhanced capabilities needed to achieve the required performance of a WCDMA system.

We consider three different Pilot Symbol Assisted (PSA) beamforming techniques, Direct Matrix Inversion (DMI), Least-Mean Square (LMS) and Recursive Least Square (RLS) adaptive algorithms. Geometrically Based Single Bounce (GBSB) statistical Circular channel model is considered, which is more suitable for array processing, and conducive to RAKE combining. The performances of the Beamformer-Rake receiver are evaluated in this channel model as a function of the number of antenna elements and RAKE fingers, in which are evaluated for the uplink WCDMA system. It is shown that, the Beamformer-Rake receiver outperforms the conventional RAKE receiver and the conventional beamformer by a significant margin. Also, we optimize and develop a mathematical formulation for the output Signal to Interference plus Noise Ratio (SINR) of a Beamformer-Rake receiver.

In this research, also, we develop, simulate and evaluate the *SINR* and Signal to Noise Ratio (E_b/N_0) performances of an adaptive beamforming technique in the WCDMA system for downlink. The performance is then compared with an omnidirectional antenna system. Simulation shows that the best performance can be achieved when all the mobiles with same Angle-of-Arrival (AOA) and different distance from base station are formed in one beam.

TABLE OF CONTENTS

STATUS OF THESIS.....	i
APPROVAL PAGE.....	ii
TITLE PAGE.....	iii
DECLARATION.....	iv
ACKNOWLEDGEMENT.....	v
ABSTRACT.....	vi
TABLE OF CONTENT.....	vii
LIST OF TABLES.....	xiii
LIST OF FIGURES.....	xiv
APPREVIATIONS AND SYMBOLS.....	xvii
 CHAPTER ONE: INTRODUCTION.....	 1
1.1 Background and Literature Survey.....	1
1.2 Problem statement.....	8
1.3 Objectives.....	9
1.4 Scope of study.....	9
1.5 Methodology.....	10
1.6 Thesis Overview.....	11
 CHAPTER TWO: FUNDAMENTAL CONCEPTS OF SPACE TIME	
PROCESSING.....	13
2.1 Introduction.....	13
2.2 Space -Time processing techniques.....	14
2.2.1 High Sensitivity Reception (HSR).....	15
2.2.2 Space division multiple access (SDMA).....	15
2.2.3 Smart Antennas.....	15
2.3 Space- Time Base stations.....	16
2.4 Space- Time Mobiles.....	17

2.5 Advantages of Space- Time processing	17
2.5 Signal processing in the Antenna Array	18
2.6.1 Uniform Linear Array (ULA)	18
2.7 Beamforming	23
2.7.1 Example of a Simple Beamforming (Null- Steering) with ULA	24
2.8 Array Ambiguity	27
2.9 Spatial Sampling Theorem.....	28
2.10 Spatial Diversity Gain.....	29
2.11 Temporal Processing: Rake Receiver for CDMA	30
2.11.1 Combining Techniques for Improved SNR.....	31
2.11.1.1 Selection Combining (SC)	32
2.11.1.2 Maximal Ratio Combining (MRC).....	32
2.11.1.3 Equal Gain Combining (EGC).....	32
2.12 Beamformer –Rake Receiver.....	32
2.13 Summary	34
 CHAPTER THREE: BEAMFORMING CRITERIA	 35
3.1 Introduction.....	35
3.2 MSNR Beamforming	35
3.2.1 Maximizing the Signal to Noise Ratio.....	36
3.2.2 Alternate SE for MSNR Beamforming.....	39
3.2.3 Phase Ambiguity in Eigen-Beamforming.....	40
3.3 MSIR Beamforming.....	42
3.4 MSINR Beamforming.....	44
3.4.1 Maximizing the Signal to Interference and Noise Ratio.....	45
3.4.2 Maximizing the Received Signal to Interference and Noise Ratio.....	47

3.5 MMSE Beamforming Criterion	48
3.6 Adaptive Beamforming Algorithms	51
3.6.1 Non-blind Algorithms.....	52
3.6.1.1 Least Mean Square Algorithm (LMS).....	53
3.6.1.2 Normalized Least Mean Square Algorithm (NLMS).....	54
3.6.1.3 Sample Matrix Inversion Algorithm (SMI).....	55
3.6.1.4 Recursive Least Square Algorithm (RLS)	56
3.6.1.5 Direct Matrix Inversion Algorithm (DMI)	57
3.6.2 Blind Algorithms	58
3.6.2.1 Constant Modulus Algorithm (CMA).....	58
3.6.2.2 Other Techniques.....	60
3.7 Summary	61
CHAPTER FOUR: SPATIO-TEMPORAL CHANNEL MODELS.....	62
4.1 Introduction.....	62
4.2 Geometrically Based Single Bounce Elliptical Model	63
4.2.1 Introduction.....	63
4.2.2 Assumptions.....	63
4.2.3 Geometry and Notation.....	64
4.2.4 Mathematical Formulation.....	65
4.2.5 Generation of Samples of the Elliptical Channel Model	67
4.3 Geometrically Based Single Bounce Circular Model.....	69
4.3.1 Introduction.....	69
4.3.2 Assumptions.....	70
4.3.3 Geometry and Notation.....	70
4.3.4 Mathematical Formulation	72
4.3.5 Generation of Samples of the Circular Channel Model	73
4.4 Channel parameters from the WCDMA system perspective.....	74
4.4.1 Power –delay profile	75
4.4.2 Angle Spread.....	75
4.5 Summary	76

CHAPTER FIVE: WCDMA..... 77

5.1 Introduction..... 77

5.2 Cellular Standards: From 1G to 3G 77

5.2.1 First Generation (1G) Cellular Systems.....78

5.2.2 Second Generation (2G) Cellular Systems78

5.2.3 Transition towards 3G: 2.5G Cellular Systems79

5.2.4 Third Generation Cellular Systems80

5.3 WCDMA: Air Interface for 3G..... 82

5.3.1 WCDMA Key Features.....82

5.3.2 WCDMA Key Technical Characteristics.....83

5.4 WCDMA Physical Layer at the Uplink 84

5.4.1 Physical Channel Structure.....84

5.4.1.1 Uplink Spreading and Modulation.....85

5.4.1.2 Uplink Frame Structure.....86

5.4.1.3 Uplink Channelization Codes88

5.4.1.4 Uplink Scrambling Codes.....90

5.4.1.4.1 Uplink Long Scrambling Codes.....92

5.4.1.4.2 Properties of Uplink Long Scrambling Code.....93

5.4.1.5 Summary of WCDMA Uplink Modulation94

5.4.2 Channel Coding94

5.4.2.1 Error Detection.....95

5.4.2.2 Error Correction.....95

5.5 Summary..... 95

CHAPTER SIX: SYSTEM MODELING AND ANALYSIS 97

6.1 Introduction..... 97

6.2 Transmitter Model 98

6.3 Channel Description..... 100

6.4 Receiver Model..... 102

6.4.1 Direct Matrix Inversion (DMI) beamforming.....106

6.4.2 Least Mean Square (LMS) Adaptive beamforming.....108

6.4.3 Recursive Least Square (RLS) Adaptive Beamforming.....	109
6.5 Generalized Optimum Output SINR Analysis.....	112
6.6 Summary	113

CHAPTER SEVEN: SIMULATION RESULTS AND DISCUSSION FOR

UPLINK-DOWNLINK SCENARIOS	115
7.1 Introduction For Uplink Scenario	115
7.2 Simulation Set Up For Uplink	116
7.2.1 Transmitter Specifications	116
7.3 Multipath Channel Generation For Uplink	118
7.3.1 Macrocelluar Environments.....	118
7.4 Receiver Operational Block For Uplink	120
7.5 Simulation Environment	122
7.6 Simulation Results For Uplink.....	122
7.6.1 BER performance Versus Number of Users.....	122
7.6.1.1 Macrocelluar Circular Channel Environment.....	123
7.6.1.1.1 LMS Beamforming	123
7.6.1.1.2 DMI Beamforming.....	126
7.6.1.1.3 RLS Beamforming.....	127
7.6.2 BER Performance vs. Eb/No	130
7.6.2.1 Macrocelluar Circular Channel Environment.....	130
7.6.2.1.1 LMS beamforming.....	130
7.6.2.1.2 DMI Beamforming.....	134
7.6.2.1.3 RLS Beamforming.....	136
7.7 Performance of Adaptive Antennas for Downlink Scenario.....	138
7.7.1 Introduction.....	138
7.7.2 Topology	138
7.7.3 Simulation Scenario	139
7.7.3.1 Antenna Parameter	140
7.7.3.2 Adaptive Beamforming Technique.....	141
7.7.3.3 Downlink Interference Analysis	143

7.7.3.3.1 Intracell Interference	143
7.7.3.3.2 Intrabeam Interference	143
7.7.3.3.2.1 Interbeam Interference	143
7.7.3.3.2.2 Intercell Interference	144
7.7.4 Program Flowchart	145
7.7.5 Input Parameters	151
7.7.6 Simulation Output	152
7.7.7 Simulation Results and Discussion For Downlink Scenario	153
7.7.7.1 Introduction	153
7.7.8 Performance of adaptive array antenna	153
7.7.9 Performance comparison between adaptive array antenna and omnidirectional antenna	157
7.7.10 Downlink power control of adaptive array antenna	158
7.7.11 Summary	164
CHAPTER EIGHT: CONCLUSIONS AND FUTURE WORK	165
8.1 Conclusion	165
8.2 Future Work	166
REFERENCES	168
PUBLICATIONS	191

LIST OF TABLES

TABLE 5.1: 3G data rate requirements	80
TABLE 5.2: WCDMA key technical characteristics.....	83
TABLE 5.3: Uplink data rate vs. spreading factor	88
TABLE 5.4: Parameters of WCDMA spreading and modulation at the uplink	94
TABLE 7.1: Uplink WCDMA Frame-Slot parameters.	116
TABLE 7.2: Uplink WCDMA transmitter parameters for simulation	118
TABLE 7.3: Simulation input parameters.	151
TABLE 7.4: Simulation input parameters (user-defined).....	151
TABLE 7.5: User data rates.....	152
TABLE 7.6: Input parameters for the simulation of adaptive array antenna performance in downlink WCDMA system performance comparison.....	153
TABLE 7.7: Eb/No threshold for each bit rate	156
TABLE 7.8: Input parameters for the simulation of the user data rate effect.....	158

LIST OF FIGURES

Figure 2.1: Plane wave incident on a ULA with an AOA of θ	19
Figure 2.2a: Digital beamformer principle.	24
Figure 2.2b: Typical array gain pattern.....	24
Figure 2.3: Beam pattern for the elementary beamformer. The AOA of the desired user is 0° and the AOA of the interferer is 45°	27
Figure 2.4a: Rake Receiver.....	30
Figure 2.4b: Multipath diversity	31
Figure 2.5a: Beamformer-Rake structure (CSTP)	33
Figure 2.5b: Different weight vector accentuates different multipath component of the desired user	33
Figure 3.1: Classification of adaptive beamforming algorithms	52
Figure 4.1: Geometry of the GBSB elliptical channel model.....	64
Figure 4.2: Geometry of the Circular Scattering Channel Model.....	71
Figure 5.1: Evolution towards 3G.....	81
Figure 5.2: Uplink spreading and modulation.	85
Figure 5.3: Frame structure for uplink DPDCH/DPCCH.....	87
Figure 5.4: Code – tree for generation of OVSF codes	88
Figure 5.5: Auto-correlation for two OVSF codes of SF = 256	90
Figure 5.6: Generation of scrambling codes.....	91
Figure 5.7: Uplink long scrambling code generator	93
Figure 6.1: WCDMA uplink transmitter model.....	98
Figure 6.2: Base station antenna array receiver model.	102
Figure 7.1: Multipath propagation model for macrocelluar environment	120
Figure 7.2: Block diagram of a PSA 2-D RAKE receiver used for simulation.....	121
Figure 7.3: BER performance of a 2-D RAKE receiver with 2-element LMS beamformer	124

Figure 7.4: BER performance of a 2-D RAKE receiver with 4-element LMS beamformer	125
Figure 7.5: BER performance of a 2-D RAKE receiver with 2-element DMI beamformer	126
Figure 7.6: BER performance of a 2-D RAKE receiver with 4-element DMI beamformer	127
Figure 7.7: BER performance of a 2-D RAKE receiver with 2-element RLS beamformer	128
Figure 7.8: BER performance of a 2-D RAKE receiver with 4-element RLS beamformer	129
Figure 7.9: BER vs. E_b/N_0 performance for a 2-element LMS 2-D RAKE receiver with 2-user scenario	131
Figure 7.10: BER vs. E_b/N_0 for a 2-element LMS 2-D RAKE receiver with 4-user scenario	132
Figure 7.11: BER vs. E_b/N_0 for a 6-element LMS 2-D RAKE receiver with 6-user scenario	133
Figure 7.12: BER vs. E_b/N_0 for a 6-element LMS 2-D RAKE receiver with 12-user scenario	133
Figure 7.13: BER vs. E_b/N_0 for a 2-element DMI 2-D RAKE receiver with 2-user scenario	134
Figure 7.14: BER vs. E_b/N_0 for a 4-element DMI 2-D RAKE receiver with 8-user scenario	135
Figure 7.15: BER vs. E_b/N_0 for a 6-element DMI 2-D RAKE receiver with 12-user scenario	135
Figure 7.16: BER vs. E_b/N_0 for a 2-element RLS 2-D RAKE receiver with 2-user scenario	136
Figure 7.17: BER vs. E_b/N_0 for a 4-element RLS 2-D RAKE receiver with 8-user sceanrio	137
Figure 7.18: BER vs. E_b/N_0 for a 6-element RLS 2-D RAKE receiver with 12-user scenario	137

Figure 7.19: Cells layout and MSs Distribution (x refers to MS).....	138
Figure 7.20: Actual beam formation algorithm parameters, (b) Examples of beam formation and (c) Beam reformation to accommodate a new call.....	142
Figure 7.21: Intrabeam interference and Interbeam interference.....	144
Figure 7.22: Adaptive array antennas in WCDMA downlink simulation algorithm Calculating SINR and EbNo vs. No MSs Algorithm	147
Figure 7.23: Adaptive array antennas in WCDMA downlink simulation algorithm Calculating SINR and EbNo vs. separation angle algorithm.....	148
Figure 7.24: Comparison between adaptive array antenna and omnidirectional antenna for downlink WCDMA system simulation algorithms	149
Figure 7.25: Adaptive array antenna power control for downlink WCDMA system simulation algorithms.....	150
Figure 7.26: Average SNR for adaptive array antenna in downlink WCDMA vs. Separation Angle of Arrival (AOA)	154
Figure 7.27: SINR vs. Number of users for adaptive array antenna in downlink WCDMA system	155
Figure 7.28: SNR vs. Number of users for adaptive array antennas in downlink WCDMA system.....	156
Figure 7.29: Average downlink SNR vs. Number of users for omnidirectional and adaptive array antennas.....	157
Figure 7.30: Eb/No for each mobile before and after power control	158
Figure 7.31: EIRP before and after power control.....	159
Figure 7.32: Eb/No for each mobile before and after power control	159
Figure 7.33: EIRP before and after power control.....	160
Figure 7.34: Eb/No for each user before and after power control for R= 144 kb/s.....	162
Figure 7.35: EIRP before and after power control for R= 144 kb/s.....	162
Figure 7.36: Eb/No for each user before and after power control for R= 384 kb/s.....	163
Figure 7.37: EIRP before and after power control for R= 384 kb/s.....	163

ABBREVIATIONS AND SYMBOLS

AOA	Angle of Arrival
ARIB	Association of Radio Industry and Business
ATIS	Alliance for Telecommunications Industry Solutions
BPSK	Binary Phase Shift Keying
BTS	Base Station Transceiver
BS	Base Station
CFA	Code Filtering Approach
CSTP	Concatenated Space Time Processor
CCPCH	Common Control Physical Channels
CRC	Cyclic Redundancy Check
DS-CDMA	Direct sequence Code Division Multiple Access
IMT-2000	International Mobile Telecommunications
MAI	Multiple Access Interference
RTT	Radio Transmission Technology
ETSI	European Telecommunications Standards Institute
ISI	Inter- symbol interference
DSPs	Digital signal processors
PSA	Pilot Symbol Assisted
GBSB	Gaussian Based Single Bounce
ML	Maximum Likelihood
MVDR	Minimum Variance Distortion less Response
TDL	Taped Delay Line
MEM	Maximum Entropy Method
MLM	Maximum Likelihood Method
DOA	Direction of Arrival
MUSIC	Multiple Signal Classification
ESPRIT	Estimation of Signal Parameters via Rotational Invariance Technique
ULA	Uniform Linear Array
WSF	Weighted Subspace Fitting
LSCMA	Least Squares Constant Modulus Algorithm
GPM	Generalized Power Method
GE	Generalized Eigenvalue problem
GLM	Generalized Lagrange Multiplier
SE	Simple Eigenvalue problem
TDMA	Time Division Multiple Access
SFIR	Spatial Filtering Interference Reception
HSR	High Sensitivity Reception
SDMA	Space Division Multiple Access
FDMA	Frequency Division Multiple Access
SINR	Signal to Interference plus Noise Ratio
SIR	Signal to Interference Ratio

SNR	Signal to Noise Ratio
WCDMA	Wideband Code Division Multiple Access
FIR	Finite Impulse Response
MRC	Maximal Ratio Combining
EGC	Equal Gain Combining
SC	Selection Combining
MSNR	Maximum Signal to Noise Ratio
MSIR	Maximum Signal to Interference Ratio
MSINR	Maximum Signal to Interference and Noise Ratio
MMSE	Minimum Mean Square Error
MSIR	Maximum Signal to Interference Ratio
DF	Direction Finding
RSNR	Received Signal to Noise Ratio
DPCCH	Dedicated Physical Control Channel
DPDCH	Dedicated Physical Data Channel
MRSINR	Maximum Received Signal to Interference and Noise Ratio
MSE	Mean Square Error
LMS	Least Mean Square
NLMS	Normalized Least Mean Square
SMI	Sample Matrix Inversion
RLS	Recursive Least Square
DMI	Direct Matrix Inversion
CMA	Constant Modulus Algorithm
SCORE	Self-Coherence Restoral
DD	Decision Directed
ISI	Intersymbol Interference
LOS	Line Of Sight
AOD	Angle of Arrival
1G	First Generation
3G	Third Generations
AMPS	Advanced Mobile Phone System
NAMPS	Narrowband AMPS
TACS	Total Access Cellular System
NMT-900	Nordic Mobile Telephone System
FM	Frequency Modulation
2G	Second Generation
USDC	United States Digital Cellular
GSM	Global System for Mobile communications
PDC	Pacific Digital Cellular
GPRS	General Packet Radio Service
EDGE	Enhanced Data-rates for Global Evolution
EGPRS	EDGE for GPRS
ECSD	EDGE for Circuit Switched Data traffic
PSTN	Public Switched Telephone Network
ITU	International Telecommunication Union
SMG	Special Mobile Group

UMTS	Universal Mobile Telecommunication System
UTRA	UMTS Terrestrial Radio Access
FDD	Frequency Division Duplex
TDD	Time Division Duplex
DPCH	Dedicated Physical Channel
SCH	Synchronization Channel
PRACH	Physical Random Access channel
QPSK	Quadrature Phase Shift Keying
OVSF	Orthogonal Variable Spreading Factor
HPSK	Hybrid Phase Shift Keying
FBI	Feedback Information
TPC	Transmit Power Control
TFCI	Transport Format Combination Indicator
SF	Spreading Factor
LSB	Least Significant Bit
UL	Uplink
SCCC	Serial Concatenated Convolutional Code
W-H	Wiener-Hopf
BER	Bit Error Rate
MSs	Mobile Stations
EIRP	Effective isotropically radiated power

$(.)^*$	Complex conjugate
$*$	Convolution
$(.)^H$	Complex conjugate transposition
$(.)^T$	Transposition
$A_i(t)$	The signal Amplitude
$A_{l,i}[n]$	$N \times G_i$ discrete channel matrix for the l th path of user i
$\underline{a}(\theta)$	The array response vector
a_m	The semimajor axis
$\underline{a}(\theta_i)$	The $N \times 1$ antenna response vector
$\underline{a}(\theta_d)$	The array response vector for an AOA of θ_d
\underline{a}^H	Hermitian transpose of array response vector
$\underline{a}(\theta_{l,i})$	The $N \times 1$ array response vector or the steering vector
$a_{l,i}(t)$	Spatial signature vector or the channel vector
B	Number of base stations interfering with the user

b_m	The semiminor axis
c	The velocity of light
C_1	Real chip rate code
C_2'	Decimated version of a real chip rate code C_2
C_{sc}	Scrambling code
$C_{1,n}, C_{2,n}$	The real chip rate codes of n th scrambling code
c_i^D	Channelization code vector for i th user's DPDCH
c_i^C	Channelization code vector for i th user's DPCCH
c_i^{scr}	Complex scrambling code for i th user
d	Element spacing between adjacent antenna elements
d	The distance between two adjacent antenna elements
$d^*(l)$	Conjugate of the actual sample sent
d_l	The multipath propagation distance
$d^j[n]$	Pilot bits for the j th slot
d	The MS-BS separation distance
D	The directivity
d	desired symbol or reference signal
D	The separation distance between the transmitter and the receiver
$e(k)$	The error signal
E	Ensemble expectation operator
$e^j[n]$	The error signal for the j th slot
f_c	The carrier frequency
$f_{\theta_b}(\theta_b)$	AOA pdf elliptical channel model
$G_t(\theta_d)$	Transmit antenna as function of the angle of departure θ_d
$G_r(\theta_a)$	Receive antenna as function of the angle of arrival θ_a
$g(\theta)$	Frequency response of an FIR filter
$G(\theta)$	Antenna response beam pattern
G	The gain
G_i	The i th user's spreading factor
G_p	processing gain
$g(t)$	Chip pulse shaping waveform
$h_i(t)$	The channel impulse response of the i th user

h_t	The base station antenna height above rooftop
h_b	The rooftop height
h_m	The mobile station antenna height
\underline{i}	The interference.
I	$N \times N$ identity matrix
$I[n]$	user's self interference
I_{intra_beam}	Intrabeam interference
I_{inter_beam}	Interbeam interference
$I_{intercell}$	Intercell interference
J	Mean Square Error MSR
k	Sample index
K	The number of active users
$k(n)$	Gain vector
L_i	The number of resolvable multipaths from the i th user
L_r	The path loss
$M[n]$	Multiple access interference (MAI)
M	The number of RAKE fingers used in the receiver
M	The number of beams interfering with the user
N	The number of users in the same cell
N	The number of antenna elements
\underline{n}	Complex additive Gaussian noise vector
$\underline{n}(t)$	The thermal noise vector.
\underline{n}	Spatially and temporally white noise
n	The bit index
$\hat{N}[n]$	Single interference plus noise matrix
$\hat{N}_{dscr}[n]$	$N \times G_i$ interference plus noise matrix after descrambling
$N[n]$	$N \times G_i$ received sampled noise matrix
N_d	The number of pilot bits per slot
P_r	The received power
P_s	Power of the desired signal
P_n	Power of the noise

P_{ref}	The reference power
P_T	The transmitted power
$P_0(dBm)$	The power of the direct path component (LOS)
P_{ki}	The transmit power for kth BS and ith MS
$\underline{\underline{R}}_{ss}$	Covariance matrix of the desired signal vector
$\underline{\underline{R}}_{nn}$	Noise covariance matrix
$\underline{\underline{R}}_{xx}$	The received signal covariance matrix
R_{uu}	Covariance matrix of the array element input for the interferes
\underline{r}_{xd}	Cross-correlation vector between the received signal vector \underline{x} and the reference signal d
$R(n)$	Covariance matrix for n iterations
r_b	Distance from the base station of a scatterer located at the boundary of the ellipse
$\hat{\underline{\underline{R}}}_{xx}(n)$	Estimated window of received signal covariance matrix
$\hat{\underline{r}}_{xd}(n)$	Estimated window of Cross-correlation vector between the received signal vector \underline{x} and the reference signal d
$R_{uu}^D[n]$	Autocorrelation matrix of interference plus noise vector for data channel
$R_{uu}^C[n]$	Autocorrelation matrix of interference plus noise vector for control channel
\underline{s}	Desired signal vector
$s_i(t)$	The i^{th} signal
\underline{s}^H	Hermitian transpose of desired user signal vector
SF	Spreading factor
$s_i[n]$	$G_i \times 1$ transmitted chip sequence vector for the user i
T_b, T_c	Bit and chip duration
\underline{u}	Undesired signal vector
$v_i[n]$	Spreaded chip sequence vector for the n th bit
$w_{l,OPT}^D$	The optimum weight vectors for the l th beamformer data

	channel
$w_{l,OPT}^C$	The optimum weight vectors for the l th beamformer control channel
$\underline{w}^H(t)$	Hermitian transpose of the antenna weight vector
\underline{w}	Antenna weight vector
$\hat{\underline{w}}$	Estimated window of antenna weight vector
w_1	Repetition of $\{1 \ 1\}$ at the chip rate
w_2	Repetition of $\{1 \ -1\}$ at the chip rate
ω_c	Angular carrier frequency
w_l^j	Weight vector of the l th beamformer for the j th slot
\hat{w}_{OPT}	Optimum weight vector estimate given by Wiener-Hopf (W-H) solution
$\underline{x}(t)$	The received signal vector
χ_{\max}	The reciprocal of the maximum delay
\underline{x}	Received signal vector at the antenna array
$\underline{x}(l)$	Collected sample of the received signal over a block of L samples
$\underline{x}(t)$	The total received $N \times 1$ signal vector at the base station antenna array
$x_{l,i}^D[n]$	The resulting despreaded data bit
$x_{l,i}^C[n]$	The resulting despreaded control bit
$x_{l,i}^D[n]_j$	Despreaded data channel bits for the j th slot
$x_{l,i}^C[n]_j$	Despreaded control channel bits for the j th slot
$X_{l,i}[n]$	$N \times G_i$ received chip sample matrix
$\gamma(t)$	The information
$y(n)$	The array output
$z_{l,i}^D[n]$	The output of l th beamformer for the j th data channel
$z_{l,i}^C[n]$	The output of l th beamformer for the j th control channel
$z_i^D[n]_j$	The output of the MRC coherent RAKE combiner data channel
$z_i^C[n]_j$	The output of the MRC coherent RAKE combiner control channel
θ	Angle of Arrival

τ	Time delay
β	The random phase
λ	RF waveform length
σ^2_n	Noise variance
λ_{\max}	Maximum eigenvalue
ρ	Complex scalar
σ_s^2	Output signal power
σ_u^2	Total interfering signal power
β_{SIR}	Signal to interference ratio scalar coefficient
$\nabla(J)$	Gradient vector
$\frac{\partial}{\partial \underline{w}^*}$	Conjugate derivative with respect to vector \underline{w}
μ	Step size parameter of LMS algorithm
$\varepsilon(n)$	Cost function
λ	Forgetting factor of RLS algorithm
$\alpha(n)$	Estimation error
δ	Small positive constant
$\nabla(J(n))$	Instantaneous estimate of the gradient vector
τ_{\max}	Maximum specified delay
θ_b	AOA at the base station
τ_l	The propagation delays of the multipaths
$\theta_{b,l}$	The angle of arrivals (AOA) of the multipaths at the base station
γ_l	The phase of the multipath components
α_l	The complex amplitudes of the multipath components
σ_{θ_b}	Ensemble average angle spread for AOA at the receiver
β_i^D	The gain factor for i th user's DPDCH
β_i^C	The gain factor for i th user's DPCCH
$diag(\cdot)$	The diagonalization operation
ϕ_i	Unknown carrier phase
$\alpha_{l,i}(t)$	Complex path amplitude

$\tau_{l,i}$	Path delay for l th resolvable multipaths and i th user
$\theta_{l,i}$	AOA of the l th path from i th user
Δ_i	Angle spread of the i th user
$\eta(t)$	$N \times 1$ complex additive Gaussian noise vector
$\hat{\eta}_l^D[n]$	$N \times 1$ total interference plus noise vectors for the n th bit for data channel
$\hat{\eta}_l^C[n]$	$N \times 1$ total interference plus noise vectors for the n th bit for control channel
$\sigma_{\hat{\eta}_l^D}^2$	The variances of $\hat{\eta}_l^D[n]$
$\sigma_{\hat{\eta}_l^C}^2$	The variances of $\hat{\eta}_l^C[n]$
$\hat{\alpha}_{l,i}[n]_j$	The modified channel gain at the beamformer output
γ_l^D	Arbitrary constant for data channel
γ_l^C	Arbitrary constant for control channel
$SINR_{OPT}^D$	The output signal to noise plus interference ratio for data channel
$SINR_{OPT}^C$	The output signal to noise plus interference ratio for control Channel
β	3-dB antenna beam width
ϕ	Deviation angle from the main lobe
α_{ij}	i th angle of arrival on j th base station
α_{kj}	k th angle of arrival on j th base station
γ_{ik}^j	The separation angle between adjacent mobiles
α	Orthogonal factor.

CHAPTER ONE

INTRODUCTION

1.1 Background and Literature Survey

A Beamformer-Rake [1] receiver is a concatenation of a beamformer [2] and a Rake receiver [3], [4]. This provides a higher degree of freedom since the signal can be processed in both the temporal and the spatial domains. The signal processing of the Beamformer-Rake combats against the Multiple Access Interference (MAI) and mitigates fading. Wireless service providers throughout the world are working to introduce the third generation (3G) [5] cellular service that will provide higher data rates and better spectral efficiency. Wideband Code Division Multiple Access (WCDMA) [6], [7], [8], [9], [10] has been widely accepted as one of the air interfaces for 3G. A Beamformer-Rake receiver can be an effective solution to provide the receivers enhanced capabilities needed to achieve the required performance of a WCDMA system.

Wideband direct sequence Code Division Multiple Access (W-CDMA) has been widely accepted as the radio access scheme for the third generation (3G) wireless system known as International Mobile Telecommunications-2000 (IMT-2000). One of the major objectives of IMT-2000 is to support high and widely variable data rate users with high quality and achieve enhanced system coverage and capacity. For example, the target specified by IMT-2000 for minimum user data rate is 144 kbps in vehicular environments and 384 kbps in pedestrian environments [11]. But in a Direct Sequence CDMA (DS-CDMA) system where all the users communicate simultaneously within the same frequency band, the high data rate users may cause large Multiple Access Interference (MAI) due to their increased transmission power. This problem is particularly severe in the uplink (mobile to base station) where the users transmit asynchronously, producing the well known near-far problem. In addition to MAI, the received signal is also subjected to multipath fading due to the relative motion between the mobile and the local

scatterers. Also, distance dependent path loss and long term fading (shadowing) exist. All of these significantly degrade the uplink system capacity. A promising technique to reduce the MAI and thereby increase the uplink system capacity is to employ an adaptive antenna array [12], [13], [14],[15].

An adaptive antenna array is capable of forming a beam towards the desired user and directing the nulls towards the interferers, which is commonly known as beamforming. By doing so, it can reduce the co-channel interference from the other users within its own cell as well as in the neighboring cells, thereby increasing the system capacity. There exist many adaptive antenna array algorithms or beamforming techniques, both blind and non blind or Pilot Symbol Assisted (PSA) that offer different advantages for different environments.

The term adaptive antenna has been used in the literature since the late 50.s and early 60.s [16], [17], [18], [19], [20], [21]. A multitude of different adaptive antenna techniques have been proposed in the last four decades or so. In this section we present a literature survey of adaptive antennas. Vector channel models [22] are required to investigate the performance of a receiver equipped with adaptive antenna processing. A null-steering beamformer is used to cancel a plane wave coming from a particular direction by placing a null at the Angle of Arrival (AOA) of that plane wave in the beam pattern. One of the earliest schemes [23] proposed to achieve this by estimating the signal arriving from a known direction by steering a conventional beam in the direction of the source and then subtracting the output of this from each antenna element. Although this process is very effective in canceling strong interference, the scheme becomes unwieldy as the number of interfering signals grows. Therefore null steering based on constraints was proposed in [24]. The basic idea is to form a beam with unity gain in the direction of the desired user and nulls in the direction of the interferers [24], [25], [26]. This beamformer does not minimize the uncorrelated noise at the output of the beamformer. This was achieved in [27]. Null steering schemes towards known locations have been also shown to be effective in a transmit beamforming array to minimize the interference towards other co-channel mobiles in a cellular system [28].

The null-steering schemes do not maximize the output Signal to Noise Ratio (SNR). A beamformer that maximizes the SNR and at the same time tends to minimize the interference was therefore proposed by various researchers [29]-[32]. This beamformer termed as the optimal beamformer maximizes the Signal to Interference and Noise Ratio (SINR) at the output of the beamformer. The optimum beamforming technique can be attributed to [33] whose early work by finding the Maximum Likelihood (ML) estimate of the power of the desired signal led to its development. The optimum beamformer is often time termed as the Minimum Variance Distortionless Response (MVDR) Beamformer. In mobile communications literature, the optimal beamformer is often referred to as the optimal combiner. Discussion on the use of the optimal combiner to cancel interferences and to improve the performance of mobile communications systems can be found in [34]-[37].

A beamformer that utilizes a reference signal to calculate the weights was proposed in [16]. The beamformer utilizes the Wiener solution arising from the Minimum Mean Squared Error (MMSE) criterion. Further analysis of this technique can be found in [38], [39], [40], and [32]. This scheme was also shown to be effective in acquiring a weak signal in the presence of strong jammers in [41]. The MMSE beamformer was compared to an MVDR Beamformer in [42]. Similar study in a mobile communication environment based on simulation was performed in [43]. The study of reference based beamforming for mobile communications system have also been reported in [44]-[47].

Beam-space processing is a two stage scheme where the first stage takes the array signals as input and produces a set of multiple outputs, which are then weighted and combined to produce the array output. Since beam-space beamforming is not very closely related to the research work presented in this dissertation, only references [39, 48-55] are provided here for interested readers. As the signal bandwidth increases and the narrowband assumption no longer holds, a Tapped Delay Line (TDL) structure or a lattice structure can be an effective solution. We will just present some pertinent references [56-63] here. The application of TDL structure for broadband beamforming in mobile communication environment has been reported in [44], [64], [65].

Estimation of Direction of Arrival (DOA) is one of the major branches of adaptive beamforming. Spectral estimation technique is one of the oldest methods for DOA estimation. Bartlett method is probably the most elementary method for spectral estimation. This method involves weighting the signals from all the antenna elements and finding the average power at different directions. The application of the Bartlett method to the mobile communications environment has been investigated in [66]. Finding the ML estimate of the direction can improve the resolution of the direction finding technique [67] over the Bartlett method. The application of linear prediction [68], Maximum Entropy Method (MEM) [69] and Maximum Log-likelihood Method (MLM) [67] has also been investigated.

The DOA estimate techniques based on the Eigenstructure methods are to some extent similar in principle to the beamforming techniques employed in our research. The basic idea is to utilize the structure of the received signal covariance matrix which can be partitioned into two orthogonal subspaces corresponding to the directional signal and the noise. The Eigenstructure methods try to find an eigenvector that is in the noise subspace and then search for directions for which the steering vector is orthogonal to this eigenvector. The Eigenstructure methods have been investigated in details in [70-78]. The MUSIC method and its several variations are probably the most investigated of the Eigenstructure based DOA estimate techniques. The spectral MUSIC estimates the noise space by employing the Eigen-decomposition of the estimated array covariance matrix [79] or the singular value decomposition of the data covariance matrix [80]. The application of MUSIC for mobile communications has been investigated in [81]. A variation of MUSIC termed as the Root-MUSIC is applicable to Uniform Linear Array (ULA) [82] and has better performance compared to the MUSIC. There are other variations of the MUSIC like the constrained MUSIC [80] and beam-space MUSIC [83], [84]. There have been also investigations of the min-Norm method [85], [86] and the CLOSEST method [97].

ESPRIT [88] is a computationally efficient and robust method of DOA estimation that employs two identical arrays so that the second element of each pair is displaced by the

same distance and in the same direction relative to the first element. Different variations of the ESPRIT algorithm can be found in [89-96]. The application of ESPRIT in estimating the DOA at the reverse link of CDMA cellular system has been reported in [97]. WSF is another DOA estimation method that has been widely investigated [98], [99].

The optimal beamforming techniques mentioned a little earlier requires the estimate of the inverse interference and noise covariance matrix. The Sample Matrix Inversion (SMI) makes a running estimate of the matrix and utilizes matrix inversion lemma to get a simple estimate of the inverse. The SMI method is well described in [30], [100], and [101].

The Least Mean Squared (LMS) algorithm [102] is the most computationally simple algorithm to find the weight vector that satisfies the MMSE beamforming criterion. Ever since the publication of their seminal paper by Windrow *et. al* [16], the LMS has been the subject of numerous research investigations. There are different variations of the LMS algorithm, the unconstrained LMS [103-109], sign algorithm LMS [110], [111], normalized LMS [112-115] and the constrained LMS [116-118] are to name a few. The LMS algorithm is not a very robust algorithm in a fast fading channel. This fact was demonstrated in [119] in the context of spatial equalization.

The convergence of LMS is very slow when the signal covariance matrix (the pertinent matrix in the Wiener solution) has a large spread in its Eigenvalue. The recursive Least Square (RLS) algorithm [102] avoids this at the cost of higher computational complexity. The details of RLS algorithm and its employment in adaptive beamforming can be found in [120-127]. Simulation study has shown the RLS algorithm to be superior to the LMS and the SMI algorithms for flat fading under mobile communications environment [128]. The capacity gain with an RLS based adaptive array at the reverse link of the CDMA system has been reported in [129].

The Constant Modulus Algorithm (CMA) is a gradient based blind adaptive technique. The CMA is widely attributed to [130] and [131]. The main disadvantage of this method

is its slow convergence. Faster converging CMA namely the Orthogonalized CMA [132] and Least Squares CMA (LSCMA) [133], [134] have been proposed in the literature. The development and analysis of CMA is described in detail in [135].

Adaptive beamforming based on the optimal or MSINR criterion can lead to a Generalized Eigenvalue problem (GE) [1]. The Generalized Power Method (GPM) [136] is probably the most common method to solve the GE. However the high computational complexity of the GPM makes it unsuitable for real time implementation. Computationally simple algorithms like the Generalized Lagrange Multiplier method (GLM) [137] and the Adaptive Inversion Method [138], [139] have been proposed.

The conventional (MSNR criterion based) beamforming can be implemented by solving for a Simple Eigenvalue problem (SE) [140]. The Power method [136] can be used to solve the SE. The Conjugate Gradient Method has been proposed to implement the MSNR based beamforming [140-142]. The Lagrange multiplier method has also been proposed as a low complexity solution to the SE [143]. The power method has been simplified in [144] to reduce the computational complexity. An alternate method applying the Lagrange multiplier to solve the GE has been proposed in [145]. A similar technique has been proposed in [146] to solve the SE.

A Rake receiver is used in a CDMA system to exploit the multipath diversity. Combining the adaptive antenna array with the Rake structure, a Beamformer-Rake receiver was proposed [36], [147]. This receiver utilizes the Code Filtering Approach (CFA) [1] to formulate the GE required to perform MSINR based beamforming. The system capacity improvement for this receiver is analyzed in [37], [148], and [149]. Kwon *et. al*, [137] proposed an alternative technique to the CFA to form the Generalized Eigenvalue problem. Another alternative to CFA was proposed by [150]. This method termed as the Code Gated Algorithm (CGA) employs a combination of high-pass and low-pass filter and form the GE with the signals at the output of these filters. A Beamformer-Rake receiver that utilizes the LMS algorithm to perform MMSE based beamforming was proposed in [151]. A thorough analysis of a Beamformer-Rake receiver that performs

optimal and conventional combining in both the spatial and temporal domain can be found in [152]. Performance of the receiver at the uplink of a WCDMA system is also reported in that study.

It is essential to have vector channel models [22] in order to investigate the performance of a receiver equipped with spatio-temporal processing. Vector channel models describe the temporal or spectral parameters like power delay profile, Doppler spread as well as spatial parameters like AOA distribution, angle spread. Geometrically based vector channel models define a region in space where the objects are distributed and the distribution of these objects. The objects are responsible for scattering and/or reflection. Typically a multipath signal is viewed as a single bounce from the transmitter to the receiver. Therefore these models are often termed as Geometrically Based Single Bounce (GBSB) models [153], [154]. Circular channel model [155-158] is a popular model to describe the macro-cellular environment. In a circular channel model the transmitter is surrounded by local scatterers that are distributed within a circle centered on the transmitter. Typical urban and bad urban models are special cases of the circular channel model [159-161]. The elliptical channel model [22], [153], [154] is a typical GBSB model to describe the microcellular environment. The objects are uniformly distributed within an ellipse and the transmitter and the receiver are located at the foci of the ellipse. The maximum delay defines the boundary of the ellipse. The elliptical model provides a much greater angle spread than the previously mentioned models. There are other geometrical models that can be found in the literature [162], [163]. There is also a separate class of vector channel models known as the statistical vector channel model that can be found in the literature [155], [160],[164]-[167]. A special statistical channel model based on the Jake's model [155], [167] can be employed to generate the complex coefficient of a resolvable multipath as a summation of a number of unresolvable components. This model provides very good control over the angle spread of the unresolvable components.

The third generation (3G) mobile telecommunication systems are being deployed and expected to be running globally in the near future. Wideband Code Division Multiple

Access (WCDMA) has emerged as the mainstream air interface solution for the 3G networks. It was also selected as the Radio Transmission Technology (RTT) for Universal Mobile Telecommunications System (UMTS), which is the European Third Generation mobile communications system developed by European Telecommunications Standards Institute (ETSI). The system performances are expected to be improved in term of spectral efficiency, capacity, data rates, and support for multimedia and packet switched services and innovative seamless applications such as mobile video conferencing and web browsing. However, this technology needs to tackle challenges like path loss, multi-path fading, inter- symbol interference (ISI) and power control.

The concept of using multiple antennas and innovative signal processing to serve cells more intelligently has existed for many years. In fact, varying degrees of relatively costly smart antenna systems have already been applied in defense systems. Until recent years, cost barriers have prevented their use in commercial systems. The advent of powerful low-cost digital signal processors (DSPs), and general purpose processors as well as innovative software-based signal-processing techniques (algorithms) have made intelligent antennas practical for cellular communications systems.

Today, when spectrally efficient solutions are increasingly a business imperative, these systems are providing greater coverage area for each cell site, higher rejection of interference, and substantial capacity improvements.

In truth, antennas are not smart—antenna systems are smart. Generally co-located with a base station, a smart antenna system combines an antenna array with a digital signal-processing capability to transmit and receive in an adaptive, spatially sensitive manner. In other words, such a system can automatically change the directionality of its radiation patterns in response to its signal environment. This can dramatically increase the performance characteristics (such as capacity) of a wireless system.

The most important reason lead us to work in this research is to improve the capacity of WCDMA system and accommodate higher number of users in certain bit rate and cell radius.

In this research we improve the performance of adaptive array antenna under different conditions by minimizing the beam width, optimizing the effective parameters and applying downlink power control for WCDMA system.

1.2 Problem statement

The capacity of a cellular system is limited by two different phenomena, namely multipath fading (it's phenomena due to signal power fluctuate or faded in wireless channel or the signal power dropped significantly, so the wireless channel is said to be faded or a phenomena due to presence of obstacles in between the transmitter & receiver, so the signal may reflected, refracted or scattered, so the transmitted signal receive the receiver with different time delays and different multiple copies or replicas) and multiple access interference MAI (it's interference between direct sequences in CDMA system, or due to high data rate CDMA users, in addition , CDMA is interference limited system because all users sharing the all radio resources (Time slot, Frequency band) in the whole bandwidth, but in different PN sequences or codes). A Two Dimensional (2-D) or beamformer-Rake receiver [1] combats both of these by processing the signal both in the spatial and temporal domain. An ideal 2-D receiver would perform joint space-time processing. But this will provide optimum performance at the cost of high computational complexity. So we propose a computationally simpler technique termed as beamformer-Rake receiver.

Adaptive antenna arrays can be used to combat either fading or MAI with the employment of spatial processing only. Since the users of a cellular system transmit from different spatial locations, the received signal from each user has a unique spatial signature associated with it. Adaptive antenna arrays [2] can exploit this spatial property of the signal to reduce the MAI by performing beamforming. The beamformer may be a very practical solution to improve the performance of a Code Division Multiple Access (CDMA) system which is designed to operate in co-channel interference. The capacity of a CDMA system can be effectively increased with a small reduction in the co-channel interference levels.

1.3 Objectives

The main goal of this research is to enhance the performance of the beamformer-Rake receiver established for uplink WCDMA system to give better results and enhance or develop the performance of an adaptive beamforming algorithm in downlink WCDMA system. The objectives of this research include:

1. To develop and study different beamformer-Rake receivers for different adaptive beamforming algorithms or pilot symbol assisted beamforming (PSA) techniques that are suitable for WCDMA systems and investigate their performance under different operating conditions.
2. To compare the performance of these beamformer-Rake receivers with the conventional RAKE receiver and the conventional beamformer.
3. To optimize and generalize a mathematical formulation for the output SINR of a beamformer-Rake receiver.
4. To study the effectiveness of controlling the power in downlink WCDMA system with adaptive array antenna.
5. To develop, simulate and evaluate the SINR and E_b/N_0 performances of an adaptive beamforming technique in WCDMA system for downlink scenario with and without power control algorithm.

1.4 Scope of study

In this research, we consider the beamformer-Rake receiver for the uplink of the W-CDMA system. Our approach is to combine different PSA adaptive beamforming algorithms with a coherent Maximal Ratio Combining (MRC) RAKE receiver. The reason we concentrate on the PSA beamforming techniques is that the W-CDMA standard specifies pilot symbols in the uplink. These pilot symbols can be used for both beamformer weight calculation and channel estimation required for subsequent coherent RAKE combining. We consider the Direct Matrix Inversion (DMI), Least Mean Square (LMS) and Recursive Least Square (RLS) based adaptive beamforming techniques,

which use the pilot symbols as the reference signal. We simulate these PSA based beamformer-RAKE receivers with the W-CDMA reverse link transmitted signal using the Geometrically Based Single Bounce (GBSB) statistical channel model.

CDMA is interference limited multiple access system. Because all users transmit on the same frequency, internal interference generated by the system is the most significant factor in determining system capacity and call quality. The transmit power for each user must be reduced to limit interference, however, the power should be enough to maintain the required E_b/N_0 (signal to noise ratio) for a satisfactory call quality. Maximum capacity is achieved when E_b/N_0 of every user is at the minimum level needed for the acceptable channel performance. As the MS moves around, the RF environment continuously changes due to fast and slow fading, external interference, shadowing, and other factors. The aim of the dynamic power control is to limit transmitted power on both the links while maintaining link quality under all conditions. Additional advantages are longer mobile battery life and longer life span of BTS power amplifiers. In this research, our approach is to improve performance of adaptive array antenna under different conditions by minimizing the beam width, optimizing the effective parameters and applying downlink power control and improve the capacity of WCDMA system and accommodate higher number of users with a certain bit rate and cell radius.

1.5 Methodology

The most obvious way to achieve both MAI suppression and fading reduction is to combine an adaptive antenna array with a RAKE receiver. Such a receiver is commonly known as a space-time or beamformer-Rake receiver due to the fact that both the spatial and the temporal processing are used to estimate the user's transmitted data. A beamformer-Rake receiver is composed of a beamformer connected to each finger of the subsequent RAKE combiner. The beamformer in a particular RAKE finger tries to direct the beam in the direction of a desired user's multipath component to which the finger is synchronized and steer nulls to the other signals. In doing so, it improves the overall SINR and outperforms both the plain adaptive array and the conventional RAKE receiver.

A software simulation of MATLAB 7 has been used to simulate our beamformer-Rake receiver for WCDMA reverse link, also has been used for simulating and evaluating the SINR and Eb/No performances of an adaptive beamforming technique in the WCDMA system for downlink with and without power control algorithm.

1.6 Thesis Overview

Chapter one gives a general background and literature survey of adaptive antenna arrays and wireless mobile communication systems like wideband CDMA systems, Problem statements, objectives and scope of study are also outlined. Chapter two introduces the fundamental concept of spatial and temporal processing and the idea of Beamformer-Rake receivers. Chapter three is devoted towards different beamforming criteria that can be employed in a CDMA based cellular environment. Chapter four describes two GBSB spatio-temporal channel models, which are suited for our space- time processing system and used in our simulation. Chapter five we introduce the current W-CDMA uplink standard used to simulate the transmitted signal. We briefly present the uplink physical channel format, modulation and spreading, scrambling and spreading code generation and allocation. Chapter six we develop a detailed mathematical description of the overall system. We formulate the W-CDMA uplink transmitter model, a spatio-temporal parametric channel and perform a detailed analysis of a PSA beamformer-Rake receiver. We also derive the output SINR expression for a generalized beamformer-Rake receiver. Chapter seven describes the simulation environments and presents the simulation results. A detailed performance comparison of the various PSA beamformer-Rake receivers in the proposed GBSB channel model is provided in this chapter. Chapter eight provides a simulation model employed to study the performance of adaptive array antenna in downlink WCDMA system with and without power control algorithm. The performance is then compared with an omnidirectional antenna system. Chapter nine shows a brief summary and conclusion in along with some suggestions for future work.

CHAPTER TWO

FUNDAMENTAL CONCEPTS OF SPACE TIME PROCESSING

2.1 Introduction

The capacity of a cellular system is limited by two different phenomena, namely multipath fading and multiple access interference (MAI). A Two Dimensional (2-D) receiver [1] combats both of these by processing the signal both in the spatial and temporal domain. An ideal 2-D receiver would perform joint space-time processing. But this will provide optimum performance at the cost of high computational complexity. In this chapter we will introduce the idea of a computationally simpler technique termed as a Concatenated Space Time Processor (CSTP) or Beamformer-Rake [168].

Adaptive antenna arrays can be used to combat either fading or MAI with the employment of spatial processing only. Since the users of a cellular system transmit from different spatial locations, the received signal from each user has a unique spatial signature associated with it. Adaptive antenna arrays [2] can exploit this spatial property of the signal to reduce the MAI by performing beamforming. The beamformer may be a very practical solution to improve the performance of a Code Division Multiple Access (CDMA) system which is designed to operate in co-channel interference. The capacity of a CDMA system can be effectively increased with a small reduction in the co-channel interference levels. This is a marked contrast from Time Division Multiple Access (TDMA) systems which do not benefit as much from a small reduction in interference [135]. Adaptive antenna array can also attain diversity gain [22] if the received signals at the different antenna elements are relatively uncorrelated. The spatial diversity gain can help mitigate multipath fading. The opportunity to employ temporal diversity processing is an inherent advantage of a CDMA system. In a CDMA system, Rake [3] receivers are

used to combat the fading by processing the different time resolvable copies of the received signal in the temporal domain. The CSTP cascades an antenna array with a Rake receiver to take advantage of both the antenna array and a Rake receiver. In a CSTP the output of a spatial processor is fed into a succeeding temporal processor or it can be the other way around.

In this chapter we will discuss a special class of CSTP popularly known as a Beamformer-Rake [1]. A Beamformer-Rake is a concatenation of a beamformer with temporal Rake.

This chapter begins with a discussion on space-time processing techniques, space-time Base stations, space-time Mobiles and the advantages of space-time processing. Also presented an overview of antenna arrays and the fundamental concepts of beamforming. The description of temporal processing in the form of Rake receiver and its Rake combining techniques comes next. We conclude with a discussion on Beamformer-Rake receiver.

2.2 Space -Time processing techniques

Through the use of space- time processing techniques, the levels of MAI and fading a receiver has to cope with can be significantly reduced, thereby increasing the capacity of the overall system. So Space- Time Processing is the minimization of fading and MAI through the integrated use of multiple antennas , advanced signal processing techniques , advanced receiver structures and forward error correction.

From the definition it is clear that techniques such as SFIR,HSR, SDMA and various others are all different forms of space- time processing where the emphasis of the space-time processing technique is on different ways to reduce fading and MAI , these as follows:

2.2.1 High Sensitivity Reception (HSR)

It refers to the use of adaptive antenna arrays in the uplink of a cellular network to focus the antenna beam on a specific user, thereby increasing the antenna gain in the direction of the user and suppressing transmissions received from interfering users. In the case of TDMA and FDMA systems the HSR system may use pencil antenna beams to focus on the active users, whereas in CDMA systems, the HSR system can be increase the SNR in the uplink by introducing nulls in the antenna pattern in the direction of strong interfering signals.

In the same manner to HSR, spatial filtering for interference reception (SFIR) can be used in the downlink of a cellular system to focus all the energy radiated by the base station onto a single user or cluster of users. Where as HSR and SFIR techniques increase cellular spectral efficiency by decreasing the total co-channel interference levels in a cell, SDMA techniques increase cellular spectral efficiency by decreasing $A_{cluster}$. In other words, the same physical cellular network resources can be re-used more often.

2.2.2 Space division multiple access (SDMA)

It is a multiple access technique which enables two or more subscribers, affiliated to the same base station, to use the same Time, Frequency and Code (T/F/C) resources on the grounds of their physical location or spatial separation. The overall system gains that can be achieved with the techniques described above depend heavily on the type of cellular structure employed. A plethora of different cellular structures has been defined in the literature [136, 169]. Among these, the best known are macro-cells, micro-cells, Pico cells and hierarchical cells.

2.2.3 Smart Antennas

Are the combinations of antennas with signal processing algorithms to yield an antenna system with dynamic properties. These dynamic properties may, for example be a radiation pattern those changes according to the motion of the mobile. Based on these

definitions the main aim of space –time techniques for mobile systems is to maintain an acceptable level of error performance and, hence to maximize the signal to interference and noise ratio (SINR) for each user in the system.

2.3 Space- Time Base stations

A base station with space-time techniques can take on many different forms. In its simplest form, multiple antennas at the base station may be used to form multiple fixed beams to cover the whole cell site. For example three beams with a beam width of 120° each or six beams with a beam width of 60° each may be used. Each beam may then be treated as a separate cell and the frequency assignment may be performed in the usual manner, with mobiles handed to the next beam as they leave the area covered by the current beam, using the normal hand –off process when a mobile crosses a cell boundary.

To realize such a base station, the ability to locate and track mobiles would be required in order to adapt the system parameters to meet traffic requirements. Another important technology related to dynamic or adaptive beamforming is so- called Intelligent technology .This technology allows cell shapes and sizes to be changed based upon traffic conditions, channels to be assigned dynamically as per traffic need , and transmitter power to be adapted according to receiver requirements.

In contrast to steering beams toward the desired mobile, one may adjust the antenna pattern so that it has nulls toward other mobiles, thereby reducing interference. Formation of nulls in the antenna pattern toward co-channel mobiles helps to reduce the co-channel interference in two ways. In transmit mode, less energy is transmitted from the base toward these mobiles, thereby reducing the interference from the base station. In receive mode, this helps to reduce the interference contribution from these mobiles.

2.4 Space- Time Mobiles

Due to space limitations on current mobile phones, implementation of space-time techniques is not yet reality .It is expected that this will change in future as new antenna structures and more power efficient digital signal processors become available. However, not only mobile phones will be available in the near future .Other types of mobile terminals, e.g. notebook type terminals, will incorporate space-time processing techniques.

2.5 Advantages of Space- Time processing

Space-time techniques have the ability to improve the performance of a mobile communication system in a number of ways. Specific advantages of space-time techniques are that they yield:

- Increased capacity (spectrum efficiency) by increasing the number of active users for a given BER quality.
- Reduction of co-channel interference to improve service quality and/ or increase the frequency re-use factor. This point is especially important in CDMA –based systems in which the system capacity is interference limited.
- Reduction in delay spread and fading, by beamforming and diversity techniques, the SINR of the system can be improved in a fading environment. Related to this is the reduction of the effect of angular spreading of the received signal due to scatterers around the mobile by narrow beams being formed on the arriving signals.
- Reduction in outage probability. Outage probability is the probability of a channel being inoperative due to an increased error rate.
- Increase in transmission efficiency. Due to the high directivity and gain of the space-time system ,base station range may be extended , and a mobile may be able to transmit using less power resulting in longer battery life

- Dynamic channel assignment. Making use of SDMA, channels may be dynamically assigned as a function of the traffic demand in the cell.

2.6 Signal processing in the Antenna Array

An antenna array consists of a set of antenna elements that are spatially distributed at known locations with reference to a common fixed point [170], [171]. The antenna elements can be arranged in various geometries. Some of the popular geometrical configurations are Linear, Circular and Planar. In a linear array, the centers of the elements of the array are aligned along a straight line. In case of a circular array, the centers of the elements lie on a circle. For a planar array configuration, the centers of the array lie on a single plane. Both the linear and circular array are obviously special cases of the planar array.

The radiation pattern of an array is determined by the radiation pattern of the individual elements, their orientation and relative positions in space, and the amplitude and the phase of the feeding current [170]. If each element of the array is an isotropic point source, the radiation pattern of the array will depend solely on the geometry and feeding current of the array. In that case the radiation pattern is commonly known as the array factor. If each of the elements of the array is similar but nonisotropic, by the principle of pattern multiplication [2], the radiation pattern can be computed as a product of the array factor and the individual element pattern [172].

2.6.1 Uniform Linear Array (ULA)

If the spacing between the elements of a linear array is equal, it is known as Uniform Linear Array (ULA). Figure 2.1 shows an N element ULA. The spacing between the array elements is d and a plane wave arrives at the array from a direction θ off the array *broadside*. The array broadside is perpendicular to the line containing the center of the elements. The angle θ measured clockwise from the array broadside is called Direction of Arrival (DOA) or the Angle of Arrival (AOA) of the received signal.

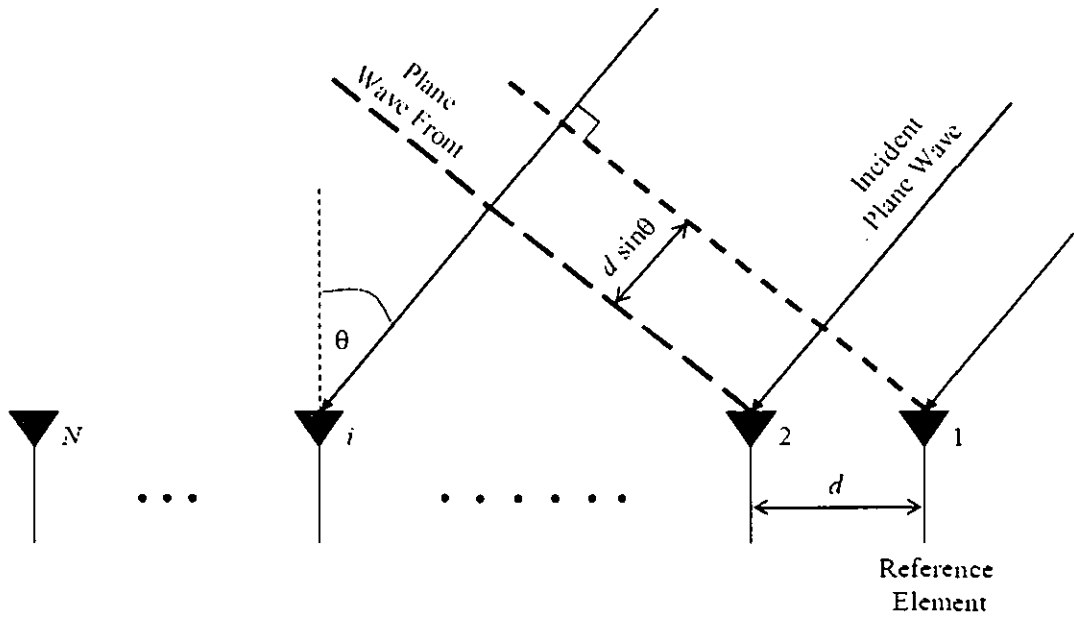


Figure 2.1: Plane wave incident on a ULA with an AOA of θ [170]

The received signal at the first element can be written as [170]

$$\tilde{x}_1(t) = A_1(t) \cos\{2\pi f_c t + \gamma(t) + \beta\}, \quad (2.1)$$

Where;

$A_1(t)$ is the amplitude of the signal

f_c is the carrier frequency

$\gamma(t)$ is the information

β is the random phase

Note that the complex envelope of the signal at the first element is given by

$$x_1(t) = A_1(t) e^{j\{\gamma(t) + \beta\}} \quad (2.2)$$

Let us assume that the signals originate far away from the array and the plane wave associated with the signal advances through a non-dispersive medium that only

introduces propagation delay. Under these circumstances, the signal at any other element can be represented by a time advanced or time delayed version of the signal at the first element. Referring to Figure 2.1, the wave front impinging on the first element travels an additional $d \sin \theta$ distance to arrive at the second element. The time delay due to this additional propagation distance is given by

$$\tau = \frac{d \sin \theta}{c} \quad (2.3)$$

Where c is the velocity of light.

So the received signal at the second element is given by

$$\begin{aligned} \tilde{x}_2(t) &= \tilde{x}_1(t - \tau) \\ &= A_1(t - \tau) \cos\{2\pi f_c(t - \tau) + \gamma(t - \tau) + \beta\} \end{aligned} \quad (2.4)$$

If the carrier frequency f_c is large compared to the bandwidth of the impinging signal, the signal maybe treated as quasi-static during time intervals of order τ and we can write

$$\tilde{x}_2(t) = A(t) \cos\{2\pi f_c t - 2\pi f_c \tau + \gamma(t) + \beta\} \quad (2.5)$$

Thus the complex envelope of the signal at the second antenna element can be written as

$$\begin{aligned} x_2(t) &= A(t) e^{j\{-2\pi f_c \tau + \gamma(t) + \beta\}} \\ &= x_1(t) e^{j\{-2\pi f_c \tau\}} \end{aligned} \quad (2.6)$$

It is thus evident from Equation 2.6 that the time delay of the signal can now be represented by a phase shift. From Equations 2.3 and 2.6, we can write

$$x_2(t) = x_1(t) e^{j\left\{-2\pi f_c \frac{d \sin \theta}{c}\right\}} \quad (2.7)$$

$$= x_1(t) e^{-j \left\{ 2\pi \frac{d}{\lambda} \sin \theta \right\}}$$

Therefore the complex envelope of the received signal at the i^{th} ($i = 1, 2 \dots N$) elements can be expressed as

$$x_i(t) = x_1(t) e^{-j \left\{ 2\pi \frac{d}{\lambda} (i-1) \sin \theta \right\}} \quad (2.8)$$

Let us define a column vector whose each element contains the received signal at the corresponding array element. Therefore the received signal vector is defined as

$$\underline{x}(t) = [x_1(t) \ x_2(t) \ \dots \ x_N(t)]^T, \quad (2.9)$$

Where T represents transpose.

We can also define

$$\underline{a}(\theta) = [1 \ e^{-j \left\{ 2\pi \frac{d}{\lambda} \sin \theta \right\}} \ \dots \ e^{-j \left\{ 2\pi \frac{d}{\lambda} (N-1) \sin \theta \right\}}]^T \quad (2.10)$$

$\underline{a}(\theta)$ is known as the array response vector or the steering vector of an ULA. The array response vector is a function of the AOA, individual element response, the array geometry and the signal frequency. We will assume that for the range of operating carrier frequency, the array response vector does not change. Since we have already fixed the geometry (Uniform Linear Array) and the individual element response (identical isotropic elements), the array response vector is a function of the AOA only. The received signal vector can now be written in a compact vector form as

$$\underline{x}(t) = \underline{a}(\theta)x(t) \quad (2.11)$$

We would like to point out that so far we have assumed that the bandwidth of the impinging signal is much smaller than the reciprocal of the propagation time across the array. This assumption, commonly known as the narrowband assumption [2] for the signal, made it possible to represent the propagation delay within the elements of the array by phase shifts in the signal. Although the narrowband model is exact for sinusoidal signals, this is usually a good approximation for a situation where the bandwidth of the signal is very small compared to the inverse of the propagation time across the array. Any deviation from the narrowband model is detrimental to the performance of a narrowband beamformer usually manifesting as a limit in the ability to null interferers [135]. In such a scenario, a wideband beamformer [2], [170] must be used. Throughout this research we will assume that the WCDMA signal satisfies the narrow band assumption. We provide with a justification next:

The delay the wave front experiences to propagate from the first element to the N^{th} element is given by

$$\tau_{\max} = \frac{(N-1)d \sin \theta}{c} \quad (2.12)$$

If the spacing between the elements is half the carrier wavelength,

$$\begin{aligned} \tau_{\max} &= \frac{(N-1)\frac{\lambda}{2}}{c} ; \max(\sin \theta) = 1 \\ &= \frac{(N-1)\frac{c}{2f_c}}{c} = \frac{(N-1)}{2f_c} \end{aligned} \quad (2.13)$$

If there are 4 elements and the carrier frequency is 2 GHz, $\tau_{\max} = \frac{3}{2 \times 2000 \times 10^6}$ seconds.

So for the WCDMA signal which has a bandwidth of 5 MHz, the ratio of the reciprocal of the maximum delay and the signal bandwidth is given by

$$\begin{aligned}\chi_{\max} &= \frac{3 \times 5 \times 10^6}{2 \times 2000 \times 10^6} \\ &= 0.0037\end{aligned}\tag{2.14}$$

Therefore the narrowband assumption holds for WCDMA signal.

2.7 Beamforming

Beamforming is the most common spatial processing technique that an antenna array can utilize. In a cellular system, the desired and the interfering signals originate from different spatial locations. This spatial separation is exploited by a beamformer which can be regarded as a spatial filter separating the desired signal from the interference. The signals from different antenna elements are weighted and summed to optimize the quality of the signal. Figure 2.2 illustrates the idea of a narrowband beamformer [2], [170], which is concentrated in the following discussion. With the proper selection of beamforming criterion, it is possible to point the beam towards the direction of the desired user and/or place nulls in the direction of the interferers.

If we have K total signals with distinct Angle of Arrival (AOA) impinging on an antenna array consisting of N elements, the received signal vector can be written as

$$\underline{x}(t) = \sum_{i=1}^K s_i(t) \underline{a}(\theta_i) + \underline{n}(t), \tag{2.15}$$

Where $s_i(t)$ is the i^{th} signal with an AOA of θ_i , $\underline{a}(\theta_i)$ is the $N \times 1$ antenna response vector for the AOA of θ_i and $\underline{n}(t)$ is the thermal noise vector. The output of the antenna array is given by

$$y(t) = \underline{w}^H(t) \underline{x}(t) \tag{2.16}$$

Here $\underline{w} = [w_1 \ w_2 \ \dots \ w_N]^T$ is the $N \times 1$ Weight vector and H denotes Hermitian transpose. The weight vector is chosen to optimize some beamforming criterion, these are Popular adaptive beamforming techniques used for weight computation, which include Minimum Mean Square Error (MMSE) [2], Maximum Signal to Interference and Noise Ratio (MSINR) [2], Maximum Signal to Noise Ratio (MSNR)[173], Constant Modulus (CMA) [135], Maximum Likelihood (ML) [2], Least Mean Square (LMS), Direct Matrix Inversion (DMI), Recursive Least Square (RLS), etc. We will discuss some of these beamforming criteria in chapter 3.

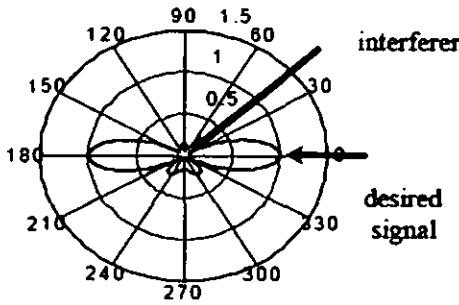
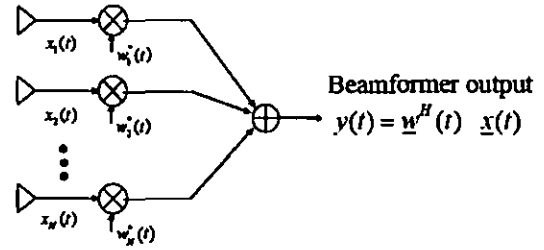


Figure 2.2b: Typical array gain pattern



$$\underline{x}(t) = \sum_{i=1}^K s_i(t) \underline{a}(\theta_i) + \underline{n}(t)$$

Figure 2.2a: Digital beamformer principle

2.7.1 Example of a Simple Beamforming (Null- Steering) with ULA

We will use a very simple example to demonstrate the principle of beamforming. Let us assume that the desired users signal is coming from the broadside of the ULA so that its AOA is 0° . Let us also assume that there is an interfering signal being received with an AOA of 45° . The array response vector for the desired user is given by:

$$\underline{a}_{desired} = \underline{a}(0) = \begin{bmatrix} 1 \\ 1 \end{bmatrix} \quad (2.17)$$

Similarly, the array response vector of the interferer is given by:

$$\underline{a}_{\text{int}} = \underline{a}\left(\frac{\pi}{4}\right) = \begin{bmatrix} 1 \\ e^{-j2\pi \times \frac{1}{2} \sin\left(\frac{\pi}{4}\right)} \end{bmatrix} = \begin{bmatrix} 1 \\ e^{-j\frac{\pi}{\sqrt{2}}} \end{bmatrix} = \begin{bmatrix} 1 \\ -0.6057 - j0.7957 \end{bmatrix} \quad (2.18)$$

A beamformer will try to increase the gain in the direction of the desired user and at the same time will try to minimize the gain in the direction of the interferer. So an *ideal weight vector* will satisfy the following criterion:

$$\begin{aligned} \underline{w}^H \underline{a}_{\text{desired}} &= 1 \\ \underline{w}^H \underline{a}_{\text{int}} &= 0 \end{aligned} \quad (2.19)$$

We can solve Equation 2.19 to get

$$\underline{w} = \begin{bmatrix} 0.5 - j0.2478 \\ 0.5 + j0.2478 \end{bmatrix}$$

The beamformer response (analogous to frequency response of an FIR filter) to a particular AOA θ is given by:

$$g(\theta) = \underline{w}^H \underline{a}(\theta) \quad (2.20)$$

The beam pattern is defined as the magnitude of $g(\theta)$, i.e.

$$G(\theta) = |g(\theta)| \quad (2.21)$$

The beam pattern which describes the array gain versus AOA for a particular weight vector is in many ways analogous to the magnitude response of an FIR filter. The beam pattern for the above example is illustrated in Figure 2.3. As we can clearly observe, the beamformer has unity gain for the desired user and a null at the direction of the interferer. Since the beamformer can place nulls in the direction of the interfering user, it is often time referred to as null steering beamformer (see section 1.1) in the literature. Note that this elementary beamforming will work only if the total number of discrete signals is equal to or less than the number of elements. In fact a beamformer with N elements can

steer $N - 1$ nulls which makes it unsuitable for a CDMA cellular environment. When the number of incident signals exceeds the number of antenna elements, the array is called overloaded. However the processing gain of the CDMA receiver is a big ally against the overloading of an array and spatial diversity gain can improve the performance the antenna array.

We can also make the following observations from the simple beamforming example:

- Even though we have placed a null at the direction of the interferer, the antenna gain is not maximized at the direction of the desired user. So we can employ more refined beamforming criterion. We will discuss some of these beamforming criteria in the next chapter.
- We have implicitly assumed that have a priori knowledge of the array response vectors corresponding to different users. In an urban cellular environment, each resolvable multipath may be comprised of several unresolved components coming from significantly different angles. In such case, it is not possible to associate a discrete (AOA) with a signal impinging the antenna array and the knowledge of the array response vector may not be very reliable. It is also necessary to estimate the (AOA) to find the array response vector. But one of the key assumptions all high resolution (AOA) estimation techniques require is that the number of signal wave fronts including co-channel interference signals must be less than the number of elements in the array. This is not a very realistic scenario for a commercial CDMA system. Eigen-Beamforming techniques, discussed in the next chapter, can be an effective solution since they do not need apriori knowledge of the array response vectors, even so there is no need to explicitly estimate the (AOAs).

We have used the beam pattern to illustrate the working principle of the elementary null-steering beamformer. However one should not put too much importance on the beam pattern as it only describes the magnitude response of the beamformer and does not

provide any information of the phase. The weight vector is intended to satisfy a particular beamforming criterion. A MSINR weight vector for example, will maximize the output SINR and the beam pattern may not show a high gain at the (AOA) of the desired user or a null at the (AOA) of the interferer. This is especially true in a multipath environment when the array response vector is replaced by the composite channel vector.

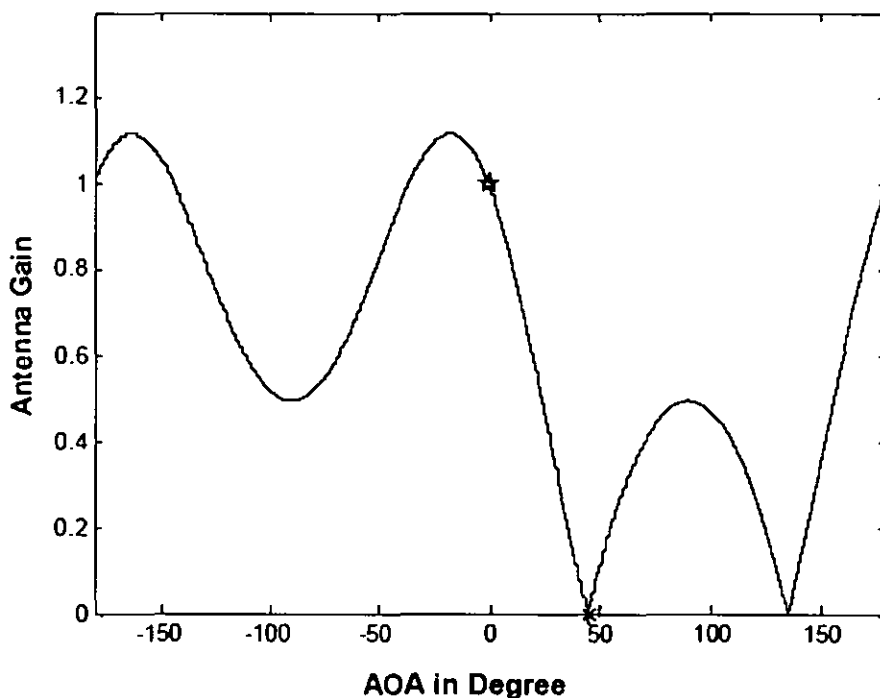


Figure 2.3: Beam pattern for the elementary beamformer. The AOA of the desired user is 0° and the AOA of the interferer is 45° [1]

2.8 Array Ambiguity

Let us consider the array response vector of a ULA given by Equation 2.10. It is obvious that any two AOAs θ_1 and θ_2 related as $\theta_2 = \pi - \theta_1$ will have the same array response vector i.e. $\underline{a}(\theta_1) = \underline{a}(\theta_2)$. As a result it is impossible for a ULA to distinguish between the desired signal coming from the direction θ_1 and an interfering signal coming from the direction θ_2 . This ambiguity makes it impossible to place a null in the direction of the

interferer without nulling the desired signal itself. Any linear array suffers from this ambiguity although the relation between the ambiguous AOAs depends on the inter-element spacing. This ambiguity can be avoided if sectorization [3] is employed and/or the individual elements are not isotropic. Throughout this work we will assume that the cellular system employs a 3 sector per cell arrangement which is a valid assumption for WCDMA systems.

2.9 Spatial Sampling Theorem

Theorems applied to the FIR filter in the time domain may sometimes also be applied to an ULA in the spatial domain because of the analogous relation between an FIR filter and an ULA [189]. In the time/frequency domain, the Nyquist sampling theorem [4] states that for a band limited signal with highest frequency f , the signal is uniquely determined by its discrete time samples if the sampling rate is equal to or greater than $2f$. If the sampling rate is less than $2f$, there will be aliasing. Similarly to avoid spatial aliasing, the beamformer must satisfy the following criterion [135], [170]

$$d \leq \frac{\lambda}{2} \quad (2.22)$$

This is known as the Nyquist sampling theorem in the spatial domain. Therefore to perform beamforming without spatial aliasing, the element spacing of the array must be less than or equal to half of the carrier wavelength. (Note that the ambiguity resulting from the spatial aliasing is different from the ambiguity that mentioned in section 2.8) However the element spacing cannot be made arbitrarily small because of mutual coupling effects between elements. As a result, in a practical beamformer, the antenna elements are spaced close to half wavelength so that the spatial aliasing is avoided and the mutual coupling effect is minimized as well. For the beamformers employed in this work, we assume that the element spacing of the ULA is at half of the carrier wavelength unless explicitly mentioned otherwise.

2.10 Spatial Diversity Gain

The adaptive antenna array can achieve spatial diversity and mitigate multipath fading. This is in addition to the interference cancellation attained from steering beams towards the desired user and/or steering nulls in the direction of interferers. The signal envelopes observed across the elements of an antenna array should have very little cross-correlation in order to achieve diversity gain. As a result, if the signal at one of the elements is going through a deep fade, it is highly unlikely that the signals at the other elements are encountering that at the same time. So there is nearly always good signal reception on one of the antenna elements. Therefore combining the signals from various elements will increase the SNR and the fidelity of the received signal. This gain in SNR is termed as the spatial diversity gain. The spatial diversity gain depends mainly on two factors [22]. The cross correlation of the fading envelopes across the elements of the array and the mean power level of the signal. The lower the cross-correlation the lower the chances of the signals across various elements encountering simultaneous fades and therefore higher the diversity gain is. If the mean power level of the signals at the different elements is not equal, the element at higher power will dominate the combined output. It will be difficult to improve the SNR when the stronger branch is going through a deep fade. As a result the diversity gain is higher when the signals are received with equal mean power level on various antenna elements.

Ideally, a diversity combiner would need zero cross-correlation between signals across elements. The elements may be required to be separated by distance that is on the order of several carrier wavelengths to ensure low cross-correlation between signals across elements. Therefore the elements of a diversity combiner are not usually Nyquist-spaced. The spacing between the elements depends on the angle spread of the channel. The higher the angle spread, smaller the element spacing can be. So there is an obvious trade-off between the diversity gain and spatial aliasing while deciding on the inter-element spacing of an adaptive antenna array.

2.11 Temporal Processing: Rake Receiver for CDMA

In a frequency selective channel, there are multiple replicas (that are resolvable in time) of the transmitted signal at the receiver, traversing different multipath. These multiple copies can be combined to improve the signal to noise ratio (SNR) at the receiver. Since the signals are coming from different paths, they encounter independent fading. This means that if one of the paths is undergoing a deep fade, it is very unlikely that the signals from the other paths are also encountering fading. As a result the receiver still has a good chance to attain acceptable fidelity. In a CDMA system the receiver can employ multiple correlators to separate the multiple copies of the signal and mitigate fading. This receiver, commonly known as a Rake receiver [3], (see figure 2.4a), has been extensively employed by the second generation CDMA based cellular systems like the IS-95. Temporal processing by the Rake receiver lets the CDMA system exploit multipath diversity (see figure 2.4b) and makes it inherently resistant to fading. There are different techniques that can be applied to combine the output of the correlators. If the combining weights are matched to the discrete channel gain coefficients corresponding to the respective multipath components, it is called Maximal Ratio Combining (MRC). MRC is a coherent combining scheme. For non-coherent combining, all the weights can be set equal and this is termed as Equal Gain Combining (EGC). Both the MRC and the EGC are intended to improve SNR. However it is also possible to set the combining weights such that SINR instead of SNR is maximized

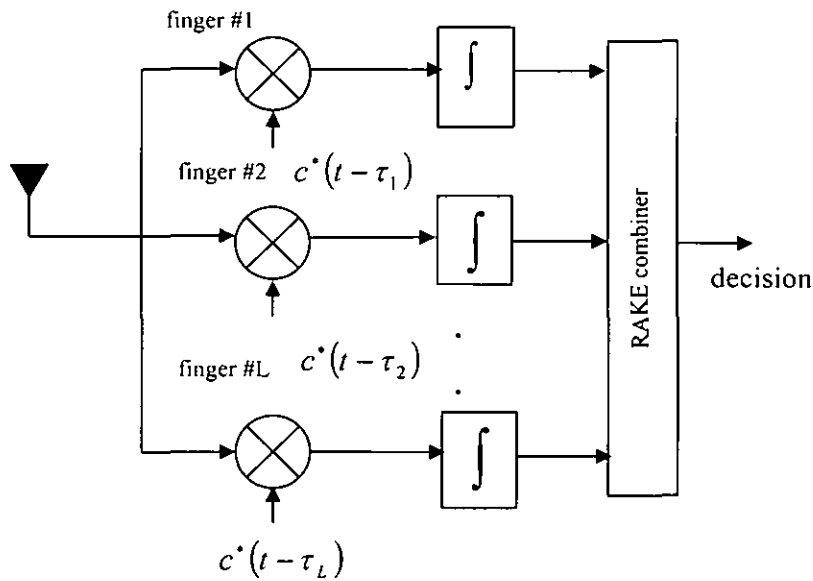


Figure 2.4a: Rake Receiver [3]

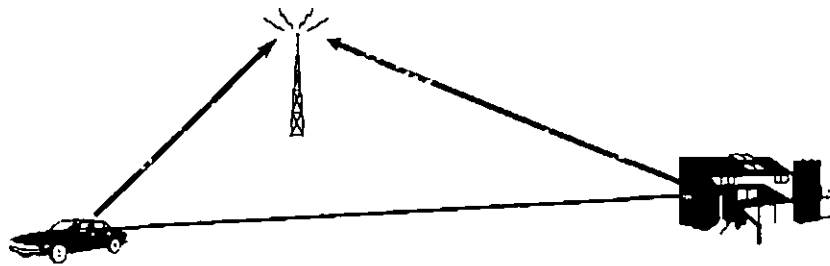


Figure 2.4b: Multipath diversity

2.11.1 Combining Techniques for Improved SNR

Different combining techniques can be implemented to improve the SNR with spatial diversity. The most common strategies are Selection Diversity, Maximal Ratio Combining and Equal Gain Combining. These techniques are equally applicable to temporal diversity, in other words they can be applied for combining signals from different fingers of a Rake receiver.

2.11.1.1 Selection Combining (SC)

At any given instant, the receiver selects only the signal from one antenna element. In the ideal case, the receiver would select the element with the best SNR. However this means additional system complexity as the receiver would need to measure and monitor the instantaneous SNR at all the elements continuously. One practical solution is to monitor the SNR of the current branch and then switch to other branch if the SNR gets below some threshold. This is often known as switched diversity [22].

2.11.1.2 Maximal Ratio Combining (MRC)

The co-phased desired signal from each antenna element is combined after weighting them by the individual branch SNR. MRC provides the maximum SNR if the interference and noise is “white”. However this scheme requires continuous measurement and monitoring of the instantaneous SNR at all the branches. This is the combining scheme that has been employed through out this work for temporal combining.

2.11.1.3 Equal Gain Combining (EGC)

The signals from different branches are co-phased and added together. This eliminates the need to estimate the SNR at each branch. However there is approximately 1dB performance penalty compared to MRC [22], [155].

2.12 Beamformer –Rake Receiver

A Beamformer-Rake [1] or 2-D Rake Receiver or Concatenated Space-Time Processor (CSTP) all gives the same name of our receiver, in which cascades a beamformer with Rake reception to process the signal both in the spatial and the temporal domain. For each finger of the temporal Rake processor, there is a beamformer to improve the fidelity of the signal of that particular branch. Figure 2.5 illustrates the structure and operating principle of a Beamformer-Rake. At the front end of the receiver is an antenna array. The signals from the array are fed into a set of spatial combiners that perform beamforming

for different multipath and each weight vector accentuates the signal from a particular multipath component of the desired user. A temporal combiner follows the spatial combiner where the contribution from different multipath (from their corresponding spatial combiner) is combined to exploit the multipath diversity. We will discuss briefly the structure and operational functional block of this receiver in chapter 7.

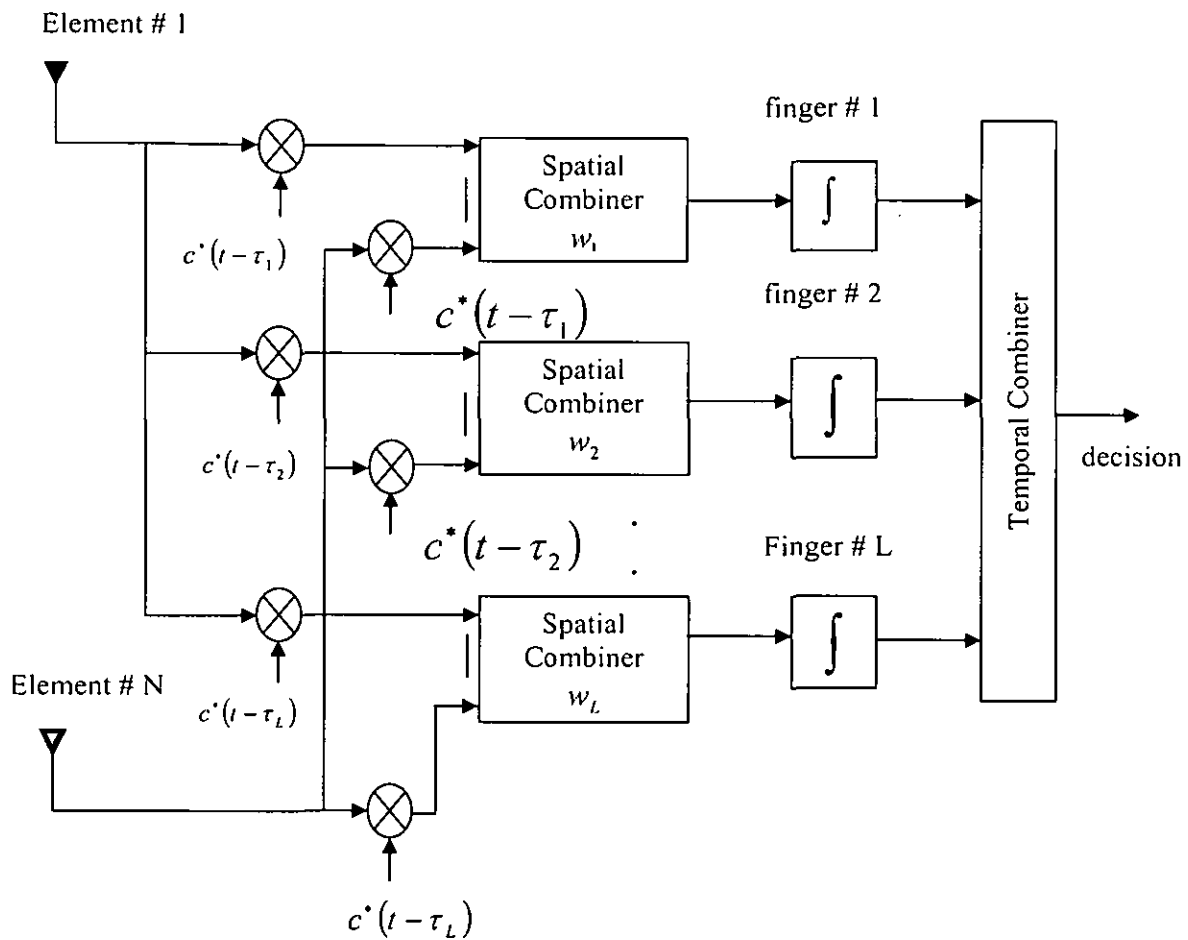


Figure 2.5a: Beamformer-Rake structure (CSTP) [1]

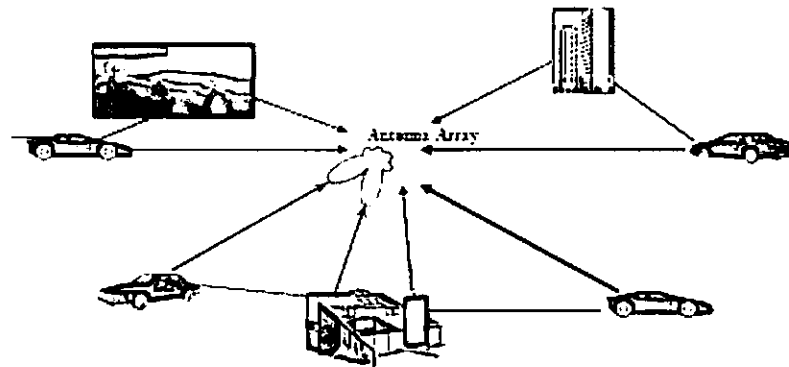


Figure 2.5b: Different weight vector accentuates different multipath component of the desired user [1]

2.13 Summary

This chapter presented an overview of the fundamental concepts of our space-time processing on CDMA system, also presented an overview of smart antenna array and provided a mathematical analysis of the signal at the output of the smart antenna array and discussed relevant terminologies and concepts related to antenna array and adaptive beamforming. The correspondence between a narrowband beamformer and finite impulse response (FIR) filter was introduced. The description of temporal processing in the form of Rake receiver and its combining techniques for improving SNR was presented. The performance improvement that can be achieved with the application of a beamformer-Rake which enjoys the collective benefit of the temporal and spatial processing none of their individual weaknesses was introduced.

CHAPTER THREE

BEAMFORMING CRITERION

3.1 Introduction

In this chapter we describe different techniques that can be applied for beamforming in a CDMA based cellular environment. The four beamforming criteria discussed in this chapter are the Maximum Signal to Noise Ratio (MSNR), the Maximum Signal to Interference Ratio (MSIR), the Maximum signal to Interference and Noise Ratio (MSINR) and the Minimum Mean Square Error (MMSE). The chapter starts with the formulation of the MSNR solution as a Simple Eigenvalue problem (SE). We present a discussion on MSIR in which the weight vectors are chosen to maximize the output signal to-interference ratio (SIR) [2]. We then go on to discuss the MSINR beamforming criterion and formulate that as a Generalized Eigenvalue problem (GE). The MMSE based beamforming comes next. We end the chapter with a discussion on adaptive beamforming algorithms (blind and non-blind algorithms).

3.2 MSNR Beamforming

The MSNR beamforming criterion as the name suggests is intended to maximize the Signal to Noise Ratio (SNR) at the output of the beamformer. In the literature, it is often termed as the conventional beamformer (see section 1.1 for detail references). The weight vector that maximizes the SNR is the *principal eigenvector* of the covariance matrix of the desired signal. If the interference and noise is spatially white, this is the optimum beamforming.

3.2.1 Maximizing the Signal to Noise Ratio

Let us consider the case of maximizing the Signal to Noise Ratio (SNR) of the desired signal in *white* noise. . The received signal can be written as

$$\underline{x} = \underline{s} + \underline{n} \quad (3.1)$$

Here \underline{s} and \underline{n} are the $N \times 1$ desired signal vector and complex additive Gaussian noise vector respectively with N being the number of antenna elements. The noise is zero mean and the covariance is given by

$$\underline{\underline{R}}_{nn} = E[\underline{n}(t)\underline{n}^H(t)] = \sigma_n^2 I_N \quad (3.2)$$

where σ_n^2 is the noise variance. Equation 3.2 implies that the noise is spatially white. Let us for the time being further assume that the noise is temporally white also so that

$$E[\underline{n}(t_1)\underline{n}^H(t_2)] = \sigma_n^2 I_N \delta(t_1 - t_2) \quad (3.3)$$

Now the power of the desired signal at the output of the beamformer, assuming that the signal is a zero mean stationary process, is given by

$$\begin{aligned} P_s &= E\left(\left\|\underline{w}^H \underline{s}\right\|^2\right) \\ &= E\left(\underline{w}^H \underline{s} \underline{s}^H \underline{w}\right) \\ &= \underline{w}^H E\left(\underline{s} \underline{s}^H\right) \underline{w} \\ \Rightarrow P_s &= \underline{w}^H \underline{\underline{R}}_{ss} \underline{w} \end{aligned} \quad (3.4)$$

Here $\underline{\underline{R}}_{ss} = E\left(\underline{s} \underline{s}^H\right)$ is the covariance matrix of the desired signal vector \underline{s} and \underline{w} is the $N \times 1$ antenna weight vector.

Similarly, the power of the noise at the output of the beamformer is

$$\begin{aligned}
P_n &= E\left(\left\|\underline{w}^H \underline{n}\right\|^2\right) \\
&= \underline{w}^H \underline{R}_{nn} \underline{w} \\
&= \sigma_n^2 \underline{w}^H \underline{w}
\end{aligned} \tag{3.5}$$

Therefore the SNR at the beamformer output is given by

$$SNR = \frac{\underline{w}^H \underline{R}_{ss} \underline{w}}{\sigma_n^2 \underline{w}^H \underline{w}} \tag{3.6}$$

To find the optimum weight vector that maximizes the SNR, we take the derivative of the right hand side of Equation 3.6 with respect to \underline{w}^H and set it equal to a null vector. Therefore we get,

$$\begin{aligned}
\frac{(\underline{w}^H \underline{w}) \underline{R}_{ss} \underline{w} - (\underline{w}^H \underline{R}_{ss} \underline{w}) \underline{w}}{(\underline{w}^H \underline{w})^2} &= \underline{0} \\
\Rightarrow \underline{R}_{ss} \underline{w} &= \left[\frac{\underline{w}^H \underline{R}_{ss} \underline{w}}{\underline{w}^H \underline{w}} \right] \underline{w}
\end{aligned} \tag{3.7}$$

The value of $\frac{\underline{w}^H \underline{R}_{ss} \underline{w}}{\underline{w}^H \underline{w}}$ is bounded by the minimum and the maximum eigenvalue of the symmetric matrix \underline{R}_{ss} [2], the maximum eigenvalue λ_{\max} satisfying

$$\underline{R}_{ss} \underline{w} = \lambda_{\max} \underline{w} \tag{3.8}$$

is the maximum value of the SNR. The eigenvector \underline{w}_{MSNR} corresponding to λ_{\max} is the optimum weight vector that maximizes the SNR at the output of the antenna array.

So, the MSNR solution for the optimum weight vector is given by the principal eigenvector (the eigenvector corresponding to the maximum eigenvalue) of the following Simple Eigenvalue problem (SE):

$$\underline{R}_{ss} \underline{w}_{MSNR} = \lambda_{\max} \underline{w}_{MSNR} \quad (3.9)$$

This type of MSNR based beamforming is often known as Eigen-Beamforming for obvious reason.

If we could assign a single AOA θ_d to the desired signal, the desired signal vector can be written as,

$$\underline{s}(k) = d(k) \underline{a}(\theta_d), \quad (3.10)$$

where d is the desired symbol, k is the sample index and $\underline{a}(\theta_d)$ is the array response vector for an AOA of θ_d . So we can write

$$\underline{R}_{ss} = E(\|\underline{d}\|^2) \underline{a}(\theta_d) \underline{a}^H(\theta_d). \quad (3.11)$$

So from Equation 3.9, we can write

$$E(\|\underline{d}\|^2) \underline{a}(\theta_d) \underline{a}^H(\theta_d) \underline{w}_{MSNR} = \lambda_{\max} \underline{w}_{MSNR} \quad (3.12)$$

By defining $\zeta = \frac{E(\|\underline{d}\|^2) \underline{a}^H(\theta_d) \underline{w}_{MSNR}}{\lambda_{\max}}$, the MSNR weight vector is given by

$$\underline{w}_{MSNR} = \zeta \underline{a}(\theta_0). \quad (3.13)$$

A similar expression can be derived for a scenario when a resolvable path is a summation of several unresolvable paths with distinct AOAs. The array response vector is replaced by the channel vector.

Equation 3.13 makes sense intuitively. Since there is no particular directivity or spatial structure associated with the noise, co-phasing the received signals from different antenna elements will maximize the SNR. It also suggests that MSNR beamforming could be implemented with the help of any high resolution direction finding (DF) technique [66-101] However DF techniques are not applicable for a large number of propagation conditions. Moreover the direction finding techniques usually require that the number of

signal wave fronts including the co-channel interference signals be less than the number of antenna elements in the antenna array [1]. This is not a realistic scenario for a commercial, especially CDMA based, cellular system.

3.2.2 Alternate SE for MSNR Beamforming

Observation of Equation 3.9 indicates that we will need an estimate of the covariance matrix of the desired signal, $\underline{\underline{R}}_{ss}$ to perform the Eigen-Beamforming. However it may be difficult to separate the signal from the noise to form an estimate $\underline{\underline{R}}_{ss}$ of and if we could separate the signal from the noise, we might not require beamforming. However there is an alternative technique that would not require estimating the desired signal covariance matrix. If the desired signal is independent of the noise, the received signal covariance matrix can be written as

$$\underline{\underline{R}}_{xx} = \underline{\underline{R}}_{ss} + \sigma_n^2 I_N \quad (3.14)$$

So the Received Signal to Noise Ratio is given by

$$RSNR = 1 + SNR \quad (3.15)$$

It is obvious from Equation 3.15 that maximizing the RSNR will maximize the SNR. If we follow the same procedure detailed by Equation 3.4 to 3.9 we get that the weight vector that maximizes the SNR is given by the principal eigenvector of the following SE:

$$\underline{\underline{R}}_{xx} \underline{\underline{w}}_{MSNR} = \lambda \underline{\underline{w}}_{MSNR} \quad (3.16)$$

The principal eigenvector of the covariance matrix $\underline{\underline{R}}_{xx}$ constitutes a single dimensional signal and noise subspace. The remaining eigenvectors corresponding to $N-1$ equal eigenvalues constitute a non-unique orthonormal basis to the noise-only subspace which is orthogonal to the signal and noise subspace. So by applying the weight, the beamformer

takes a projection of the signal to a subspace (the signal and noise subspace) that is orthogonal to the noise-only subspace.

If the noise is stronger than the desired signal, the maximum eigenvalue does not correspond to the desired signal and as a result the principal eigenvector of Equation 3.16 is not the MSNR weight vector. However in a CDMA environment, such a scenario is not very likely to occur because of the processing gain and the power control mechanism. The CDMA receivers are equipped with a bank of correlators and the output of the correlators contain the narrowband desired signal and in-band interference and noise (typically not very large compared to the desired signal because of the CDMA processing gain). Therefore the covariance matrix can be formed at the output of the CDMA correlators to formulate the required SE for the MSNR solution.

In the previous analysis we have rather conveniently consolidated the entire undesired signal as noise and assumed it to be white. We could split the noise component of Equation 3.1 into two different components so that

$$\underline{n} = \underline{n}' + \underline{i}' \quad (3.17)$$

where \underline{n}' is spatially and temporally white noise and \underline{i}' is the interference. In this scenario if the interference is white, MSNR weight is the optimum weight vector. But if the interference is not white, the eigenvector corresponding to the maximum eigenvalue of the received signal does not correspond to the MSNR weight vector. However this is a moot point since the spatial structure of the interference requires to be taken into account and the optimum weigh vector will be the weight that maximizes the Signal to Interference and Noise Ratio (SINR). We will discuss maximum SINR (MSINR) based Eigen-Beamforming a little later in this chapter.

3.2.3 Phase Ambiguity in Eigen-Beamforming

Before we move on to other beamforming techniques, we would like to point out a potential drawback of Eigen-Beamforming techniques commonly known as the phase

ambiguity. Since the beamformer is intended to maximize the SNR (or the SINR as we will see shortly), there is no constraint on the beamformer to preserve the phase of the signal. The MSNR weight vector maximizes the SNR $\frac{\underline{w}^H \underline{R}_{ss} \underline{w}}{\sigma_n^2 \underline{w}^H \underline{w}}$ and is the principal eigenvector of the SE given by Equation 3.9

The SNR at the output of the beamformer is given by

$$SNR_{\max} = \frac{\underline{w}_{MSNR}^H \underline{R}_{ss} \underline{w}_{MSNR}}{\sigma_n^2 \underline{w}_{MSNR}^H \underline{w}_{MSNR}} \quad (3.18)$$

Let us see what the SNR would be if the beamformer employs a weight vector $\hat{\underline{w}} = \rho \underline{w}_{MSNR}$ where ρ is a complex scalar. The SNR at the output of the beamformer is given by

$$\begin{aligned} SNR' &= \frac{\hat{\underline{w}}^H \underline{R}_{ss} \hat{\underline{w}}}{\sigma_n^2 \hat{\underline{w}}^H \hat{\underline{w}}} \\ &= \frac{(\rho \underline{w}_{MSNR})^H \underline{R}_{ss} (\rho \underline{w}_{MSNR})}{\sigma_n^2 (\rho \underline{w}_{MSNR})^H (\rho \underline{w}_{MSNR})} \\ &= \frac{|\rho|^2 \underline{w}_{MSNR}^H \underline{R}_{ss} \underline{w}_{MSNR}}{\sigma_n^2 |\rho|^2 \underline{w}_{MSNR}^H \underline{w}_{MSNR}} \\ &= \frac{\underline{w}_{MSNR}^H \underline{R}_{ss} \underline{w}_{MSNR}}{\sigma_n^2 \underline{w}_{MSNR}^H \underline{w}_{MSNR}} \\ &= SNR_{\max} \end{aligned} \quad (3.19)$$

Therefore the weight vector $\hat{\underline{w}}$ also maximizes the SNR and there is no way to guarantee that the solution of the SE will preserve the phase. Similar phase ambiguity is present for MSINR based Eigen-beamforming. As a result Eigen-Beamforming is applicable where

- there is no phase modulation
- non-coherent detection is possible
- pilot assisted coherent detection is possible

Since the WCDMA uplink has pilot symbols in the DPCCH, it is possible to perform Eigen-Beamforming at the WCDMA reverse link.

3.3 MSIR Beamforming

In this performance criterion, the weights vectors can be chosen to maximize the output Signal to-interference ratio (SIR) [2]. Let the vector of the desired signal sampled at the array element input is $s(k)$, the ratio of the output signal power is σ_s^2 and the total interfering signal power is σ_u^2 . The output signal power of the beamformer can be expressed as

$$\begin{aligned}
 \sigma_s^2 &= E \left[\left| w^H s(k) \right|^2 \right] \\
 &= E \left[\left\{ w^H s(k) \right\} \left\{ w^H s(k) \right\}^* \right] \\
 &= w^H E \left\{ s(k) s(k)^H \right\} w \\
 &= w^H R_{ss} w
 \end{aligned} \tag{3.20}$$

Where $R_{ss} = E \left[s(k) s(k)^H \right]$ is the covariance matrix of the array element input for the desired user. Similarly, the output interfering power σ_u^2 can be written as

$$\begin{aligned}
 \sigma_u^2 &= E \left[\left| w^H u(k) \right|^2 \right] \\
 &= E \left[\left\{ w^H u(k) \right\} \left\{ w^H u(k) \right\}^* \right] \\
 &= w^H E \left\{ u(k) u(k)^H \right\} w \\
 &= w^H R_{uu} w
 \end{aligned} \tag{3.21}$$

where $R_{uu} = E[u(k)u(k)^H]$ is the covariance matrix of the array element input for the interferes. The output SIR, $(SIR)_0$ is given by

$$(SIR)_0 = \frac{\sigma_s^2}{\sigma_u^2} \quad (3.22)$$

$$= \frac{w^H R_{ss} w}{w^H R_{uu} w}$$

To find out the optimum weight vector that maximizes the output SIR, the derivative of the right hand side of equation 3.22 is taken with respect to w^H and set equal to zero as:

$$\frac{(w^H R_{uu} w) R_{ss} w - (w^H R_{ss} w) R_{uu} w}{(w^H R_{uu} w)^2} = 0$$

or

$$R_{ss} w = \frac{w^H R_{ss} w}{w^H R_{uu} w} R_{uu} w \quad (3.23)$$

Equation 3.23 appears to be a joint eigenvalue problem. The value of $\frac{w^H R_{ss} w}{w^H R_{uu} w}$ is bounded by the minimum and maximum eigenvalue of the symmetric matrix $R_{uu}^{-1} R_{ss}$. The maximum eigenvalue λ_{\max} satisfying

$$R_{uu}^{-1} R_{ss} w = \lambda_{\max} w \quad (3.24)$$

The optimum weight vector w_{opt} is obtained by finding the largest eigenvalue λ_{\max} of the symmetric matrix $R_{uu}^{-1} R_{ss}$. Therefore,

$$R_{ss} w_{opt} = SIRR_{uu} w_{opt} \quad (3.25)$$

where the optimum value of SIR is λ_{\max} . Since $R_{ss} = E[d^2(k)]a(\theta)a^H(\theta)$, the optimum weight vector can be expressed in terms of the Winner solution as follow:

$$w_{opt} = \beta_{SIR} R_{uu}^{-1} a(\theta) \quad (3.26)$$

$$\text{Where } \beta_{SIR} = \frac{E[d^2(k)]}{SIR} a^H(\theta) w_{opt} \quad (3.27)$$

In which β_{SIR} is a scalar coefficient. This equation gives the expression for the optimum weight vectors for SIR.

3.4 MSINR Beamforming

In this section we introduce the idea of Eigen-Beamforming resulting from the Maximum Signal to Interference and Noise Ratio (MSINR) criterion for beamforming. In the literature, it is often termed as the optimal beamformer (see section 1.1 for detail references). In the previous section we discussed the MSNR beamforming criterion which is optimum only if the interference and noise is spatially white. In a WCDMA system, the users will have different data rate i.e. different spreading factors. At the same time they will have different target Bit Error Rate (BER). As a result some of the higher data rate users might be required to operate at a higher power level compared to their lower data rate counterparts and the interference is not spatially white. Under these operating conditions, the MSINR beamforming is the optimum beamforming criterion. Unlike the MSNR beamforming criterion that leads to a simple eigenvalue problem, the MSINR beamforming results in a Generalized Eigenvalue problem (GE). In addition to the signal covariance matrix, the interference and noise covariance matrix becomes a factor in order to fine tune the weight according to the spatial distribution of the interference and noise.

3.4.1 Maximizing the Signal to Interference and Noise Ratio

Let us write the received signal vector as

$$\underline{x} = \underline{s} + \underline{u} \quad (3.28)$$

where \underline{s} is the desired signal and \underline{u} is the undesired signal which comprises of interference and thermal noise.

The power of the desired signal at the output of the antenna array after combining is given by Equation 3.4 which is repeated for convenience,

$$P_s = \underline{w}^H \underline{R}_{ss} \underline{w} \quad (3.29)$$

Here $\underline{R}_{ss} = E(\underline{s}\underline{s}^H)$ is the covariance matrix of the desired signal vector \underline{s}

Similarly, the power of the undesired signal at the output of the antenna array is

$$P_u = E\left(\left\|\underline{w}^H \underline{u}\right\|^2\right) = \underline{w}^H \underline{R}_{uu} \underline{w} \quad (3.30)$$

with $\underline{R}_{uu} = E(\underline{u}\underline{u}^H)$ being the covariance matrix of the interference and noise signal vector \underline{u} .

So the output Signal to Interference and Noise Ratio (SINR) is

$$SINR_{out} = \frac{\underline{w}^H \underline{R}_{ss} \underline{w}}{\underline{w}^H \underline{R}_{uu} \underline{w}} \quad (3.31)$$

To find the optimum weight vector that maximizes the output SINR, we have to take the derivative of the right hand side of Equation 3.31 with respect to \underline{w}^H and set it equal to a null vector. Therefore,

$$\underline{R}_{ss} \underline{w} = \left(\frac{\underline{w}^H \underline{R}_{ss} \underline{w}}{\underline{w}^H \underline{R}_{uu} \underline{w}} \right) \underline{R}_{uu} \underline{w} \quad (3.32)$$

The value of $\frac{\underline{w}^H \underline{R}_{ss} \underline{w}}{\underline{w}^H \underline{R}_{uu} \underline{w}}$ is bounded by the minimum and the maximum eigenvalue of the symmetric matrix $\underline{R}_{uu}^{-1} \underline{R}_{ss}$ [2]. The maximum eigenvalue λ_{\max} satisfying

$$\underline{R}_{uu}^{-1} \underline{R}_{ss} \underline{w} = \lambda_{\max} \underline{w} \quad (3.33)$$

is the optimum (maximum) value of the SINR. The eigenvector \underline{w}_{MSINR} corresponding to λ_{\max} is the optimum weight vector that maximizes the SINR at the output of the antenna array.

So, the MSINR solution for the optimum weight vector is given by the principal eigenvector (the eigenvector corresponding to the maximum eigenvalue) of the following Generalized (or joint) Eigenvalue problem (GE):

$$\underline{R}_{ss} \underline{w}_{MSINR} = \lambda \underline{R}_{uu} \underline{w}_{MSINR} \quad (3.34)$$

We can observe that the covariance matrix of the interference and noise signal has been introduced in the Eigen-Equation to take the spatial structure of the undesired signal into account. The matrix \underline{R}_{uu} can be regarded as an operator modifying the weight vector that one would otherwise obtain from solving a simple eigenvalue problem like $\underline{R}_{ss} \underline{w} = \lambda \underline{w}$. The MSINR beamforming can be viewed as a technique that maximizes the SNR for spatially colored noise, or the MSNR beamforming can be regarded as a special case of MSINR beamforming for spatially white noise.

As discussed in the previous section, if we could assign a single AOA θ_d to the desired signal, the covariance matrix of the desired signal can be written as

$$\underline{\underline{R}}_{ss} = E\left(\|d\|^2\right) \underline{a}(\theta_d) \underline{a}^H(\theta_d) \quad (3.35)$$

So from Equation 3.34, we can write

$$\underline{\underline{R}}_{uu}^{-1} \left\{ E\left(\|d\|^2\right) \underline{a}(\theta_d) \underline{a}^H(\theta_d) \underline{w}_{MSINR} \right\} = \lambda_{\max} \underline{w}_{MSINR} \quad (3.36)$$

By defining $\xi = \frac{E\left(\|d\|^2\right) \underline{a}^H(\theta_d) \underline{w}_{MSINR}}{\lambda_{\max}}$ the MSINR weight vector is given by

$$\underline{w}_{MSINR} = \xi \underline{\underline{R}}_{uu}^{-1} \underline{a}(\theta_0). \quad (3.37)$$

Once again we can observe that the interference and noise covariance matrix modifying the MSNR weight to compute the MSINR weight. The expression for the weight vector can be easily extended for a scenario when a resolvable path is a summation of several unresolvable paths with distinct AOAs.

3.4.2 Maximizing the Received Signal to Interference and Noise Ratio

If the desired signal is independent of the interference and noise, the received signal covariance matrix can be written as

$$\underline{\underline{R}}_{xx} = \underline{\underline{R}}_{ss} + \underline{\underline{R}}_{uu} \quad (3.38)$$

The Received Signal to Interference and Noise Ratio (RSINR) becomes

$$RSINR = 1 + SINR \quad (3.39)$$

So maximizing RSINR amounts to maximizing SINR and we will end up with the same set of weights. As a result we will not distinguish between the MSINR and the Maximum RSINR (MRSINR) criterion. However let us formally state the MRSINR beamforming criterion as The MRSINR solution for the optimum weight vector is given by the

principal eigenvector (the eigenvector corresponding to the maximum eigenvalue) of the following Generalized (or joint) Eigenvalue problem (GE):

$$\underline{\underline{R}}_{xx} \underline{\underline{w}}_{MRSINR} = \lambda \underline{\underline{R}}_{uu} \underline{\underline{w}}_{MRSINR} \quad (3.40)$$

Equation 3.40 offers us another insight to the property of the optimum weight vector for colored noise. In case of the MSNR based Eigen-Beamforming (the solution of the Simple Eigenvalue problem), the objective is to split the eigenspace [174] of the received signal covariance matrix into two orthogonal subspaces and then find the eigenvector that defines the subspace (signal and noise subspace) orthogonal to the noise only subspace and corresponds to the desired signal. The two subspaces in the case of the MRSINR beamforming (or equivalently MSINR beamforming) are orthogonal to each other with respect to the covariance matrix of the interference and noise signal. This permits the adjustment of the weight vector according to the spatial signature of the undesired signal.

3.5 MMSE Beamforming Criterion

The Minimum Mean Squared Error (MMSE) criterion intends to find a weight vector that will minimize the Mean Squared Error (MSE) between the combined signal and some desired (or reference) signal. The error signal can be defined as [2]

$$e(k) = d(k) - \underline{\underline{w}}^H \underline{\underline{x}}(k), \quad (3.41)$$

where d is the reference signal, $\underline{\underline{w}}$ is the antenna weight vector, $\underline{\underline{x}}$ is the received signal vector at the antenna array, k is the sample index.

So the MSE is given by:

$$J = E[\|e(k)\|^2] \quad (3.42)$$

Here E denotes the ensemble expectation operator.

Thus we can rewrite Equation 3.42 the following way.

$$\begin{aligned}
J &= E \left[\left\| d(k) - \underline{w}^H \underline{x}(k) \right\|^2 \right] \\
&= E \left[\left\{ d(k) - \underline{w}^H \underline{x}(k) \right\} \left\{ d(k) - \underline{w}^H \underline{x}(k) \right\}^* \right] \\
&= E \left[\left\| d(k) \right\|^2 - d(k) \underline{x}^H(k) \underline{w} - d^*(k) \underline{w}^H \underline{x}(k) + \underline{w}^H \underline{x}(k) \underline{x}^H(k) \underline{w} \right] \\
&= E \left[\left\| d(k) \right\|^2 \right] - \underline{r}_{xd}^H \underline{w} - \underline{w}^H \underline{r}_{xd} + \underline{w}^H \underline{R}_{xx} \underline{w}
\end{aligned} \tag{3.43}$$

where, $\underline{R}_{xx} = E[\underline{x}(k) \underline{x}^H(k)]$ is the covariance matrix of the received signal and $\underline{r}_{xd} = E[\underline{x}(k) d^*(k)]$ is the cross-correlation vector between the received signal vector \underline{x} and the reference signal d . The MSE J is minimized when the gradient vector $\nabla(J)$ is equal to a null vector. Now the gradient vector is defined as

$$\nabla(J) = 2 \frac{\partial}{\partial \underline{w}^*} \tag{3.44}$$

where $\frac{\partial}{\partial \underline{w}^*}$ is the conjugate derivative with respect to vector \underline{w} .

So we can write

$$\begin{aligned}
\nabla(J) \big|_{\underline{w}_{MMSE}} &= \underline{0} \\
-2 \underline{r}_{xd} + 2 \underline{R}_{xx} \underline{w}_{MMSE} &= \underline{0}
\end{aligned} \tag{3.45}$$

Thus we arrive at the well-known Wiener-Hopf equation [8]

$$\underline{R}_{xx} \underline{w}_{MMSE} = \underline{r}_{xd} \tag{3.46}$$

We can premultiply Equation 3.46 by \underline{R}_{xx}^{-1} and get

$$\underline{w}_{MMSE} = \underline{R}_{xx}^{-1} \underline{r}_{xd} \tag{3.47}$$

The above solution for MMSE weight is often called the Wiener solution [2]. In order to obtain the optimum weight vectors, Equation 3.47 shows the need of the knowledge of two statistics as follows:

- The covariance matrix $\underline{\underline{R}}_{xx}$ of the array input $\underline{x}(k)$, and
- The cross-correlation vector \underline{r}_{xd} between the array input vector $\underline{x}(k)$ and the reference or desired signal $d(k)$.

If the desired signal is uncorrelated with the interference and noise,

$$\underline{\underline{R}}_{xx} = \underline{\underline{R}}_{ss} + \underline{\underline{R}}_{uu} \quad (3.48)$$

Now if the desired signal had a single AOA θ_d associated with it and the reference signal was the actual desired signal,

$$\begin{aligned} \underline{\underline{R}}_{ss} &= E(\|d\|^2) \underline{a}(\theta_d) \underline{a}^H(\theta_d) \\ \underline{r}_{xd} &= E(\|d\|^2) \underline{a}(\theta_d) \end{aligned} \quad (3.49)$$

By applying Woodbury's Identity [2], we get

$$\underline{\underline{R}}_{xx}^{-1} = \left\{ \frac{1}{1 + E(\|d\|^2) \underline{a}^H(\theta_d) \underline{\underline{R}}_{uu}^{-1} \underline{a}(\theta_d)} \right\} \underline{\underline{R}}_{uu}^{-1} \quad (3.50)$$

So the MMSE weight is given by

$$\underline{w}_{MMSE} = \chi \underline{\underline{R}}_{uu}^{-1} \underline{a}(\theta_0), \quad (3.51)$$

$$\text{where } \chi = \left\{ \frac{E(\|d\|^2)}{1 + E(\|d\|^2) \underline{a}^H(\theta_d) \underline{\underline{R}}_{uu}^{-1} \underline{a}(\theta_d)} \right\}. \quad (3.52)$$

By comparing Equation 3.51 with Equation 3.37, we observe that the MMSE weight vector differs from the MSINR weight vector by a scalar. Since the SINR at the output of the beamformer does not depend on the scalar, the *MMSE* weight vector in fact maximizes *SINR*.

3.6 Adaptive Beamforming Algorithms

The previous section describes some of the beamforming criteria for calculating the optimum weight vector. In order to obtain the optimum weight vector, one needs to know the second order statistics. Since these statistics are usually unknown and change over time, adaptive beamforming algorithms are employed to estimate and update the weight vector over time. As the weight vectors are iteratively adjusted, the performance of the beamformer is closer to the desired criterion. The algorithm is said to be converged when such a performance criterion is met. Most of these algorithms can be categorized into blind and non blind algorithms according to whether a training signal is used or not, as shown in Figure 3.1. This section describes some of the adaptive beamforming algorithms [175]

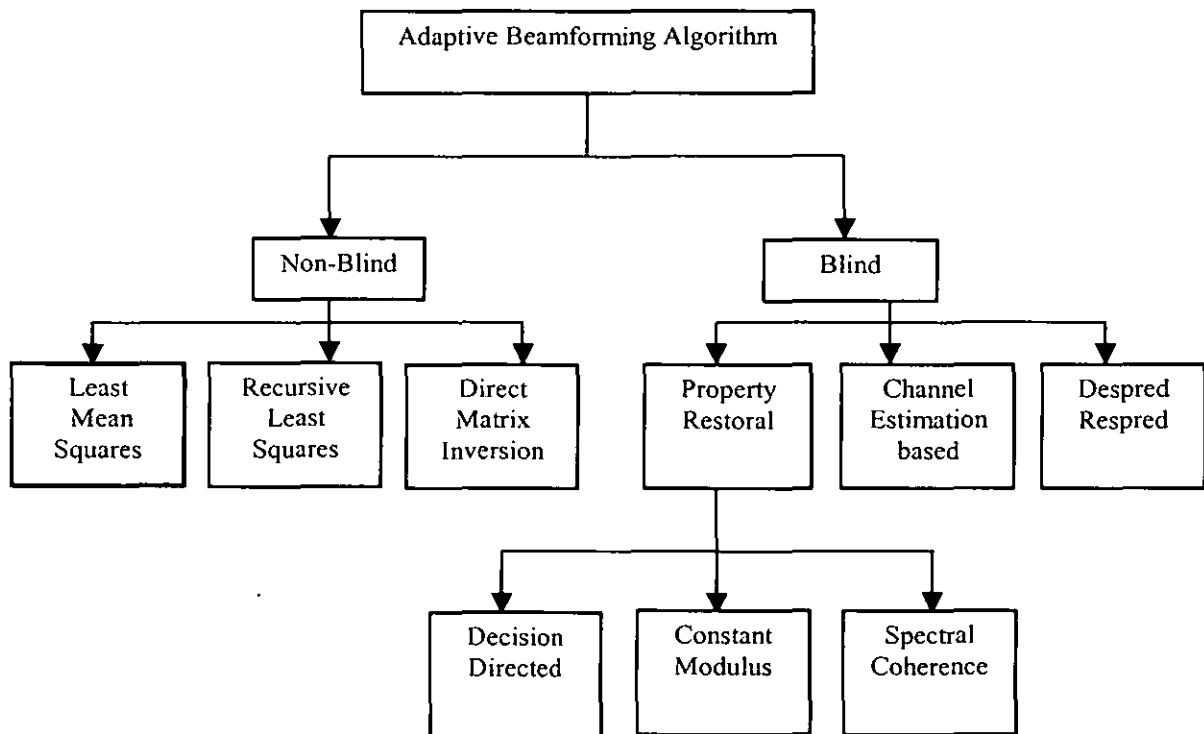


Figure 3.1: Classification of adaptive Beamforming algorithms [175]

3.6.1 Non-blind Algorithms

A training signal is used to adjust the array weight vector in non-blind adaptive algorithm. A training signal is sent from the transmitter to the receiver during the training period which is known to both the transmitter and receiver. The beamformer in the receiver uses the information of the training signal to compute the optimal weight vector. This technique requires synchronization. After the training period, data is sent and the beamformer uses the weight vector computed previously to process the received signal. The non-blind algorithms minimize the MSE between the desired signal and the array output.

3.6.1.1 Least Mean Square Algorithm (LMS)

It is obvious that an exact measurement of the gradient vector $\nabla\{J(n)\}$ as well as a judicious choice of the step size μ is required for the convergence of the steepest descent method to the optimum MMSE weight vector. However an exact measurement of the gradient vector requires prior knowledge of the covariance matrix of the received signal and the correlation vector between the received signal vector and the reference signal. As a result the gradient vector must be measured from the observed data. The Least Mean Square (LMS) algorithm proposes a very simple instantaneous estimate [102] of the gradient vector so that

$$\hat{\nabla}\{J(n)\} = -2\underline{x}(n)e^*(n) \quad (3.53)$$

The weight update equation for the LMS algorithm becomes

$$\underline{w}(n+1) = \underline{w}(n) + \mu\underline{x}(n)e^*(n). \quad (3.54)$$

The following two equations thus define the LMS algorithm:

$$\begin{aligned} e(n) &= d(n) - \underline{w}^H(n)\underline{x}(n) \\ \underline{w}(n+1) &= \underline{w}(n) + \mu\underline{x}(n)e^*(n) \end{aligned} \quad (3.55)$$

We can observe that the LMS has a computational complexity of $O(2N)$. This low computational complexity is the most attractive feature of the LMS algorithm. The response of the LMS algorithm is determined by the following three principal factors [102]:

- The step-size
- The size of the weight vector
- Eigen-value distribution of the received signal covariance matrix.

The LMS algorithm is described in detail in [102], [16].

We have shown in a previous study [176], [177] that the LMS is not a very suitable algorithm for spatial processing in a Beamformer-Rake receiver (2-D Rake Receiver). One of the reasons for this is the eigenvalue distribution of the covariance matrix of the received signal. Since the control channel has a large processing gain (because of a spreading factor of 256) the covariance matrix has a large dominant eigenvalue (corresponding to the desired signal) followed by quite small eigenvalues (corresponding to interference and noise). The LMS algorithm has difficulty to converge in such a scenario [102]. Also it has been shown that [119] the LMS based MMSE beamforming is not a very robust technique in a fast fading channel. Therefore we propose a Beamformer-Rake receiver for WCDMA uplink that computes the MMSE weight vector by employing the Direct Matrix Inversion (DMI) and/or Recursive Least Square (RLS) techniques outlined in the coming sections.

3.6.1.2 Normalized Least Mean Square Algorithm (NLMS)

Theoretically, LMS method is the most basic method for calculating the weight vectors. However, in practice, an improved LMS method, the Normalized –LMS (NLMS) is used to achieve stable calculation and faster convergence. The NLMS algorithm can be formulated as a natural modification of the LMS algorithm based on stochastic gradient algorithm [175].

Gradient noise amplification problem occurs in the standard form of LMS algorithm. This is because the product vector $\mu \underline{x}(n)e^*(n)$ in Equation 3.54 at iteration, n applied to the weight vector $\underline{w}(n)$ is directly proportional to the input vector $\underline{x}(n)$. This can be solved by normalized the product vector at iteration $n + 1$ with the square Euclidean norm of the input vector $\underline{x}(n)$ at iteration n [175]. The final weight vector can be updated by

$$\underline{w}(n+1) = \underline{w}(n) + \frac{\mu}{\|\underline{x}(n)\|^2} \underline{x}(n)e^*(n) \quad (3.56)$$

where the NLMS algorithm reduces the step size μ to make the large changes in the update weight vectors. This prevents the update weight vectors from diverging and makes the algorithms more stable and faster converging than when a fixed step size is used.

3.6.1.3 Sample Matrix Inversion Algorithm (SMI)

The SMI method is a technique to approximate the solution to the MMSE problem. This algorithm is a block adaptive approach which uses a block of data to estimate the adaptive beamforming weight vector. The idea of SMI algorithm [2] is to estimate the covariance matrix R and the cross-correlation vector r based on the array antenna element input in an observation interval i.e.,

$$R = \sum_{n=N_1}^{N_2} x(n)x^H(n) \quad (3.57)$$

$$r = \sum_{n=N_1}^{N_2} d^*(n)x(n) \quad (3.58)$$

where N_1 and N_2 are the lower and upper limits of the observation interval respectively. The weight vector w is then calculated using the optimum Wiener solution as:

$$\underline{w}_{opt} = R^{-1}r \quad (3.59)$$

In order to allow the array antenna to adapt as the signal environment changes, the covariance matrix R and the cross-correlation vector r are estimated for each observation interval. Data that are outside the current observation interval do not have any effect on the calculation of the weight vector for the current observation interval. The rate of convergence for SMI algorithm is faster than the LMS algorithm but the algorithm is computationally complex.

3.6.1.4 Recursive Least Square Algorithm (RLS)

Unlike the LMS algorithm which uses the method of steepest-descent to update the weight vector, the RLS algorithm uses the method of least squares to adjust the weight vector [2]. In this method of least squares, the weight vector $w(n)$ is chosen to minimize a cost function that consists of the sum of error squares over a time window. On the other hand, in the method of steepest-descent, the weight vector is chosen to minimize the ensemble average of the error squares.

In the RLS algorithm, at time n , the weight vector is chosen to minimize the cost function as

$$\varepsilon(n) = \sum_{i=1}^n \lambda^{n-i} |e(i)|^2 \quad (3.60)$$

where error signal $e(i)$ is defined in Equation 3.41 and the forgetting factor λ is a positive constant close to but less than one, which determines how quickly the previous data are de-emphasized. In stationary environments, however, λ should be equal to 1, since all the data should have equal weight. The RLS algorithm is obtained from minimizing Equation 3.60 by expanding the magnitude squared and applying the matrix inversion lemma. The RLS algorithm can be described by the following equations [175]:

$$k(n) = \frac{\lambda^{-1} R(n-1) x(n)}{1 + \lambda^{-1} x^H(n) R(n-1) x(n)} \quad (3.61)$$

$$\alpha(n) = d(n) - w^H(n-1) x(n) \quad (3.62)$$

$$w(n) = w(n-1) + k(n) \alpha^*(n) \quad (3.63)$$

$$R(n) = \lambda^{-1} R(n-1) - \lambda^{-1} k(n) x^H(n) R(n-1) \quad (3.64)$$

In the above equations, $k(n)$, $\alpha(n)$ and $R(n)$ are gain vectors, estimation error and covariance matrix correspondingly. The initial value of $R(n)$ can be set to $R(0) = \delta^{-1} I$ where, I is the identity matrix, and δ is a small positive constant.

The RLS algorithm utilizes the information contained in the input data and extending back to the instant of time when the algorithm is initiated. The convergence rate is therefore an order of magnitude faster than the LMS algorithm. This improvement in the performance, however, is achieved at the expense of a large increase in computational complexity.

3.6.1.5 Direct Matrix Inversion Algorithm (DMI)

The received signal matrix can be estimated by using an L sample rectangular averaging window as

$$\hat{\underline{R}}_{xx}(n) = \frac{1}{L} \sum_{l=n-L+1}^n \underline{x}(l) \underline{x}^H(l) \quad (3.65)$$

Here $\underline{x}(l)$ is collected sample of the received signal over a block of L samples. Similarly, the cross correlation vector can be estimated as

$$\hat{\underline{r}}_{xd}(n) = \frac{1}{L} \sum_{l=n-L+1}^n \underline{x}(l) d^*(l) \quad (3.66)$$

where $\underline{x}(l)$ is collected samples of the received signal, $d^*(l)$ is the conjugate of the actual sample sent. As before the estimation is performed over a block of L samples. The DMI involves computing the inverse of the estimated received signal matrix $\hat{\underline{R}}_{xx}$ and then calculate the MMSE weight vector by applying the Wiener solution. Based on the estimates of Equation 3.65 and 3.66, the MMSE weight can be computed as

$$\underline{w}_{MMSE}(n+1) = \hat{\underline{R}}_{xx}^{-1}(n) \hat{\underline{r}}_{xd}(n) \quad (3.67)$$

Since matrix inversion requires a lot of computation, the inverse can be computed according to a *rank 1* update:

$$\begin{aligned}
 \underline{\underline{R}}_{xx}^{-1}(n) &= \underline{\underline{R}}_{xx}^{-1}(n-1) - \frac{\underline{\underline{R}}_{xx}^{-1}(n-1)\underline{x}(n)\underline{x}^H(n)\underline{\underline{R}}_{xx}^{-1}(n-1)}{1 + \underline{x}^H(n)\underline{\underline{R}}_{xx}^{-1}(n-1)\underline{x}(n)} \\
 \underline{\underline{R}}_{xx}^{-1}(0) &= \frac{1}{\varepsilon} I, \quad \varepsilon > 0
 \end{aligned} \tag{3.68}$$

The update according to Equation 3.68 is termed as the Sample Matrix Inversion (DMI) [100], [101] technique. Each iteration of Equation 3.68 requires computational complexity on the order of $O(3.5N^2 + N)$.

If the channel does not change very rapidly, it may not be necessary to estimate and update the weight for each sample and a single set of weight for a block of L samples may be adequate. For such a scenario, the received signal covariance matrix and cross-correlation vector can be estimated only once by averaging over the entire block of samples. We can then employ the Cholesky [136], [178] factorization of \hat{R}_{xx} and the Forward – Backward solve [178] technique to get the MMSE weight.

3.6.2 Blind Algorithms

Blind algorithms do not require training signals to adapt their weight vectors. Therefore these algorithms save transmission bandwidth. Blind algorithms can be classified as property restoral algorithms, channel estimation algorithms and despread and respread algorithms. Property restoral algorithms restore certain properties of the desired signal and hence enhance the signal interference plus noise ratio (SINR). The property that is being restored can be the modulus or the spectral coherence. Blind property restoral algorithms can be classified as constant modulus algorithm (CMA), self-coherence restoral (SCORE) algorithms and decision directed (DD) algorithms [2].

3.6.2.1 Constant Modulus Algorithm (CMA)

CMA is a gradient –based algorithm that works on the premise when the desired signals have constant modulus. This algorithm adjusts complex weight vector to minimize the

fluctuation in amplitude of the output signal. CMA updates the weight vectors by minimizing the cost function [175] as

$$J(n) = E \left[\left(|y(n)|^p - 1 \right)^q \right] \quad (3.69)$$

Where E denotes the expectation operator. The convergence of the algorithm depends on the coefficients p and q in Equation 3.69. Generally, the cost function J with $p=1$, $q=2$, or $p=2$, $q=2$, is used. Using J with $p=1$, $q=2$, the CMA minimizes the cost function as follows [179]:

$$J(n) = E \left[\left(|y(n)| - 1 \right)^2 \right] \quad (3.70)$$

The gradient vector is given by

$$\begin{aligned} \nabla(J(n)) &= 2 \frac{\partial J(n)}{\partial w^*(n)} \\ &= 2E \left[\left(|y(n)| - 1 \right) \frac{\partial |y(n)|}{\partial w^*(n)} \right] \\ &= 2E \left[\left(|y(n)| - 1 \right) \frac{\partial \{y(n)y^*(n)\}^{\frac{1}{2}}}{\partial w^*(n)} \right] \\ &= E \left[\left(|y(n)| - 1 \right) \{y(n)y^*(n)\}^{\frac{-1}{2}} \frac{\partial \{y(n)y^*(n)\}}{\partial w^*(n)} \right] \\ &= E \left[\left(|y(n)| - 1 \right) \frac{1}{|y(n)|} x(n)x^H(n)w(n) \right] \\ &= E \left[\left(1 - \frac{1}{|y(n)|} \right) x(n)y^*(n) \right] \\ &= E \left[x(n) \left(y(n) - \frac{y(n)}{|y(n)|} \right)^* \right] \end{aligned} \quad (3.71)$$

Ignoring the expectation operator in Equation 3.71, the instantaneous estimate of the gradient vector can be written as

$$\nabla(J(n)) = \left[x(n) \left(y(n) - \frac{y(n)}{|y(n)|} \right)^* \right] \quad (3.72)$$

Using the method of steepest-descent and replacing the gradient vector with its instantaneous estimate, the weight vector can be updated by

$$\begin{aligned} w(n+1) &= w(n) - \mu \nabla(J(n)) \\ &= w(n) - \mu x(n) \left(y(n) - \frac{y(n)}{|y(n)|} \right)^* \end{aligned} \quad (3.73)$$

where μ is the step size parameter. Finally, the CMA can be given as follows:

$$y(n) = w^H(n)x(n) \quad (3.74)$$

$$e(n) = \frac{y(n)}{|y(n)|} - y(n) \quad (3.75)$$

$$w(n+1) = w(n) + \mu x(n)e^*(n) \quad (3.76)$$

The error signal becomes zero when the output of the array has a unity magnitude, i.e., $|y(n)| = 1$ which can be seen from Equation 3.75. Comparing the above three equations to Equation 3.55, it can be observed that the CMA is very similar to the LMS algorithm and the term $\frac{y(n)}{|y(n)|}$ in CMA plays the same role as the desired signal $d(n)$ in the LMS algorithm. However, the reference signal $d(n)$ must be sent from the transmitter to the receiver if the LMS algorithm is used. The CMA algorithm does not require reference signal to generate the error signal at the receiver.

3.6.2.2 Other Techniques

Other adaptive beamforming algorithm includes a decision –directed algorithm that is used for adaptive equalization to combat intersymbol interference (ISI) in digital

communications. In this algorithm, the tap weights of the adaptive equalizer are adjusted via an adaptive process based on the digital bit stream that is fed back from the hard decision process. Spectral self-coherence restoral (SCORE) uses the cyclostationary property of a signal which is a blind adaptive algorithm. Neural networks and maximum likelihood sequences estimations can also be used to perform beamforming. In partially adaptive arrays, some of the elements are weighted adaptively. This technique is useful for large arrays. Partial adaptively allows an array to cancel interfering signals but requires less computational complexity than adapting all the elements weights [2].

3.7 Summary

In this chapter we introduced several techniques that can be applied for beamforming in a CDMA based cellular environment. The four beamforming criteria discussed in this chapter are the Maximum Signal to Noise Ratio (MSNR), the Maximum Signal to Interference Ratio (MSIR), the Maximum signal to Interference and Noise Ratio (MSINR) and the Minimum Mean Square Error (MMSE). Adaptive array algorithms have been broadly classified into non-blind or trained and blind algorithms. This chapter also described several adaptive beamforming algorithms which are used to adjust the weight vectors so that the beamforming criteria are met under the changing environment.

CHAPTER FOUR

SPATIO-TEMPORAL CHANNEL MODELS

4.1 Introduction

In a mobile radio communication system, multipaths can affect the system performance by causing destructive interference commonly known as fading. Antenna arrays are often used to mitigate the effect of fading and thereby increasing the system capacity. Application of antenna arrays may range from fixed directional spatial-filtering to adaptive beamforming. To test the performance of antenna arrays, an accurate description of the spatio-temporal channel model is required.

Classically, the rich scattering multipath environment is modeled as the Rayleigh fading phenomena. In this model, it is assumed that the signals are arriving uniformly along the azimuthal direction. However in more realistic scenarios, the angle of arrival (AOA) of the multipaths depends on a number of factors, such as the distance between the transmitter and receiver, location of scatterers, size of the receiving antenna etc. A number of channel models have been proposed in the literature based on both measurement data and statistical properties of the channel [180]. Some of these models are suited to the microcells typically set up in urban areas, while others are more applicable for the macrocells found in the rural and suburban areas. There are also channel models based on propagation statistics in the indoor environment [181], [182]. All these models provide multipath parameters including the AOA information essential to simulate an antenna array system.

In this chapter, two statistical channel models known as Geometrically Based Single Bounce (GBSB) elliptical and GBSB circular are described for micro and macrocellular environments [183]. In these models it is assumed that the multipath reflections are

created by random placement of scatterers inside a region defined by a specific geometry. From the position of the scatterers, multipath delays, AOA and power levels are determined. Thus these models provide a statistical description of the wideband spatio-temporal radio channel, which is useful in simulating a space-time processing system.

The chapter is organized as follows: Section 4.2 gives a brief description of the GBSB elliptical channel model and the method of generating the channel parameters for simulation purpose. Section 4.3 describes the GBSB circular channel model in a similar fashion. Finally in Section 4.4 the pros and cons of the two models are evaluated from the W-CDMA system perspective. Finally we draw a short chapter summary in section 4.5

4.2 Geometrically Based Single Bounce Elliptical Model

4.2.1 Introduction

In a typical urban environment dense scattering coupled with abundance of reflection results in a rich multipath scenario. In this situation, the microcellular concept where the base station has a relatively low antenna height is more appropriate. This implies that the multipath scatterers are located near the base station as well as near the mobile. Therefore, any spatial channel model that employs a geometrical scattering region around the mobile must also consider a similar scattering region around the base station. A particular channel model, which uses an elliptical scattering region surrounding the base station and the mobile, has been proposed for the microcell environment [180]. This GBSB elliptical channel model is chosen for this research to describe a typical urban multipath propagation scenario.

4.2.2 Assumptions

The following assumptions are made in developing the elliptical channel model [180]:

- The signals arriving at the base station are plane waves propagating along the horizon. As a consequence the AOA is calculated only in the azimuthal coordinates.
- The scatterers are omni-directional re-radiating elements having identical scattering coefficients.
- All scatterers are uncoupled. In other words, the signals reflected from each scatterer are not affected by the presence of the other scatterers.
- The received multipath signals are subjected to distance-dependent path loss characterized by a path loss exponent.

4.2.3 Geometry and Notation

In the GBSB elliptical channel model the scatterers are assumed to be uniformly distributed in an elliptical region. The base station and the mobile form the foci of the ellipse. The geometry of the elliptical model is shown in Figure 4.1

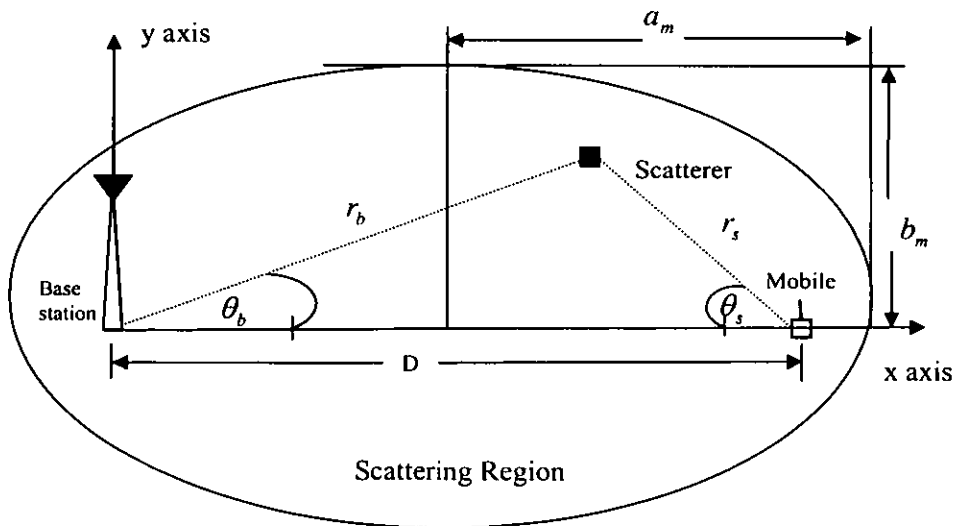


Figure 4.1: Geometry of the GBSB elliptical channel model [180]

In Figure 4.1, the base station and the mobile are separated by a distance D , with the base station at the origin. All scatterers lie in a plane that includes the base station and the mobile, implying that the reflected multipath waves will appear to have the same elevation angle. The elliptical region is completely described by its semimajor axis, a_m and its semiminor axis, b_m . The choice of these parameters is determined by the maximum delay, τ_{\max} of the multipaths. Larger values of τ_{\max} imply greater path loss for the multipaths and, consequently, lower relative power compared to those with shorter delays. Hence, this model has a nice physical interpretation in that, changing the geometry of the ellipse can automatically adjust the various channel parameters, such as multipath amplitudes, delay spread and angle spread.

4.2.4 Mathematical Formulation

The semimajor axis, a_m and the semiminor axis, b_m are related to the maximum specified delay, τ_{\max} as below

$$a_m = \frac{c\tau_{\max}}{2} \quad b_m = \frac{1}{2}\sqrt{c^2\tau_{\max}^2 - D^2} \quad (4.1)$$

Where, D is the separation distance between the transmitter and the receiver and c is the speed of propagation (3×10^8 m/s). The equation of an ellipse in Cartesian coordinates

$$\begin{aligned} \frac{\left(x - \frac{D}{2}\right)^2}{a_m^2} + \frac{y^2}{b_m^2} &= 1 \\ \Rightarrow \frac{\left(x - \frac{D}{2}\right)^2}{\left(\frac{c\tau_{\max}}{2}\right)^2} + \frac{y^2}{\left(\frac{\sqrt{c^2\tau_{\max}^2 - D^2}}{2}\right)^2} &= 1 \end{aligned} \quad (4.2)$$

Substituting, $x = r_b \cos(\theta_b)$ and $y = r_b \sin(\theta_b)$, the equation of the ellipse in Polar coordinates

$$\frac{(r_b \cos \theta_b - D/2)^2}{\left(\frac{c\tau_{\max}}{2}\right)^2} + \frac{(r_b \sin \theta_b)^2}{\left(\frac{\sqrt{c^2\tau_{\max}^2 - D^2}}{2}\right)^2} = 1 \quad (4.3)$$

Where r_b is the distance from the base station of a scatterer located at the boundary of the ellipse and θ_b is the AOA at the base station. Any scatterer inside the ellipse can be viewed as an equivalent one located at the boundary of a smaller concentric ellipse. Equation (4.3) can then be solved for r_b for different values of the multipath propagation delay, $\tau \in [\tau_{\min}, \tau_{\max}]$. However an easier way is to utilize the coordinate location of the scatterer. Referring to Figure 4.1, the total propagation distance of a multipath ray from the mobile to the base-station

$$\begin{aligned} d &= r_b + r_s \\ &= r_b + \sqrt{(D - r_b \cos(\theta_b))^2 + (r_b \sin(\theta_b))^2} \\ &= r_b + \sqrt{D^2 + r_b^2 - 2Dr_b \cos(\theta_b)} \end{aligned} \quad (4.4)$$

Substituting $d = \tau c$ in (4.4) and solving for r_b yields

$$r_b = \frac{D^2 - \tau^2 c^2}{2(D \cos(\theta_b) - \tau c)}; \quad \frac{D}{c} \leq \tau \leq \tau_m. \quad (4.5)$$

Due to the symmetric nature of the scattering region, similar expressions can be derived with respect to the mobile. A detailed analysis on the pdf of multipath delays, AOA and power spectrum of the elliptical channel model can be found in [183].

4.2.5 Generation of Samples of the Elliptical Channel Model

The elliptical model described above can be used to generate various multipath signal parameters such as multipath delay τ_i , AOA θ_i , and power P_i of the i^{th} multipath component. Usually there are two ways to generate these parameters. In one method, the geometrical definition of the elliptical scattering region can be utilized to calculate the parameters. In the other method, the delay and AOA statistics are used to generate the channel samples. The first method is more computationally efficient and it will be described below in detail. The idea is first to define an ellipse corresponding to the maximum multipath delay, τ_m and uniformly place the scatterer inside the ellipse. The relevant signal parameters can then be calculated from the coordinates of the scatterers [183]. It is assumed that the number of multipaths (scatterers), L and the transmitter to receiver separation distance, D is known. The procedure is outlined below

- Choose a value of the maximum multipath propagation delay, τ_m .
- Generate samples of two uniformly distributed random variables, x_l and y_l , $l=1, 2, \dots, L$ over the interval $[-1, 1]$. Thus, the points will be uniformly distributed in a square of arm length 2.
- Isolate the points that lie on and within a circle of unit radius centered at the origin. Translate them from the Cartesian coordinates (x_l, y_l) to the polar coordinates (r_l, θ_l) according to the following relationships

$$r_l = \sqrt{x_l^2 + y_l^2}, \quad \phi_l = \tan^{-1}\left(\frac{y_l}{x_l}\right); \quad l = 1, 2, \dots, L \quad (4.6)$$

- Now, we have L samples of a random variable described by the polar coordinates (r_l, ϕ_l) that are uniformly distributed in a circle of unit radius. To translate these samples so that they are uniformly distributed in an ellipse, the following two transformations are performed

$$x_l = a_m r_l \cos(\phi_l) + \frac{D}{2}, \quad y_l = b_m r_l \sin(\phi_l); \quad l = 1, 2 \dots L \quad (4.7)$$

Where, a_m and b_m are the semimajor and the semiminor axes of the ellipse respectively corresponding to the specified τ_m and are given by (4.1). The multipath propagation distance, d_l ; $l=1, 2 \dots L$ can be calculated as

$$d_l = \sqrt{x_l^2 + y_l^2} + \sqrt{(D - x_l)^2 + y_l^2}; \quad l = 1, 2 \dots L \quad (4.8)$$

- The propagation delays of the multipaths, τ_l ; $l=1, 2 \dots L$ will be

$$\tau_l = \frac{d_l}{c}; \quad l = 1, 2 \dots L; \quad c = 3 \times 10^8 \text{ m/s} \quad (4.9)$$

- As the base station is located at the origin of the coordinate system, so the angle of arrivals (AOA) of the multipaths at the base station are given by

$$\theta_{b,l} = \tan^{-1} \left(\frac{y_l}{x_l} \right); \quad l = 1, 2 \dots L \quad (4.10)$$

- The power of the direct path component (LOS) can be calculated as below

$$P_0(\text{dBm}) = P_{ref}(\text{dBm}) - 10n \log \left(\frac{D/c}{d_{ref}} \right) + G_t(\theta_d) + G_r(\theta_a) \quad (4.11)$$

where P_{ref} the reference power is measured at a distance d_{ref} from the transmitter using omni-directional antennas at the transmitter and the receiver. P_{ref} can be calculated using Friis' free space propagation model given by

$$P_{ref}(\text{dBm}) = P_T(\text{dBm}) - 20 \log \left(\frac{4\pi d_{ref}}{\lambda} \right) \quad (4.12)$$

where P_T is the transmitted power and $\lambda = c/f$ is the wavelength for a particular carrier frequency, f . The path loss exponent, n typically ranges from 3 to 4 in a microcell environment. $G_t(\theta_d)$ and $G_r(\theta_a)$ are the gains of the transmit and the receive antennas as functions of the angle of departure, θ_d and the angle of arrival, θ_a respectively. For the LOS component, θ_d and θ_a are both zero. The power of each of the multipath component can be calculated as below

$$P_l(dB) = P_0(dB) - 10n \log(d_l) - L_r + G_t(\theta_{d,l}) - G_t(0) + G_r(\theta_{a,l}) - G_r(0) \quad (4.13)$$

Where L_r is the path loss in dB.

- Assuming the phase of the multipath components, γ_l ; $l=1, 2 \dots L$ are uniformly distributed over the interval $[0, 2\pi)$, the complex amplitudes of the multipath components are calculated as below.

$$\alpha_l = 10^{(P_l - P_0)/20} e^{j\gamma_l}; \quad l = 1, 2 \dots L \quad (4.14)$$

4.3 Geometrically Based Single Bounce Circular Model

4.3.1 Introduction

A typical rural or suburban environment is characterized by local scatterers surrounding the mobile and no large reflectors away from the vicinity of the mobile is visible at the base station. In such environments, macro-cellular concept where the base station antenna height is considered to be above the local clutter is a more appropriate selection. Thus, the multipath channel parameters in the propagation model for rural or suburban environment are essentially determined by the distribution of the scatterers around the mobile. A number of models have been proposed in the literature that defines the geometry and the underlying distribution of the scatterer region. In one of these models, it is assumed that the scatterers are uniformly distributed within a circle of predefined

radius around the mobile [184]. This model known as Geometrically Based Single Bounce (GBSB) circular model is specially suited for macrocell environments and thus sufficient to represent a rural or suburban multipath propagation model.

4.3.2 Assumptions

A Geometrically Based Single Bounce circular model presupposes the following underlying assumptions [184], [183].

- The signals received at the base station are plane waves propagating along the horizon .Thus only the azimuthal coordinates are required to represent the corresponding AOA. This is due to the fact that the separation distance between transmitter and receiver is large compared to the respective antenna heights.
- The scatterers are considered to be omni-directional re-radiating elements with identical scattering coefficients.
- Each multipath component at the base station has interacted with only a single scatterer and thus is not influenced by the other scatterers in the channel.

4.3.3 Geometry and Notation

The Geometrically Based Single Bounce (GBSB) circular model assumes that the scatterers are uniformly distributed within a circle of radius, R around the mobile. The geometry of the circular model is shown in Figure 4.2.

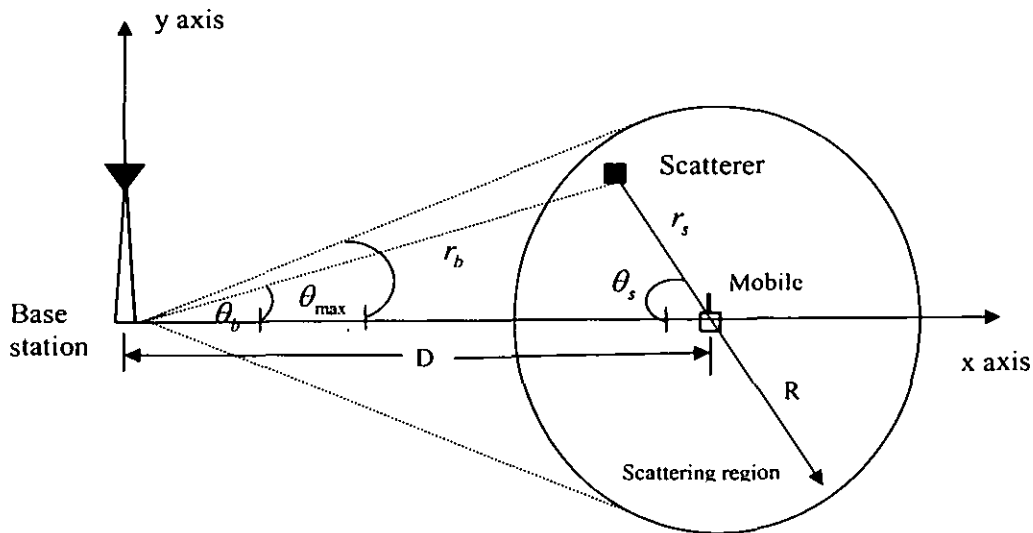


Figure 4.2: Geometry of the Circular Scattering Channel Model [184]

In Figure 4.2, the base station and the mobile are separated by a distance D , with the base station at the origin of the coordinate system and the mobile is on the x-axis. The scatterers are uniformly placed in a circle of radius R with the mobile is at the center. Typically, $R < D$, so that there are no scatterers local to the base station as is the case in a macrocell region. For simplicity, the plane of the scatterer can be viewed as horizontal, which also includes the mobile and the base station. This will ensure that the angle of arrivals (AOA) of the received signal contains only azimuthal components. The AOA of the multipath components at the base station is denoted by θ_b and depends on two parameters: the angle of departure from the mobile and the position of the scatterer. The location of the scatterer is specified by its distance from the base station, r_b , and from the mobile, r_s , respectively. Since the scatterers are confined in a circle around the mobile, the AOA at the base station, θ_b , is limited by a maximum value denoted by, θ_{\max} . Similarly, the AOA at the mobile θ_s depends on the angle of departure from the base station and the scatterer location. In this case, as the mobile is located inside the scattering region, the AOA can be any value in the interval $[0, 2\pi)$.

The radius of the circular scattering region, R , is usually determined by equating the angle spread as predicted by the model with the measured angle spread. Typical values of angle spread in a macrocell environment ranges between one to six degrees for a transmitter to receiver separation distance of $D \approx 1$ km.

4.3.4 Mathematical Formulation

The region of scatterer in the Cartesian coordinates is given by

$$(x - D)^2 + y^2 \leq R^2 \quad (4.15)$$

Substituting, $x = r_b \cos(\theta_b)$ and $y = r_b \sin(\theta_b)$ in (4.15) and expanding, the scattering region in polar coordinates

$$r_b^2 - 2r_b D \cos(\theta_b) + D^2 \leq R^2 \quad (4.16)$$

Referring to Figure 4.2, the total multipath propagation distance, d is given by

$$\begin{aligned} d &= r_b + r_s \\ &= r_b + \sqrt{(D - r_b \cos(\theta_b))^2 + (r_b \sin(\theta_b))^2} \\ &= r_b + \sqrt{D^2 + r_b^2 - 2Dr_b \cos(\theta_b)} \end{aligned} \quad (4.17)$$

Substituting $d = \tau c$ in (4.17), where τ is the total multipath propagation delay, the distance of the scatterer from the base station, r_b , can be expressed as

$$r_b = \frac{D^2 - \tau^2 c^2}{2(D \cos(\theta_b) - \tau c)} \quad (4.18)$$

As in the GBSB elliptical channel model, the symmetric nature of the scattering region allows similar expressions to be derived with respect to the mobile. A detailed analysis

on the pdf of multipath delays, AOA and power spectrum of the circular channel model can be found in [184], [183].

4.3.5 Generation of Samples of the Circular Channel Model

As in the elliptical channel model, there are two ways to generate the multipath channel parameters using the circular channel model. Exploitation of the geometry of the scattering region, which will be described below, is a much more efficient method than the one that utilizes the statistics of the channel parameters (delay, AOA). Again, the basic idea is to define a uniform circular scattering surrounding the mobile with the radius corresponds to the maximum multipath delay, τ_m . The relevant signal parameters can then be calculated from the geometry of the scattering region [183]. As in the case of elliptical model, it will be assumed that number of multipaths, L and the transmitter to receiver separation distance, D is known. The procedure is described below.

- Choose a value of the maximum multipath delay, τ_m
- Calculate the radius of the scattering region according to the following relationship

$$R_m = \frac{(c\tau_m - D)}{2} \quad (4.19)$$

Where c is the speed of propagation.

- Generate samples of two uniform random variables, x_l and y_l , $l=1, 2 \dots L$ over $[-R_m, R_m]$ and isolate those that lie on and inside a circle of radius R_m . The coordinates of these points with respect to an origin at a distance D from the center of the circle is

$$x_c = x_l + D, \quad y_c = y_l; \quad l = 1, 2 \dots L \quad (4.20)$$

- The multipath propagation distance, d_l , $l=1, 2 \dots L$ is then calculated as

$$d = \sqrt{x_c^2 + y_c^2} + \sqrt{(D - x_c)^2 + y_c^2} \quad (4.21)$$

- The propagation delay, τ_l and AOA at the base station (origin), $\theta_l, l=1,2,\dots,L$ are

$$\tau_l = \frac{d_l}{c}, \quad \theta_{b,l} = \tan^{-1}\left(\frac{y_c}{x_c}\right); \quad l = 1,2,\dots,L \quad (4.22)$$

- As in the elliptical model, the power of the multipaths components are calculated as

$$P_l(dB) = P_0(dB) - 10n \log(d_l) - L_r + G_t(\theta_{d,l}) - G_t(0) + G_r(\theta_{a,l}) - G_r(0) \quad (4.23)$$

Where the terms have the same meanings as in 4.2.5.

- Then the complex gains of the multipaths components, $\alpha_l, l=1,2,\dots,L$ are given as

$$\alpha_l = 10^{(P_l - P_0)/20} e^{j\gamma_l}; \quad l = 1,2,\dots,L \quad (4.24)$$

With the assumption that the phases $\gamma_l, l=1, 2,\dots,L$ are uniformly distributed over $[0,2\pi)$.

4.4 Channel parameters from the WCDMA system perspective

In this section, the two scattering channel models are discussed with respect to the WCDMA system. These channel models are used in our simulation and provide valuable insight into different channel parameters. The power-delay profile and the angle spread of these models will be evaluated using the geometry of the scattering region and AOA statistics that are already developed in [180], [12], [184]. They will be compared under different conditions that determine the size and shape of the geometry, such as the maximum multipath delay, τ_m , and base station to mobile distance, D . The suitability of a channel model for an environment and the range of parameters for each model is also justified.

4.4.1 Power –delay profile

The power-delay profile of a multipath channel indicates the relative strength of the multipaths with respect to their time of arrivals and can be used to create an equivalent discrete finite impulse response (FIR) model of the channel. In a CDMA type wideband system where the channel is frequency selective, the power-delay profile indicates the time dispersiveness of the channel. The power-delay profile of the elliptical and the circular models can be generated using the procedure described in section (4.2.5) and (4.3.5) respectively. In generating these profiles, it is assumed that the line of sight (LOS) power is normalized to unity. Also only the distance dependent path loss is taken into account and no long term fading (shadowing) effect is considered. The antenna gains of both the transmitter and the receiver are assumed to be unity.

4.4.2 Angle Spread

The angle spread of a channel is a measure of the angular dispersiveness of the channel. In other words, angle spread when referred to the receive side is the spread of the AOA of the multipaths at the receive antenna. Likewise, angle spread refers to the transmit side is the spread of angle of departure (AOD) of the multipaths from the transmit antenna. There are two ways to define the angle spread, central moment angle spread and ensemble average angle spread [12]. The central moment angle spread of a channel can be calculated when the measured channel impulse response is available. When the probability density functions (pdf) of the AOA/AOD of the multipaths are available, ensemble average delay spread can be used. We will use the ensemble average angle spread using the pdf of AOA derived in [180]. It is defined for AOA at the receiver (base-station) as below

$$\sigma_{\theta_b} = \sqrt{E\{\theta_b^2\} - E\{\theta_b\}^2} \quad (4.25)$$

Where θ_b is the AOA at the base station and $E\{.\}$ is the expectation operator defined as

$$E\{x\} = \int_{-\infty}^{\infty} xf(x)dx \quad (4.26)$$

For the elliptical channel model, the AOA pdf is given by [180]

$$f_{\theta_b}(\theta_b) = \frac{1}{8\pi a_m b_m} \left(\frac{\tau_m^2 c^2 - D^2}{\tau_m c - D \cos(\theta_b)} \right)^2; \quad -\pi \leq \theta_b \leq \pi \quad (4.27)$$

where the symbols have the same meaning as described in the earlier section. Using (4.26), it is found that the mean of AOA, $E\{\theta_b\}$ is zero, so the angle spread from (4.25) is

$$\sigma_{\theta_b} = \frac{(\tau_m^2 c^2 - D^2)}{8\pi a_m b_m} \int_{-\pi}^{\pi} \frac{\theta_b^2}{(\tau_m c - D \cos(\theta_b))^2} d\theta_b \quad (4.28)$$

As this expression does not have a closed form solution, so it has to be evaluated numerically.

4.5 Summary

In this chapter, we discussed two GBSB statistical channel models, which will be used as the spatio-temporal channels in our space-time processing simulation testbed. We described the geometrical configurations and mathematical formulations of these two models along with their implicit assumptions. We then outlined the procedure to generate the samples of the channel parameters in an efficient manner. These procedures will be followed extensively to simulate the multipath channel parameters. We discussed two channel property indicators, namely, the power-delay profile and the angle spread, in which will be more meaningful when simulating spatio-temporal channel for our space-time processing system.

CHAPTER FIVE

WCDMA

5.1 Introduction

we briefly discuss the different generations of cellular standards and the migration from the circuit switched voice traffic oriented older generation wireless networks to the coming third generation cellular systems that will employ packet switched networking techniques to deal with the increased demand for wireless data services. We begin with a brief discussion of the first and second generation cellular systems. Then we outline the migration towards the third generation systems and discuss the key requirements of the next generation cellular systems. We then proceed to discuss the key aspects of the physical layer of the uplink of WCDMA [6], [7], potentially the most popular of the third generation standards. The chapter concludes with a discussion on the current status of the deployment of the third generation cellular systems around the world.

5.2 Cellular Standards: From 1G to 3G

The goal for the next generation of mobile communication systems is to seamlessly provide a wide variety of communication services to anybody, anywhere, anytime. The intended services for next generation mobile phone users include services like transmitting high speed data, video and multimedia traffic as well as voice signals. The technology needed to tackle the challenges to make these services available is popularly known as the Third Generation (3G) Cellular Systems. The first-generation systems are represented by the analog mobile systems designed to carry the voice application traffic. Their subsequent digital counterparts are known as second generation cellular systems. Third generation systems mark a significant leap, both in applications and capacity, from

the current second generation standards. Whereas the current digital mobile phone systems are optimized for voice communications, 3G communicators are oriented towards multimedia message capability.

5.2.1 First Generation (1G) Cellular Systems

The first generation cellular systems generally employ analog Frequency Modulation (FM) techniques. The Advanced Mobile Phone System (AMPS) is the most notable of the first generation systems. AMPS were developed by the Bell Telephone System. It uses FM technology for voice transmission and digital signaling for control information. Other first generation systems include Narrowband AMPS (NAMPS), Total Access Cellular System (TACS) and Nordic Mobile Telephone System (NMT-900). All the first generation cellular systems employ Frequency Division Multiple Access (FDMA) with each channel assigned to a unique frequency band within a cluster of cells. The first generation networks are based on circuit switched technique.

5.2.2 Second Generation (2G) Cellular Systems

The rapid growth in the number of subscribers and the proliferation of many incompatible first-generation systems were the main reason behind the evolution towards second generation cellular systems. Second generation systems take advantage of compression and coding techniques associated with digital technology. All the second generation systems employ digital modulation schemes. Multiple access techniques like Time Division Multiple Access (TDMA) and Code Division Multiple Access (CDMA) are used along with FDMA in the second generation systems. Second generation cellular systems include United States Digital Cellular (USDC) standards IS-54 and IS-136, Global System for Mobile communications (GSM), Pacific Digital Cellular (PDC) and cdmaOne based IS-95A/IS-95B. Like their first generation counterparts, the 2G networks are also circuit switched.

5.2.3 Transition towards 3G: 2.5G Cellular Systems

The demand for wireless data services has resulted in transition towards packet switched networks. The so called 2.5 G cellular systems are currently being employed to facilitate the move from the circuit switched 2G cellular networks to the next generation packet based network. Two major 2.5G cellular systems currently being deployed are General Packet Radio Service (GPRS) and Enhanced Data-rates for Global Evolution (EDGE). The General Packet Radio Service (GPRS) is a value added service that allows information to be sent and received across a mobile telephone network. It supplements today's circuit switched data and short message service. GPRS is based on standardized open interfaces and therefore interworks with existing circuit-switched services. Since GPRS is a packet switched technology, bandwidth is only utilized during data transmission and is shared between all subscribers. This allows operators to offer billing on a usage basis rather than on connection time. Users are therefore always connected and only charged for data transfer. This makes GPRS ideally suited to bursty traffic transmission, and opens the door to a world of new services previously impractical over mobile networks.

Enhanced Data-rates for Global Evolution (EDGE) is a Third Generation (3G) compliant high-speed wireless data and Internet access technology that offers economies of scale. EDGE is a standardized set of improvements to the GSM radio interface. It defines a new modulation and new radio protocols that bring higher maximum data rates and increased spectral efficiency. EDGE is applicable to both GPRS traffic (EGPRS) and circuit switched data traffic (ECSD). EDGE can be integrated into existing GSM networks by the installation of new transceivers or new base stations. EDGE can also be applied to TDMA (D-AMPS/IS-136) networks by the addition of a complete EGPRS overlay. In the GSM context, EDGE is considered part of the 2G+/2.5G evolution, whereas for the TDMA community, it is sometimes termed as a 3G technology.

5.2.4 Third Generation Cellular Systems

Third generation cellular systems are being designed to support wideband services like high speed Internet access, video and high quality image transmission with the same quality as the fixed networks. The primary requirements of the next generation cellular systems are [5], [185]:

- Voice quality comparable to Public Switched Telephone Network (PSTN).
- Support of high data rate. The following table shows the data rate requirement of the 3G systems

Table 5.1: 3G data rate requirements

Mobility Needs	Minimum Data Rate
Vehicular	144 kbps
Outdoor to indoor & pedestrian	384 kbps
Indoor Office	2 Mbps

- Support of both packet-switched and circuit-switched data services.
- More efficient usage of the available radio spectrum
- Support of a wide variety of mobile equipment
- Backward Compatibility with pre-existing networks and flexible introduction of new services and technology
- An adaptive radio interface suited to the highly asymmetric nature of most Internet Communications: a much greater bandwidth for the downlink than the uplink.

Research efforts have been underway for more than a decade to introduce multimedia capabilities into mobile communications. Different standard agencies and governing bodies have been responsible for the efforts to integrate a wide variety of proposals for third generation cellular systems. Three different 3G standards emerged as the solution for the next generation cellular systems. They are WCDMA, CDMA2000, and UWC-136. WCDMA employs CDMA air interface with the GSM based networks. CDMA2000

is a multi-carrier CDMA standard and is a natural progression of the CDMA based 2G standard IS-95. UWC-136, a TDMA based standard, was proposed to upgrade the existing TDMA based 2G networks. However recent developments suggest that UWC-136 will not come into service in practice. The following figure 5.1, adopted from [5], shows the evolution of third generation cellular systems:

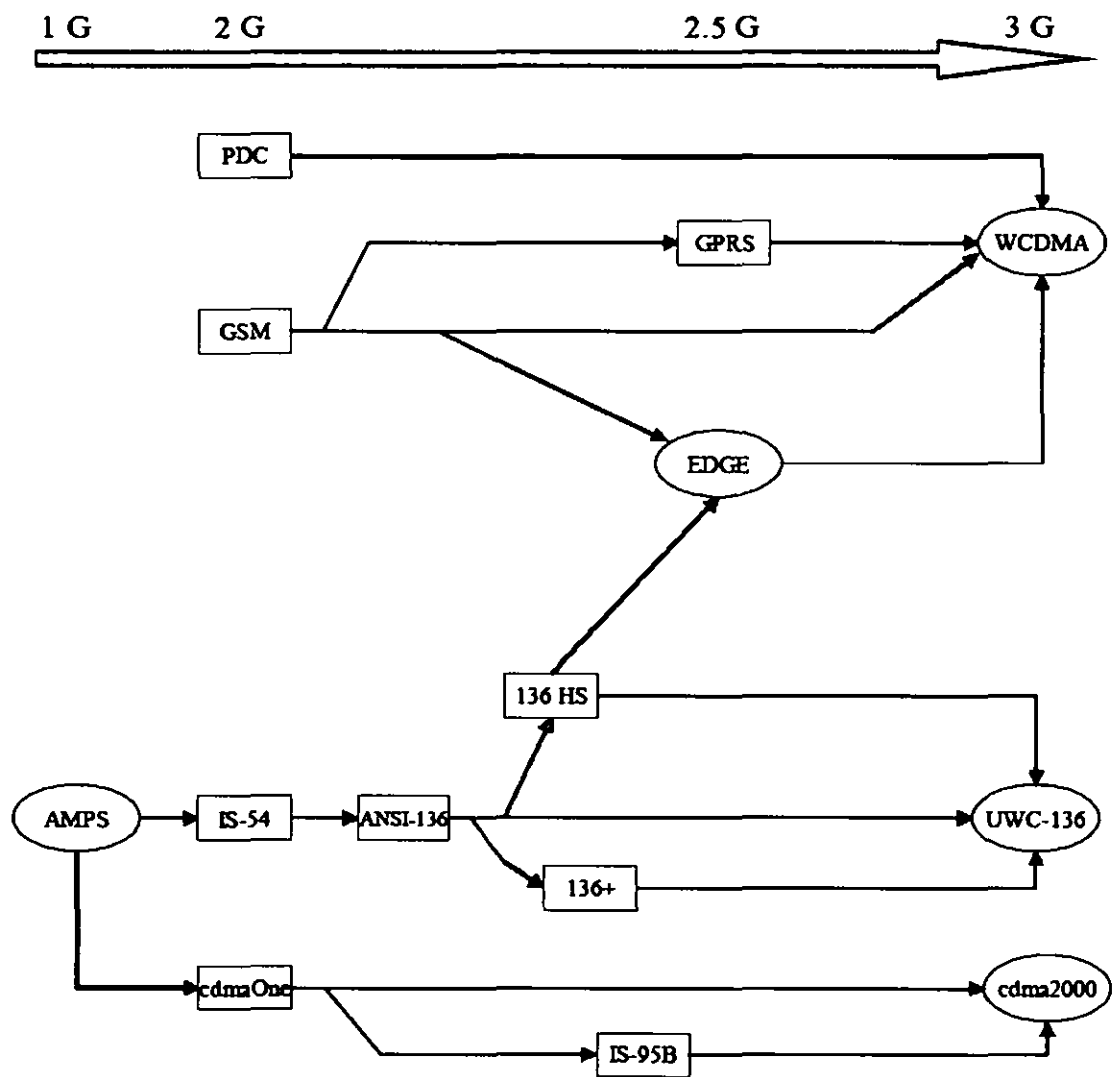


Figure 5.1: Evolution towards 3G [5]

References [5] and [8-10] provide further discussion on the evolution of third generation cellular systems.

5.3 WCDMA: Air Interface for 3G

One of the most popular approaches to 3G is to combine a Wideband CDMA (WCDMA) air interface with the fixed network of GSM. Several proposals supporting WCDMA were submitted to the International Telecommunication Union (ITU) and its International Mobile Telecommunications for the year 2000 (IMT2000) initiative for 3G. The organizations that merged their various WCDMA proposals include Japan's Association of Radio Industry and Business (ARIB), Alliance for Telecommunications Industry Solutions (ATIS), T1P1 and European Telecommunications Standards Institute (ETSI) through its Special Mobile Group (SMG). The standard that emerged is based on ETSI's Universal Mobile Telecommunication System (UMTS) and is commonly known as UMTS Terrestrial Radio Access (UTRA) [5]. This standard is intended to take advantage of the WCDMA radio techniques without ignoring the numerous advantages of the already existing GSM networks. The access scheme for UTRA is Direct Sequence Code Division Multiple Access (DS-SS). The information is spread over a band of approximately 5 MHz. This wide bandwidth is the reason for the name Wideband CDMA or WCDMA. There are two different modes namely Frequency Division Duplex (FDD) and Time Division Duplex (TDD). For the FDD mode, the uplink and downlink transmissions employ two separated frequency bands for this duplex method. A pair of frequency bands with specified separation is assigned for a connection. In the TDD duplex mode, uplink and downlink transmissions are carried over the same frequency band by using synchronized time intervals. Thus time slots in a physical channel are divided into transmission and reception part.

5.3.1 WCDMA Key Features

The key operational features of the WCDMA radio interface are listed below [9], [10]:

- Support of high data rate transmission: 384 kbps with wide area coverage, 2 Mbps with local coverage.

- High service flexibility: support of multiple parallel variable rate services on each connection.
- Both Frequency Division Duplex (FDD) and Time Division Duplex (TDD).
- Built in support for future capacity and coverage enhancing technologies like adaptive antennas, advanced receiver structures and transmitter diversity.
- Support of inter frequency hand over and hand over to other systems, including hand over to GSM.
- Efficient packet access.

5.3 .2 WCDMA Key Technical Characteristics

The following table shows the key technical features of the WCDMA radio interface:

Table 5.2: WCDMA key technical characteristics

Multiple Access Scheme	DS-CDMA
Duplex Scheme	FDD/TDD
Packet Access	Dual mode (Combined and dedicated channel)
Multi-rate/ Variable rate scheme	Variable spreading factor and multi-code
Chip Rate	3.84 Mcps
Carrier Spacing	4.4-5.2 MHz (200 kHz carrier raster)
Frame length	10 ms
Inter Base Station Synchronization	FDD: No accurate synchronization needed
Channel Coding Scheme	Convolutional Code (rate ½ and 1/3)

The chip rate may be extended to two or three times the standard 3.84 Mcps to accommodate for data rates higher than 2 Mbps. The 200 kHz carrier raster has been chosen to facilitate coexistence and interoperability with GSM.

5.4 WCDMA Physical Layer at the Uplink

This section provides a layer 1 (also termed as physical layer) description of the radio access network of a WCDMA system operating in the FDD mode. The spreading and modulation operation for the Dedicated Physical Channels (DPCH) at the reverse link is illustrated in detail. The uplink data structure for the DPCHs is described and the spreading and scrambling codes used in the uplink are reinvestigated. The spreading modulation and data structure for forward link DPCH, Physical Random Access channel (PRACH), Synchronization Channel (SCH), etc. are described in detail in [5] and [6] along with those of the uplink DPCHs.

5.4.1 Physical Channel Structure

WCDMA defines two dedicated physical channels in both links:

- Dedicated Physical Data Channel (DPDCH): to carry dedicated data generated at layer 2 and above.
- Dedicated Physical Control Channel (DPCCH): to carry layer 1 control information.

Each connection is allocated one DPCCH and zero, one or several DPDCHs. In addition, there are common physical channels defined as:

- Primary and secondary Common Control Physical Channels (CCPCH) to carry downlink common channels
- Synchronization Channels (SCH) for cell search
- Physical Random Access Channel (PRACH)

The spreading and modulation for the DPDCH and the DPCCH the uplink are described in the following two subsections.

5.4.1 .1 Uplink Spreading and Modulation

In the uplink the data modulation of both the DPDCH and the DPCCH is Binary Phase Shift Keying (BPSK). The modulated DPCCH is mapped to the Q-channel, while the first DPDCH is mapped to the I-channel. Subsequently added DPDCHs are mapped alternatively to the I or the Q-channel. Spreading Modulation is applied after data modulation and before pulse shaping. The spreading modulation used in the uplink is dual channel QPSK. Spreading modulation consists of two different operations. The first one involves replacing each data symbol by a number of chips given by the spreading factor. The second operation is scrambling where a complex valued scrambling code is applied to the chips. The bandwidth of the signal spread signal becomes 3.84 Mcps. Figure 5.2 shows the spreading and modulation for an uplink user. The uplink user has a single DPDCH only.

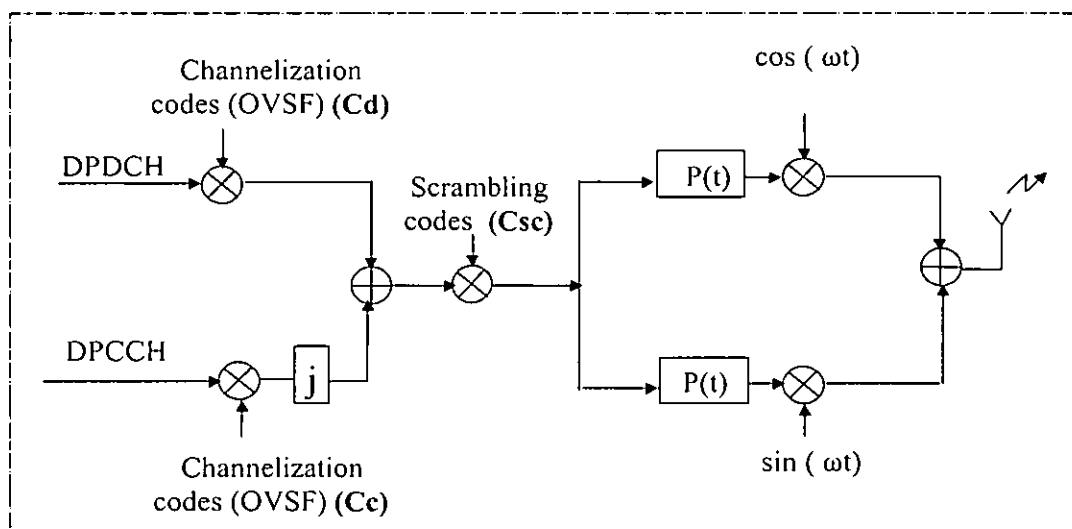


Figure 5.2: Uplink spreading and modulation [6]

The bipolar data symbols on I and Q branches are independently multiplied by different Channelization codes. The channelization codes are known as Orthogonal Variable Spreading Factor (OVSF) codes. OVSF codes are discussed in section 4.4.1.3. The resultant signal is multiplied by a complex scrambling code. The complex scrambling code is a unique signature of the mobile station. Next, the scrambled signal is pulse

shaped. Square-Root Raised Cosine filters with roll-off factor of 0.22 are employed for pulse shaping. The pulse shaped signal is subsequently up converted as shown in Figure 5.2. The application of a complex scrambling code with spreading modulation as described above is sometimes termed as Hybrid Phase Shift Keying (HPSK). HPSK reduces the peak-to average power of the mobile station by generating the complex scrambling sequence in a special way [186]. The generation of complex scrambling code is discussed in section 4.4.1.4. The spreading factor for the control channel is always set at the highest value which is 256. The channelization code of the control channel is always a sequence of 256 ones.

5.4.1.2 Uplink Frame Structure

Figure 5.3 shows the principal frame structure of the uplink dedicated physical channels. Each frame of 10 ms is split into 15 slots. Each slot is of length 2560 chips, corresponding to one power control period. The super frame length is 720 ms; i.e. a super frame corresponds to 72 frames. Pilot bits assist coherent demodulation and channel estimation. TFCI stands for transport format combination indicator and is used to indicate and identify several simultaneous services. Feedback Information (FBI) bits are to be used to support techniques requiring feedback. TPC which stands for transmit power control is used for power control purposes. The exact number of bits of these different uplink DPCCH fields is given in [7].

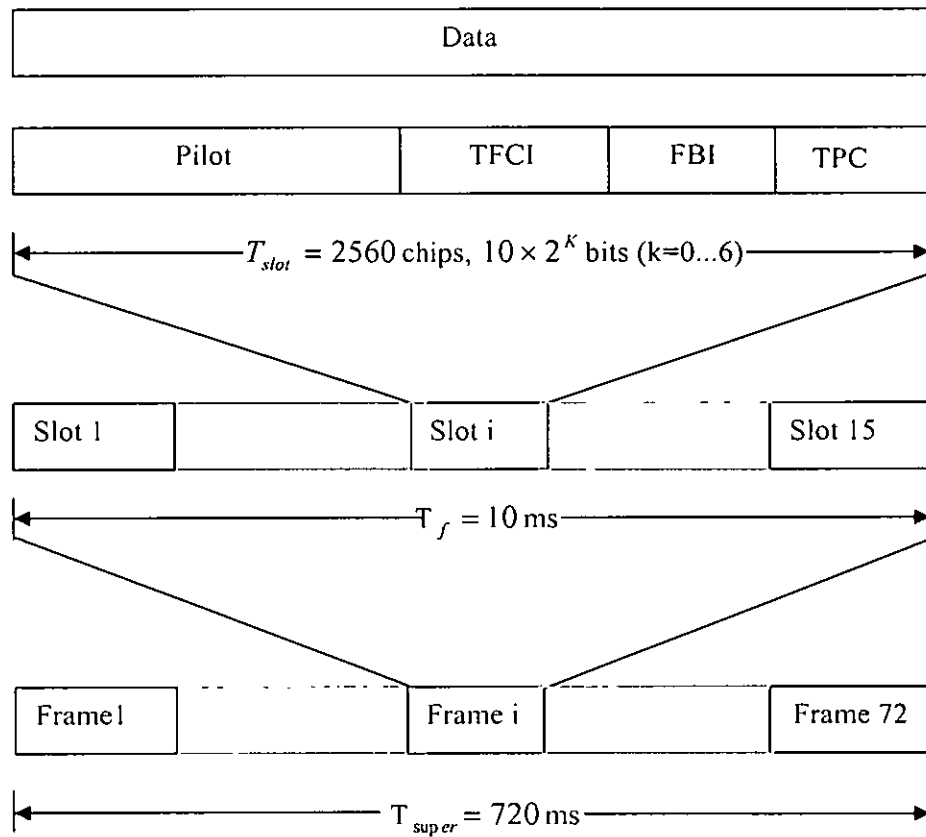


Figure 5.3: Frame structure for uplink DPDCH/DPCCH [7]

The parameter k in Figure 5.3 determines the number of bits in each slot. It is related to spreading factor (SF) of the physical channel as

$$SF = \frac{256}{2^k} \quad (5.1)$$

The spreading factor thus may range from 256 down to 4. The spreading factor is selected according to the data rate. The following table shows the spreading factor and the number of data channel for the different data rates at the WCDMA uplink

Table 5.3: Uplink data rate vs. spreading factor

Data rate (kbps)	Data channel spreading factor	Number of data channels
12.2	64	1
64	16	1
144	8	1
384	4	1
768	4	2
2048	4	6

5.4.1.3 Uplink Channelization Codes

The most important purpose of the channelization codes is to help preserve orthogonality among different physical channels of the uplink user. OVSF codes are employed as uplink spreading codes. OVSF codes can be explained using the code tree shown in Figure 5.4. The subscript here gives the spreading factor and the argument within the parenthesis provides the code number for that particular spreading factor. Each level in the code tree defines spreading codes of length SF, corresponding to a particular Spreading factor of SF. The number of codes for a particular spreading factor is equal to the spreading factor itself. All the codes of the same level constitute a set and they are orthogonal to each other. Any two codes of different levels are orthogonal to each other as long as one of them is not the mother of the other code. For example the codes c16 (2), c8 (1) and c4 (1) are all mother codes of c32 (3) and hence are not orthogonal to c32 (32).

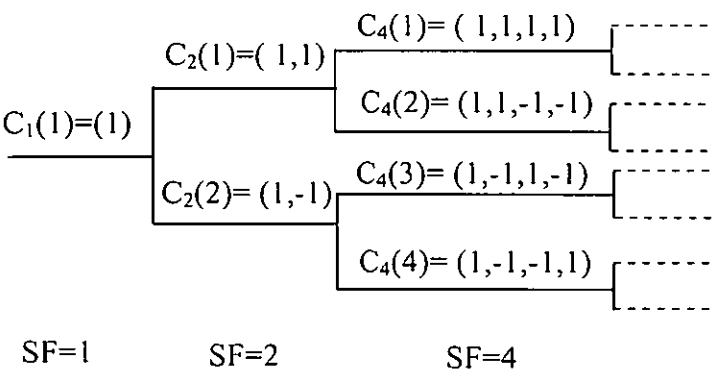


Figure 5.4: Code – tree for generation of OVSF codes [185]

The generation method of OVSF can be explained with the help of the following matrix equations [185]:

$$\begin{aligned}
 [c_1(1)] &= 1: \quad \begin{bmatrix} c_2(1) \\ c_2(2) \end{bmatrix} = \begin{bmatrix} c_1(1) & c_1(1) \\ c_1(1) & \overline{c_1(1)} \end{bmatrix} = \begin{bmatrix} 1 & 1 \\ 1 & -1 \end{bmatrix} \\
 &\quad \cdot \\
 &\quad \cdot \\
 \begin{bmatrix} c_N(1) \\ c_N(2) \\ \vdots \\ c_N(N-1) \\ c_N(N) \end{bmatrix} &= \begin{bmatrix} c_{N/2}(1) & \overline{c_{N/2}(1)} \\ c_{N/2}(1) & \overline{c_{N/2}(1)} \\ \vdots & \vdots \\ c_{N/2}(N/2) & \overline{c_{N/2}(N/2)} \\ c_{N/2}(N/2) & \overline{c_{N/2}(N)} \end{bmatrix} \quad (5.2)
 \end{aligned}$$

In the above matrix notation, an over bar indicates binary complement (e.g. $\overline{1} = -1$ and $\overline{-1} = 1$) and N is an integral power of two. The OVSF codes do not have a single, narrow auto-correlation peak as shown in figure 5.5. As a consequence code-synchronization may become difficult. OVSF codes exhibit perfect orthogonality only at zero lags and even this does not hold for partial-sequence cross-correlation. As a result the advantage of using OVSF codes could be lost when all the users are not synchronized to a single time base or when significant multipath is present.

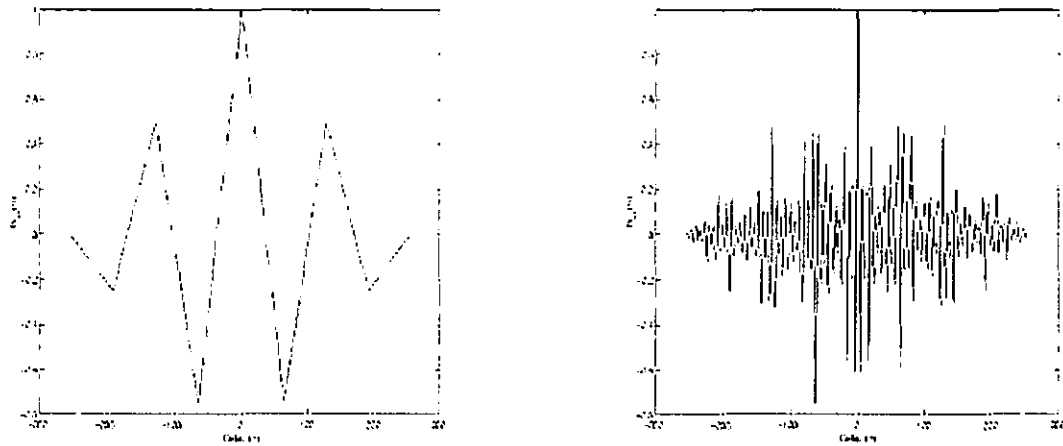


Figure 5.5: Auto-correlation for two OVSF codes of SF = 256 [185]

A sequence of 256 ones, which is the first code at the code tree for a spreading factor of 256, is used to spread the DPCCH. The first DPDCH is spread by the code number $(SF/4+1)$ where SF is the spreading factor for the data channel. As for example, the 5th code is used for spreading the first DPDCH for a spreading factor of 16. So the spreading code for the first DPDCH is always a repetition of $\{1, 1, -1, -1\}$. Subsequently added DPDCHs for multi-code transmission are spread by codes in ascending order starting from code number 2 excepting the code used for the first DPDCH. Code selection in this orderly manner along with the proper choice of scrambling code increases the spectral efficiency by limiting the diagonal transitions in the signal constellation [185]. This also results into efficient use of the power amplifier [186]. We should mention that for multi-code transmission, the spreading factor is limited to 4 only.

5.4.1.4 Uplink Scrambling Codes

Uplink Scrambling codes help maintain separation among different mobile stations. Either short or long scrambling codes can be used in the uplink [6]. Short scrambling codes are recommended for base stations equipped with advanced receivers employing multiuser detection or interference cancellation. In this research, we used long scrambling codes for the simulations.

Scrambling codes (both short and long) can be defined with the help of the following equation

$$C_{sc} = C_1(w_1 + jw_2C_2') \quad (5.3)$$

Here, C_1 is a real chip rate code, C_2' is a decimated version of a real chip rate code C_2 .

The usual decimation factor is 2 so that,

$$C_2'(2k) = C_2'(2k+1) = C_2(2k) \quad (5.4)$$

w_1 is a repetition of $\{1 \ 1\}$ at the chip rate and w_2 is a repetition of $\{1 \ -1\}$ at the chip rate

So we can write

$$C_{sc} = C_1 + jw_2C_1C_2' \quad (5.5)$$

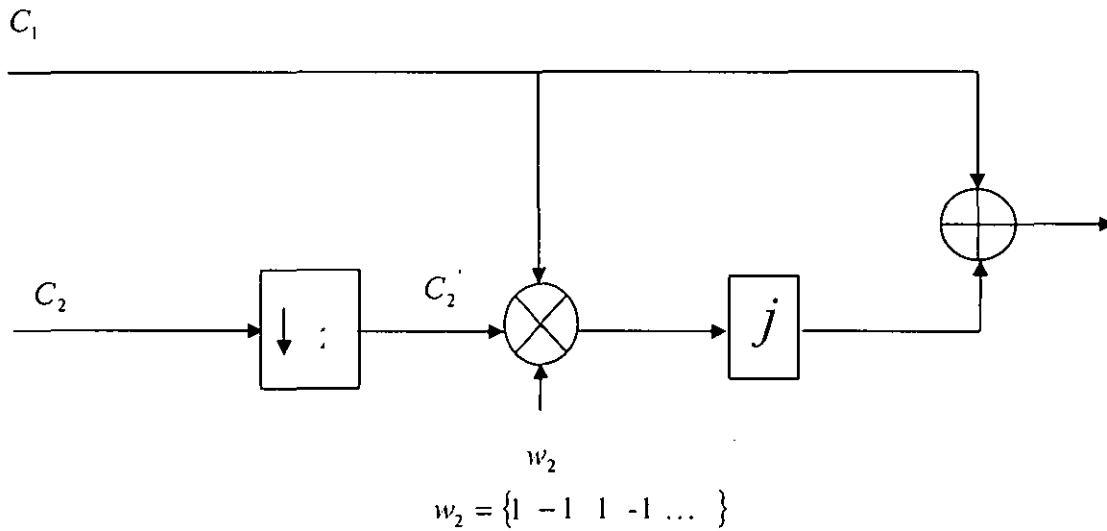


Figure 5.6: Generation of scrambling codes [6]

The above block diagram shows the implementation of Equation 5.5. All the additions and multiplications are performed in modulo 2 arithmetic.

The WCDMA standard defines a period of 10 ms or 1 frame for the period of the scrambling codes.

5.4.1.4.1 Uplink Long Scrambling Codes

Long scrambling codes are constructed as described in section 5.4.1.4. The real chip rate codes C_1 and C_2 are formed as the position wise modulo 2 sums of 38400 chip segments of two binary m sequences. The binary m sequences are generated from two generator polynomials of degree 25. This is explained in detail below following the discussion in [6].

Two binary sequences x and y are generated using the generator polynomials $x^{25} + x^3 + 1$ and $x^{25} + x^3 + x^2 + x + 1$ respectively. The resulting sequence constitutes segments of a set of Gold sequences. Let n_{23}, \dots, n_0 be the 24 bit binary representation of the scrambling code number n (decimal). In the binary representation, n_0 is the least significant bit (LSB). The x sequence depends on the choice of the scrambling code number and is thus denoted as x_n . Furthermore, let $x_n(i)$ and $y(i)$ denote the i^{th} symbol of the sequences x_n and y respectively. The m sequences are constructed the following way,

The Initial conditions are set:

$$\begin{aligned} x_n(0) &= n_0, x_n(1) = n_1, \dots, x_n(22) = n_{22}, x_n(23) = n_{23}, x_n(24) = 1 \\ y(0) &= y(1) = \dots, y(23) = y(24) = 1 \end{aligned} \quad (5.6)$$

Then subsequent symbols are generated recursively according to:

$$\begin{aligned} x_n(i+25) &= \langle x_n(i+3) + x_n(i) \rangle_{\text{mod } 2}, i = 0, 1, \dots, 2^{25} - 27 \\ y(i+25) &= \langle y(i+3) + y(i+2) + y(i+1) + y(i) \rangle_{\text{mod } 2}, i = 0, 1, \dots, 2^{25} - 27 \end{aligned} \quad (5.7)$$

The real chip rate code $C_{1,n}$ and $C_{2,n}$ for the n th scrambling code are defined as

$$C_{1,n} = \left\{ \langle x_n(0) + y(0) \rangle_{\text{mod } 2}, \langle x_n(1) + y(1) \rangle_{\text{mod } 2}, \dots, \langle x_n(N-1) + y(N-1) \rangle_{\text{mod } 2} \right\}$$

$$C_{2,n} = \left\{ \left\langle \frac{x_n(M)}{+y(M)} \right\rangle_{\text{mod } 2}, \left\langle \frac{x_n(M+1)}{+y(M+1)} \right\rangle_{\text{mod } 2}, \dots, \left\langle \frac{x_n(M+N-1)}{+y(M+N-1)} \right\rangle_{\text{mod } 2} \right\} \quad (5.8)$$

The generation of the codes $C_{1,n}$ and $C_{2,n}$ are explained in the next figure 5.7

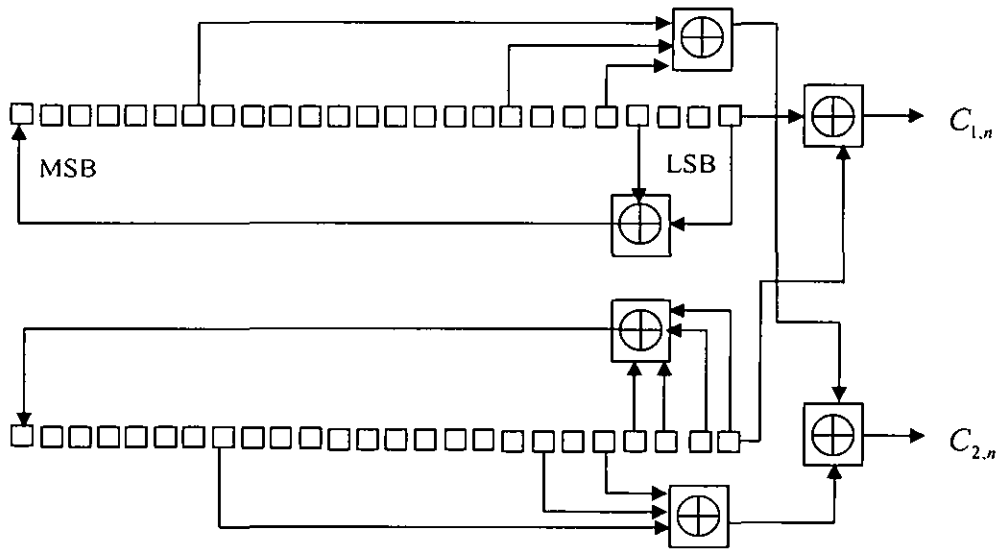


Figure 5.7: Uplink long scrambling code generator [6]

5.4.1.4.2 Properties of Uplink Long Scrambling Code

- The uplink long scrambling code has very good auto- and cross correlation properties. This is the only code that separates the asynchronous uplink users.
- Due to its good auto-correlation property, the unwanted correlation products from the desired user's multipaths will also be very small.

- The scrambling codes are designed so that they have very low cross correlation among them. This ensures good Multiple Access Interference (MAI) rejection capability

5.4.1.5 Summary of WCDMA Uplink Modulation

We can summarize the discussion on the modulation applied to the dedicated physical channels in the following table

Table 5.4: Parameters of WCDMA spreading and modulation at the uplink

Spreading Modulation	Dual Channel QPSK for UL
Data Modulation	BPSK for UL
Channelization	OVSF codes
Scrambling	Complex Scrambling
Frame Length	10 ms
Chip Rate	3.84 Mcps
Pulse Shaping	Raised Cosine with 0.22 roll off

5.4.2 Channel Coding

The main purpose of channel coding is to selectively introduce redundancy into the transmitted data and improve the wireless link performance in the process [3]. Channel codes can be used to detect as well as correct errors. The WCDMA systems have provision for both error detection and error correction. Channel coding scheme at the WCDMA system is a combination of error detection, error correction, along with rate matching, interleaving and transport channels mapping onto/splitting from physical channels [187]. This section gives a brief description on the error detection and error correction schemes recommended for the WCDMA systems

5.4.2.1 Error Detection

Error detection is provided by a Cyclic Redundancy Check (CRC) code. The CRC is 24, 16, 8 or 0 bits. The entire transmitted frame is used to compute the parity bits. Any of the following cyclic generator polynomials can be used to construct the parity bits:

$$\begin{aligned} g_{24}(D) &= D^{24} + D^{23} + D^6 + D^5 + D + 1 \\ g_{16}(D) &= D^{16} + D^{12} + D^5 + D + 1 \\ g_8(D) &= D^8 + D^7 + D^4 + D^3 + D + 1 \end{aligned} \tag{5.9}$$

A detailed description of the error detection scheme is given in [187].

5.4.2.2 Error Correction

Two alternative error correction schemes have been specified for the WCDMA system. They are Convolutional Coding and Turbo Coding. For standard services that require BER up to 10^{-3} , which is the case for voice applications, convolutional coding is to be applied. The constraint length for the proposed convolutional coding schemes is 9. Both rate 1/2 and 1/3 convolutional coding have been specified. For high-quality services that require BER from 10^{-3} to 10^{-6} , turbo coding is required. The feasibility of applying 4-state Serial Concatenated Convolutional Code (SCCC) has been investigated by different standardization bodies. Reference [187] provides a detailed description of the error correction coding schemes along with rate matching, interleaving and transport channel mapping. For the simulations performed for this research, we did not employ any error detection or error correction schemes.

5.5 Summary

In this chapter, we presented a short background on the generation of the uplink W-CDMA transmitting signal. We discussed about the designated uplink physical channels and their specific frame-slot format at the beginning. We then described the specific modulation and spreading techniques for the dedicated physical channel. For this, we

discussed the generation of the uplink spreading and scrambling codes, which are used in latter simulations. We also looked in the auto and cross correlation properties of these codes, which are crucial to justify the system performance in a qualitative manner. Even though our system does not incorporate channel coding, we looked into the proposed coding scheme for future reference. The information provided in this chapter is used extensively in the later chapters to develop our space-time processing simulation testbed.

CHAPTER SIX

SYSTEM MODELING & ANALYSIS

6.1 Introduction

In the previous chapters, we presented the necessary background for beamformer-Rake receiver structures, spatio-temporal channel models and the current W-CDMA uplink signal format. To integrate all these concepts in an orderly fashion, a mathematical formulation of the system is needed. In this chapter, we characterize the system by building mathematical models of different system components. This modeling is essential for understanding the functionality of the system as well as for analyzing the system performance. In addition, these models aid in building the simulation testbed of a base-station beamformer-Rake receiver for W-CDMA, which we will present in the next chapter. Also, a mathematical description of the system helps validate the simulation results.

We first formulate the transmitted signal in accordance with the W-CDMA uplink signal format. Then, the spatio-temporal channel is characterized by a simple parametric model. We then incorporated these models in building up a complete mathematical description of a pilot symbol assisted (PSA) coherent beamformer-Rake receiver at the base station. When necessary, the details of the functional block diagrams of different system components are included. Finally, we make a qualitative measure of the system by deriving its optimum output signal to interference plus noise ratio (SINR) performance.

The chapter is organized as follows: In section 6.2 we presented the W-CDMA uplink transmitter model. Section 6.3 gives a brief description of the spatio-temporal parametric channel model. In Section 6.4, the PSA 2-D RAKE receiver is analyzed using the input signal and channel models developed in the previous two sections. In section 6.5, we

derived the optimum output SINR performance of this space-time processing system. Finally a summary is given in section 6.6.

6.2 Transmitter Model

The block diagram of the W-CDMA uplink transmitter for the i th user as described in section 6.2 is shown in Figure 6.1.

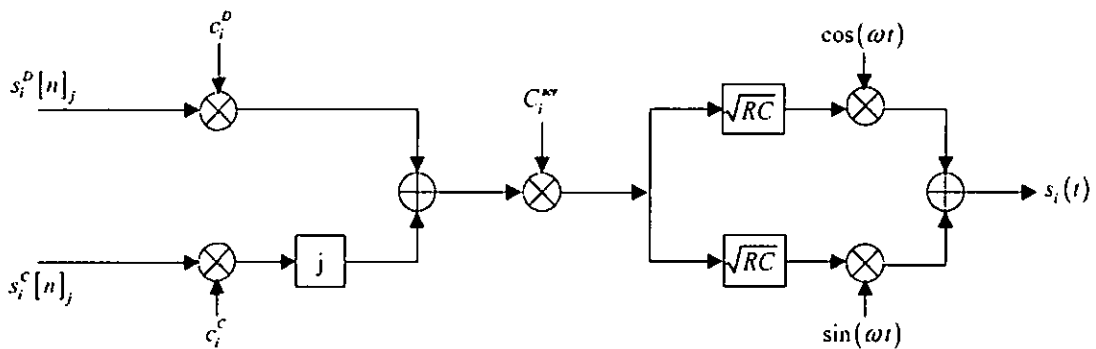


Figure 6.1: WCDMA uplink transmitter model [1]

For simplicity only one data channel (DPDCH) is shown even though the W-CDMA uplink transmitter can support up to six DPDCH. The sequences $b_i^D[n]$ and $b_i^C[n]$ are the channel coded data and control bits of the i th user respectively. In this development, these are the signals of interest, so the previous blocks such as coding and interleaving do not appear in the figure. They are mapped into the I and Q branches and subsequently spread by two different channelization code sequences c_i^D and c_i^C respectively. These codes commonly known as Orthogonal Variable Spreading Factor (OVSF) codes are orthogonal to each other and user specific. After channelization the two spreaded sequences are weighted by two different gain factors and combined orthogonally to form the baseband QPSK signal.

For simplicity of analysis, we will assume that the data and control channel have the same bit rate and the spreading factor. Then the $G_i \times 1$ spreaded chip sequence vector for the n th bit $v_i[n]$ can be expressed as

$$v_i[n] = v_i((n-1)G_i \dots nG_i) = \beta_i^D b_i^D[n] c_i^D + j \beta_i^C b_i^C[n] c_i^C; n = 1, 2, \dots, N_{Frame} \quad (6.1)$$

where n is the bit index, G_i is the i th user's spreading factor which is also the length of the channelization code vectors, c_i^D and c_i^C and β_i^D , β_i^C are the gain factor for i th user's DPDCH and DPCCCH respectively. The spreaded signal is further multiplied by a complex scrambling code, c_i^{scr} with a periodicity of one frame. The resulting signal is

$$\begin{aligned} s_i[n] &= v_i[n] \text{diag}(c_i^{scr}((n-1)G_i \dots nG_i)) \\ &= (\beta_i^D b_i^D[n] c_i^D + j \beta_i^C b_i^C[n] c_i^C) \text{diag}(c_i^{scr}[n]), n = 1, 2, \dots, N_{Frame} \end{aligned} \quad (6.2)$$

Where $\text{diag}(\cdot)$ is the diagonalization operation with the elements of $c_i^{scr}[n]$ along the main diagonal. The baseband discrete time signal is then pulse shaped by a root raised cosine filter and upconverted to form the transmitted waveform from the i th user as below

$$\begin{aligned} s_i(t) &= \sum_{n=1}^{N_{Frame}} s_i[n] c_i(t - nT_b) \exp(j\omega_c t + \phi_i) \\ &= \sum_{n=1}^{N_{Frame}} \beta_i^D b_i^D[n] \sum_{k=1}^{G_i} c_i^D(k) c_i^{scr}((n-1)G_i + k) g(t - (nG_i + k)T_c) \cos(\omega_c t + \phi_i) \\ &\quad - \beta_i^C b_i^C[n] \sum_{k=1}^{G_i} c_i^C(k) c_i^{scr}((n-1)G_i + k) g(t - (nG_i + k)T_c) \sin(\omega_c t + \phi_i). \end{aligned} \quad (6.3)$$

where $g(t)$ is the chip pulse shaping waveform, T_b and T_c is the bit and chip duration respectively, ω_c is the angular carrier frequency and ϕ_i is an unknown carrier phase. The transmitted signal is propagated through the channel characterized in the next section.

6.3 Channel Description

The spatio-temporal channel models described in Chapter 4 provides a statistical description of the multipaths channel parameters such as channel gain, propagation delays, angle of arrivals (AOA) etc. However, for the purpose of analysis, a simple parametric model represented by a summation of delta functions associated with different amplitudes, time delays and AOA is more useful. Each of these delta functions corresponds to a resolvable multipath in a frequency selective fading channel, as is the case for a W-CDMA signal. Thus the channel impulse response formed in this manner provides a mean description of the statistically distributed channel parameters in both space and time.

An important parameter that characterizes the spatial channel is the angle spread, Δ defined as the spread of the AOA of the discrete multipath components. In other words, each of the delta functions in the channel impulse response is in reality a combination of a number of delta functions (subpaths), which arrive very closely in time but may have different directions. The range of the AOA of these subpaths is characterized by the angle spread. As we will see, this parameter has an important effect on different array processing and combining techniques.

As mentioned earlier, a W-CDMA system undergoes frequency selective fading when the relative multipaths delays are more than a chip period. This time dispersiveness property of the channel is characterized by the delay spread defined in a similar way as the angle spread. That is, delay spread is a measure of spread of the multipaths in time domain. Thus, it will determine the performance of time domain processing schemes such as RAKE combining.

The time-varying property of the channel model is defined by the doppler spread. For the spatio-temporal channel models, an accurate description of doppler power spectrum is still to be formulated. However in this analysis and in our simulation we will be assuming

a Rayleigh faded temporal characteristics of the channel since it gives a close enough power spectrum to the models in chapter 4 [180], [184].

Let us consider an N -element linear antenna array at the receiver. The channel impulse response of the i th user can be expressed as

$$h_i(t) = \sum_{l=1}^{L_i} \alpha_{l,i}(t) a(\theta_{l,i}) \delta(t - \tau_{l,i}) \quad (6.4)$$

Where L_i is the number of resolvable multipaths from the i th user each characterized by a complex path amplitude $\alpha_{l,i}(t)$ and a path delay $\tau_{l,i}$. The $N \times 1$ array response vector or the steering vector $a(\theta_{l,i})$ is defined as

$$a(\theta_{l,i}) = \left[1 \quad e^{-j2\pi \frac{d}{\lambda} (N-1) \sin(\theta_{l,i} + \Delta_i)} \quad \dots \quad e^{-j2\pi \frac{d}{\lambda} (N-1) \sin(\theta_{l,i} + \Delta_i)} \right]^T \quad (6.5)$$

where d is the element spacing and $\theta_{l,i}$ is the AOA of the l th path from i th user and Δ_i is the angle spread of the i th user. In the analysis, we will use the narrowband assumption for array processing which states that the envelope of the plane wave propagating across the array remains essentially constant if the bandwidth of either the signal or the antenna is small compared to the carrier frequency. For the wideband case, this assumption is also valid provided that the time taken by the wavefront to pass across the array is small compared to the chip period T_c . Equation (6.4) can be rearranged as

$$h_i(t) = \sum_{l=1}^{L_i} a_{l,i}(t) \delta(t - \tau_{l,i}) \quad (6.6)$$

where $a_{l,i}(t) = \alpha_{l,i}(t) a(\theta_{l,i})$ is called the spatial signature vector or the channel vector of the i th user. Thus this channel model is equivalent to a tapped delay line filter with the power spectrum defining the time varying filter coefficients.

6.4 Receiver Model

The receiver portion at the base station intended to detect the i th user in the uplink is shown in Figure 6.2.

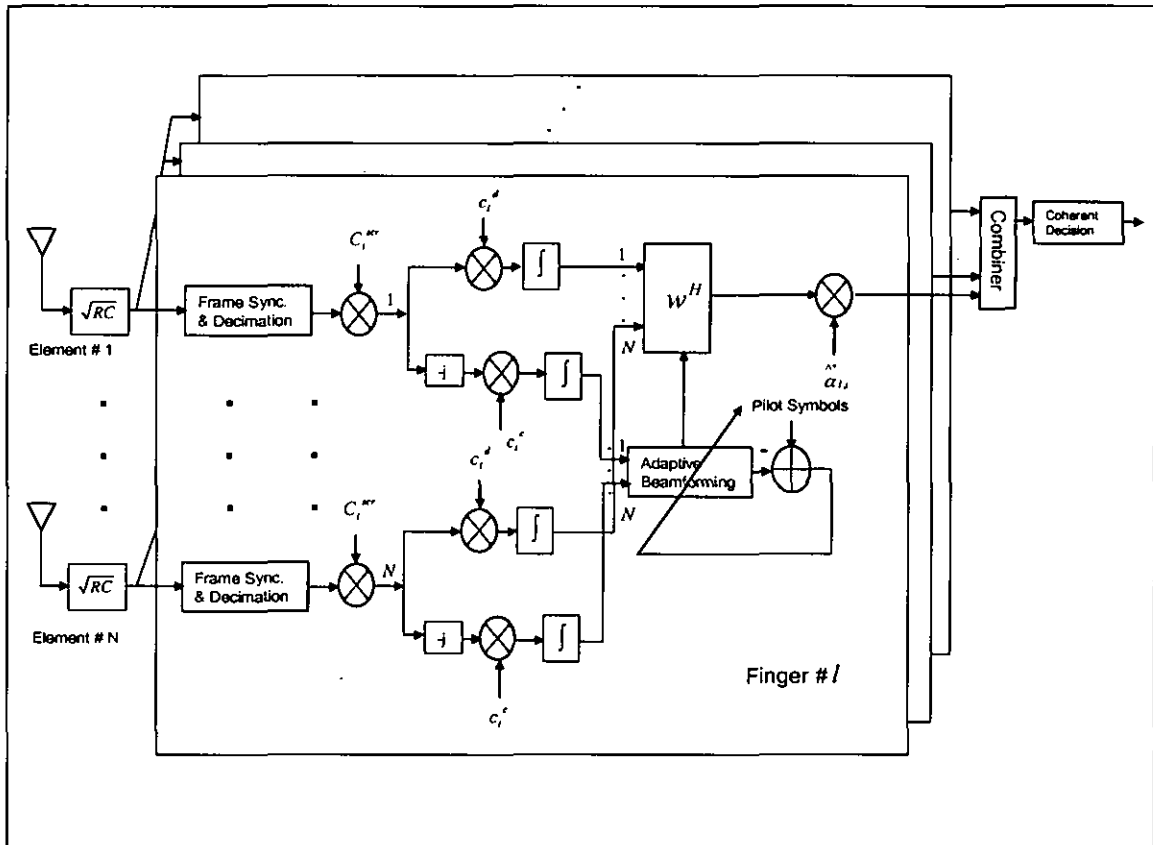


Figure 6.2: Base station antenna array receiver model [1]

The base station uses an N element antenna array receiver to demodulate the desired user's signal. After downconversion and lowpass filtering, the baseband received signal is processed by a bank of M space-time processors each assigned to one of the resolvable multipaths. To detect the l th path, the signals at different antenna elements are first time aligned to the l th path delay and discretized to form the chip samples. Then a descrambling operation is performed at each element of the antenna array followed by the despreading using the data and the control channel channelization codes. An adaptive beamforming network then takes the despreaded control channel symbols as the input and

calculates the beamformer weights using the pilot symbols in the control channel as the reference signal. Typically gradient-based algorithms such as Least-Mean Square (LMS) algorithm or the standard Recursive Least Square (RLS) algorithm are considered. The weights are updated in each slot of the W-CDMA frame and used on both the data and control channel symbols for beamforming. The outputs of the M beamformer are then coherently combined (MRC RAKE combining) by the modified channel gain through the beamformer and hard limited to get the coherent symbol decision.

The total received $N \times 1$ signal vector at the base station antenna array is given by

$$x(t) = \sum_{i=1}^K \sum_{l=1}^{L_i} a_{l,i}(t) s_i(t - \tau_{l,i}) + \eta(t) \quad (6.7)$$

where K is the total number of users in the system and $\eta(t)$ is the $N \times 1$ complex additive Gaussian noise vector with zero mean and a variance of $\sigma_n^2 = N_0/2$. All the other symbols have the same meaning as in section 6.2 and 6.3. It is assumed that the noise vector is spatially and temporally white, i.e., $E\{\eta(t_1)\eta^H(t_2)\} = \sigma_n^2 \delta(t_1 - t_2)$, where $(.)^H$ is the Hermitian (conjugate transpose) operator.

Without loss of generality, let us consider the operation of the receiver for the l th path of i th user. After downconversion, the received signal is synchronized to the l th multipath delay $\tau_{l,i}$ and low-pass filtered (root raised cosine matched filtering). The resulting discrete signal can be expressed as

$$X_{l,i}[n] = A_{l,i}[n] \text{diag}(s_i[n]) + I[n] + M[n] + N[n] ; \quad n = 1, 2, \dots, N_{Frame} \quad (6.8)$$

where again n is the bit index, $X_{l,i}[n]$ and $N[n]$ are $N \times G_i$ received chip sample matrix and sampled noise matrix respectively, $A_{l,i}[n]$ is the $N \times G_i$ discrete channel matrix for the l th path of user i , $s_i[n]$ is the $G_i \times 1$ transmitted chip sequence vector for the user i as given

by (6.2). The $N \times G_i$ matrices, $I[n]$ and $M[n]$ are the user's self interference due to multipaths and the multiple access interference (MAI) from all the other users and they are expressed as

$$I[n] = \sum_{\substack{l'=1 \\ l' \neq l}}^{L_r} A_{l',i}[n] \text{diag} \left(s_i \left[n - \left\lfloor \frac{\tau_{l',i} - \tau_{l,i}}{T_c} \right\rfloor \right] \right) \quad (6.9)$$

$$M[n] = \sum_{\substack{l'=1 \\ l' \neq i}}^K \sum_{l=1}^{L_r} A_{l,i'}[n] \text{diag} \left(s_{i'} \left[n - \left\lfloor \frac{\tau_{l,i'} - \tau_{l,i}}{T_c} \right\rfloor \right] \right)$$

Substituting (6.2) in (6.9) and treating the summation of $I[n]$, $M[n]$ and $N[n]$ as a single interference plus noise matrix, $\hat{N}[n]$, the received discrete chip samples for n th bit

$$X_{l,i}[n] = A_{l,i}[n] \text{diag} \left((\beta_i^D b_i^D[n] c_i^D + j \beta_i^C b_i^C[n] c_i^C) \text{diag}(c_i^{scr}[n]) \right) + \hat{N}[n] \quad (6.10)$$

At each antenna element, the signal is descrambled by the i th user's scrambling code sequence, c_i^{scr} as below

$$X_{l,i}^{dscr}[n] = X_{l,i}[n] \text{diag} \left((c_i^{scr})^* \right) = A_{l,i}[n] \text{diag} \left(b_i^D[n] c_i^D + j b_i^C[n] c_i^C \right) + \hat{N}_{dscr}[n] \quad (6.11)$$

where it is assumed that the amplitudes of the complex scrambling sequence, $c_i^{scr}[n]$ is normalized to unity. The resulting $N \times G_i$ interference plus noise matrix after descrambling, $\hat{N}_{dscr}[n]$ is given by

$$\begin{aligned} \hat{N}_{dscr}[n] &= I_{dscr}[n] + M_{dscr}[n] + N_{dscr}[n] \\ &= I[n] \text{diag}(c_i^{scr}[n]) + M[n] \text{diag}(c_i^{scr}[n]) + N[n] \text{diag}(c_i^{scr}[n]) \end{aligned} \quad (6.12)$$

As shown in chapter 5, the W-CDMA uplink long scrambling code, c_i^{scr} has very good auto and cross correlation properties. That means, the auto and cross correlation function of c_i^{scr} can be approximated as

$$E\{c_i^{scr}[p](c_i^{scr}[q])^*\} \cong \delta_{i,i'}(p-q), \quad p, q = 1, 2, \dots, C_{Frame} \quad i \neq i' \quad (6.13)$$

Then this has the effect of making the elements of the descrambled interference plus noise matrix, $\hat{N}_{dscr}[n]$ uncorrelated. Subsequent despreading of the resultant signal by the $G_i \times 1$ data and control channelization code vectors, c_i^D and c_i^C , respectively, collapses the chip samples over a code length into one data and control channel bit. The resulting despread data and control bits can be expressed as

$$\begin{aligned} x_{i,i}^D[n] &= \frac{1}{G_i} X_{dscr}[n] c_i^D = a_{i,i}[n] \beta_i^D b_i^D[n] + \hat{\eta}_i^D[n] \\ x_{i,i}^C[n] &= \frac{1}{G_i} (-j) X_{dscr}[n] c_i^C = a_{i,i}[n] \beta_i^C b_i^C[n] + \hat{\eta}_i^C[n] \end{aligned} \quad (6.14)$$

Where $a_{i,i}[n] = \alpha_{i,i}[n] a(\theta_{i,i})$ is the $N \times 1$ channel vector for the n th bit, $\hat{\eta}_i^D[n]$ and $\hat{\eta}_i^C[n]$ are $N \times 1$ total interference plus noise vectors for the n th bit associated with data and control channel, respectively. It is intuitive from the previous statements that the elements of the interference plus noise vectors will also be uncorrelated. Also, it is shown analytically in [188] and by simulation in [189] that when the number of user is large (heavily loaded system), autocorrelation matrices of these interference plus noise vectors are close to scaled identity matrices, which is what we expect if they are composed of independent elements. That is

$$\begin{aligned} R_{uu}^D[n] &= E\{\hat{\eta}_i^D[n](\hat{\eta}_i^D[n])^H\} \cong \sigma_{\hat{\eta}_i^D}^2 \mathbf{I} \\ R_{uu}^C[n] &= E\{\hat{\eta}_i^C[n](\hat{\eta}_i^C[n])^H\} \cong \sigma_{\hat{\eta}_i^C}^2 \mathbf{I} \end{aligned} \quad (6.15)$$

where $\sigma_{\hat{\eta}_i^D}^2$ and $\sigma_{\hat{\eta}_i^C}^2$ are the variances of $\hat{\eta}_i^D[n]$ and $\hat{\eta}_i^C[n]$ respectively and I is an $N \times N$ identity matrix. The despreaded control channel signal has a factor of $-j$ in its expression indicating the fact that it was mapped into the Q-branch in the original transmitted signal.

As mentioned in chapter 5, the current W-CDMA uplink signal format defines pilot bits in the control channel. Therefore, any beamformer that uses the pilot bits as the reference signal should take the despreaded control channel bits as the input. We considered three different pilot symbol assisted (PSA) beamforming techniques: Minimum Mean Squared Error (MMSE) based Direct Matrix Inversion (DMI) beamforming, Least Mean Square (LMS) and Recursive Least Square (RLS) adaptive beamforming. They are explained in the following sections.

6.4.1 Direct Matrix Inversion (DMI) beamforming

The DMI beamformer minimizes the mean squared error between the beamformer output and the reference signal [190], [183]. Denoting the reference signal as $d[n]$ and the input signal to the N -element beamformer as $x[n]$, the optimum weight vector estimate is given by the Wiener-Hopf (W-H) equation as below

$$\hat{w}_{OPT} = \hat{R}_{xx}^{-1} \hat{r}_{xd} \quad (6.16)$$

where the $N \times N$ matrix, \hat{R}_{xx} is a windowed estimate of the sample autocorrelation matrix, R_{xx} and is usually given by

$$\hat{R}_{xx}[i] = \sum_{n=1}^i \lambda^{i-n} x[n] x^H[n], \quad 1 \leq n \leq i \quad (6.17)$$

where λ is a weighting factor or forgetting factor defined over the interval (0,1]. The value of λ determines how much past information will be used to calculate the sample correlation matrix. For a nonstationary fading channel, λ is usually less than 1, which

defines an exponential window, thus ensuring that the data in the distant past is forgotten in order to account for the statistical variation of the data samples. For fading channels, λ is chosen so that the window length extends over the coherence time of the channel, i.e., the time over which the fading can be considered correlated. For a stationary channel, λ is taken as 1.

The $N \times 1$ vector, \hat{r}_{xd} , in (6.16) is an estimate of the sample cross correlation vector between $x[n]$ and $d[n]$ and is defined in the same way as \hat{R}_{xx} , i.e.,

$$\hat{r}_{xd}[i] = \sum_{n=1}^i \lambda^{i-n} x[n] d^*[n] ; \quad 1 \leq n \leq i \quad (6.18)$$

where the symbols have the same meaning as before. Equations (6.17) and (6.18) can be written in a recursive fashion as below

$$\begin{aligned} \hat{R}_{xx}[i] &= \lambda \left[\sum_{n=1}^{i-1} \lambda^{i-1-n} x[n] x^H[n] \right] + x[i] x^H[i] = \lambda \hat{R}_{xx}[i-1] + x[i] x^H[i] \\ \hat{r}_{xd}[i] &= \lambda \left[\sum_{n=1}^{i-1} \lambda^{i-1-n} x[n] d^*[n] \right] + x[i] d^*[i] = \lambda \hat{r}_{xd}[i-1] + x[i] d^*[i] \end{aligned} \quad (6.19)$$

As mentioned earlier, the despreaded control channel signal, $x_{l,i}^c[n]$ as given in (6.14) is the input to the l th beamformer designated for the i th user. The reference signal, $d[n]$ is the pilot in the control channel of the uplink W-CDMA signal. For each slot of a frame, the weight vectors are calculated using the pilot bits for that slot. The auto and cross correlation estimates at the end of a slot are used to update the estimates for the next slot according to (6.19). Thus if N_d is the number of pilot bits per slot, then the weight vector of the l th beamformer for the j th slot is given by

$$w_l^j = \left(\hat{R}_{x_c x_c}^j[N_d] \right)^{-1} \hat{r}_{x_c d}^j[N_d] ; \quad j = 1, 2, \dots, 15 \quad (6.20)$$

where

$$\begin{aligned}
\hat{R}_{x_c x_c}^j[N_d] &= \hat{R}_{x_c x_c}^{j-1}[N_d] + \sum_{n=(j-1)N_d+1}^{jN_d} \lambda^{jN_d-n} x_{l,i}^c[n] (x_{l,i}^c[n])^H \\
&= \hat{R}_{x_c x_c}^{j-1}[N_d] + \lambda \hat{R}_{x_c x_c}^j[N_d - 1] + x_{l,i}^c[N_d] (x_{l,i}^c[N_d])^H
\end{aligned} \tag{6.21}$$

$$\begin{aligned}
\hat{r}_{x_c d}^j[N_d] &= \hat{r}_{x_c d}^{j-1}[N_d] + \sum_{n=(j-1)N_d+1}^{jN_d} \lambda^{jN_d-n} x_{l,i}^c[n] (d^j[n])^* \\
&= \hat{r}_{x_c d}^{j-1}[N_d] + \lambda \hat{r}_{x_c d}^j[N_d - 1] + x_{l,i}^c[N_d] (d^j[N_d])^*
\end{aligned}$$

where $d^j[n]$, $n=1, 2, \dots, N_d$ are the pilot bits for the j th slot.

6.4.2 Least Mean Square (LMS) Adaptive beamforming

The DMI method as described in section 6.4.1 requires the inversion of the autocorrelation matrix R_{xx} , which involves a significant amount of computation. An attractive solution to this problem is the use of Least Mean Square (LMS) adaptive algorithm, which is a member of the so-called stochastic gradient descent algorithms [191]. The basic idea of the LMS algorithm is that it tries to get an instantaneous (symbol by symbol) estimate of the gradient vector of the cost function, which in this case is the Mean Squared error (MSE) between the reference signal and the beamformer output. In this respect, the LMS algorithm differs from the steepest descent method of solving the W-H equation in that the gradient vector estimation does not require a large windowed estimate of the correlation functions [191]. In other words, the algorithm uses a one-symbol data window to get a noisy estimate of these functions and consequently adapts to the incoming data in order to converge to the optimum Wiener solution given by (6.16).

The weight vector update using the LMS algorithm is given by the following recursive formula

$$\hat{w}[n+1] = \hat{w}[n] + \mu x[n] e^*[n] \tag{6.22}$$

where $x[n]$ is the beamformer input. $e[n]$ is the estimation error between the beamformer output and the reference signal, $d[n]$, and is represented as

$$e[n] = d[n] - \hat{w}[n]^H x[n] \quad (6.23)$$

The parameter μ in (6.22) is a small positive constant that defines the step size of the incremental correction of the weight vector. The convergence of the algorithm towards the optimum weight vector depends on the selection of μ . A larger value of μ drives the algorithm faster towards convergence but has the risk of not achieving the minimum value of the cost function and instability. On the other hand, a smaller value of μ increases the probability of reaching the minimal point but it suffers from slower convergence.

Referring to the W-CDMA frame format, the antenna weight vectors are updated in each slot using the pilot bits for that slot. The weight vector calculated at the end of a slot is used as the initial weight vector for the weight updation in the next slot. Thus the weight update equation for the j th slot can be represented as

$$\begin{aligned} w_l^j[1] &= w_l^{j-1}[N_d] \\ w_l^j[n+1] &= w_l^j[n] + \mu x_{l,i}^c[(j-1)N_d + n](e^j[n])^* ; \quad n = 1, 2, \dots, N_d \end{aligned} \quad (6.24)$$

where as in section (6.4.1), N_d is the number of pilot bits per slot and $x_{l,i}^c[n]$ is the beamformer input given by the despread control channel signal in (6.14). The error signal for the j th slot, $e^j[n]$ is expressed as below

$$e^j[n] = d^j[n] - (w_l^j[n])^H x_{l,i}^c[(j-1)N_d + n] ; \quad n = 1, 2, \dots, N_d \quad (6.25)$$

6.4.3 Recursive Least Square (RLS) Adaptive Beamforming

The RLS algorithm is a recursive technique that gives an approximate least-square (LS) estimate of the antenna weight vectors. Thus the cost function of the RLS algorithm is the sum of the squared errors over a sample window as opposed to the ensemble average of the squared error (MSE) in the LMS algorithm [191].

The key feature of the RLS algorithm is an iterative technique that estimates the inverse of the windowed autocorrelation function, R_{xx} . The steps of the RLS algorithm are given below

$$\begin{aligned}
 k[n] &= \frac{\lambda^{-1} P[n-1] x_c[n]}{1 + \lambda^{-1} x_c^H[n] \lambda^{-1} P[n-1] x_c[n]} \\
 \alpha[n] &= d[n] - \hat{w}^H[n-1] x_c[n] \\
 \hat{w}[n] &= \hat{w}[n-1] + k[n] \alpha^*[n] \\
 P[n] &= \lambda^{-1} P[n-1] - \lambda^{-1} k[n] x_c^H[n] P[n-1]
 \end{aligned} \tag{6.26}$$

where $x[n]$, $d[n]$ and λ have the same meaning as in sections (6.4.1) and (6.4.2). The $N \times N$ matrix, $P[n]$ which is updated recursively in the algorithm, is an estimate of the inverse of the autocorrelation matrix, $R_{xx}[n]$. The initial value of $P[n]$ is usually set as

$$P[0] = \delta^{-1} \mathbf{I} \tag{6.27}$$

where \mathbf{I} is the $N \times N$ identity matrix and δ is a small positive constant. As in the case of the LMS algorithm, the antenna weight vectors are updated in each slot using the pilot bits for that slot and the weights calculated at the end of a slot are used to initialize the algorithm in the next slot.

In all the three beamforming techniques described above, the weight vectors are calculated on a slot by slot basis either by taking all the pilot bits in a slot to form the

correlation estimates as in DMI or by updating the weights recursively with each pilot bits in the slot as in LMS or RLS. Thus the weight vector associated with a particular control channel slot can be used to beamform both the corresponding data and control channel slot. Continuing from Equation (6.15), the output of the l th beamformer for the j th data and control channel slot can be expressed as

$$\begin{aligned} z_{l,i}^D[n] &= (w_l^j)^H x_{l,i}^D(n)_j \\ z_{l,i}^C[n] &= (w_l^j)^H x_{l,i}^C(n)_j ; \quad n = (j-1)N_d, \dots, jN_d, \quad j = 1, \dots, \frac{N_{frame}}{N_d} \end{aligned} \quad (6.28)$$

where again j is the slot index, w_l^j is the weight vector for the j th slot and $x_{l,i}^D[n]_j$ and $x_{l,i}^C[n]_j$ are the despread data and control channel bits respectively for the j th slot given by (6.12). Substituting (6.12) in (6.13)

$$\begin{aligned} z_{l,i}^D[n]_j &= (w_l^j)^H a_{l,i}[n] \beta_i^D b_i^D[n] + (w_l^j)^H \hat{\eta}_l^D[n] \\ z_{l,i}^C[n]_j &= (w_l^j)^H a_{l,i}[n] \beta_i^C b_i^C[n] + (w_l^j)^H \hat{\eta}_l^C[n] \end{aligned} \quad (6.29)$$

In the receiver, each RAKE finger is associated with a beamformer dedicated to a specific spatio-temporal multipath. Thus, to coherently combine all the beamformer outputs the channel gains for all these paths need to be estimated. The modified channel gain at the beamformer output is given by

$$\hat{\alpha}_{l,i}[n]_j = (w_l^j)^H a_{l,i}[n] ; \quad n = (j-1)N_d, \dots, jN_d, \quad l = 1, 2, \dots, M \quad (6.30)$$

where $a_{l,i}[n] = \alpha_{l,i}[n] a(\theta_{l,i})$ is the $N \times 1$ channel vector for the n th bit and M is the number of RAKE fingers used in the receiver. In practice, this modified channel gain for each path is estimated by some sort of weighted average of the pilot bits in a single or multiple control channel slots. The output of the MRC coherent RAKE combiner is then expressed as

$$\begin{aligned}
 z_i^D[n]_j &= \sum_{l=1}^M z_{l,i}^D[n]_j (\hat{\alpha}_{l,i}[n]_j)^* \\
 z_i^C[n]_j &= \sum_{l=1}^M z_{l,i}^C[n]_j (\hat{\alpha}_{l,i}[n]_j)^* ; \quad n = (j-1)N_d, \dots, jN_d
 \end{aligned} \tag{6.31}$$

where the respective symbols have the same meaning as described before. The soft decisions, $z_i^D[n]$ and $z_i^C[n]$ are then hard-limited to get coherent decisions for the uncoded data and control channel bits.

6.5 Generalized Optimum Output SINR Analysis

In this section, the output SINR expression of the beamformer-Rake receiver employing a general optimum beamformer is derived. The approach followed here is similar to the one used in [188] and [180]. The assumptions made here will be to be validated in our future research.

The optimum weight vectors for the l th beamformer is well known to be given by [191]

$$\begin{aligned}
 w_{l,OPT}^D &= \gamma_l^D (R_{uu}^D[n])^{-1} a_{l,i}[n] \\
 w_{l,OPT}^C &= \gamma_l^C (R_{uu}^C[n])^{-1} a_{l,i}[n]
 \end{aligned} \tag{6.32}$$

where γ_l^D and γ_l^C are arbitrary constants, $R_{uu}^D[n]$ and $R_{uu}^C[n]$ the data and control interference plus noise correlation matrices respectively given as (6.15) and $a_{l,i}[n]$ is the channel vector defined in (6.15). In the case, if $R_{uu}^D[n]$ and $R_{uu}^C[n]$ can be approximated by identity matrices, the optimum weight vectors become

$$\begin{aligned}
 w_{l,OPT}^D &\cong \gamma_l^D \sigma_{\hat{\eta}_l^D}^2 a_{l,i}[n] \\
 w_{l,OPT}^C &\cong \gamma_l^C \sigma_{\hat{\eta}_l^C}^2 a_{l,i}[n]
 \end{aligned} \tag{6.33}$$

As can be seen when the interference and noise is white, the solution becomes the MRC diversity combining.

Substituting (6.32) in (6.29), the l th beamformer output can be expressed as

$$\begin{aligned} z_{l,i}^D[n] &= (\gamma_l^D)^* a_{l,i}^H[n] (R_{uu}^D[n]^{-1})^H a_{l,i}[n] \beta_i^D b_i^D[n] + (\gamma_l^D)^* a_{l,i}^H[n] (R_{uu}^D[n]^{-1})^H \hat{\eta}_l^D[n] \\ z_{l,i}^C[n] &= (\gamma_l^C)^* a_{l,i}^H[n] (R_{uu}^C[n]^{-1})^H a_{l,i}[n] \beta_i^C b_i^C[n] + (\gamma_l^C)^* a_{l,i}^H[n] (R_{uu}^C[n]^{-1})^H \hat{\eta}_l^C[n] \end{aligned} \quad (6.34)$$

According to (6.30), the weights of the RAKE combiner is then

$$\begin{aligned} \hat{\alpha}_{l,i}^D[n] &= (w_{l,OPT}^D)^H a_{l,i}[n] = (\gamma_l^D)^* a_{l,i}^H[n] (R_{uu}^D[n]^{-1})^H a_{l,i}[n] \\ \hat{\alpha}_{l,i}^C[n] &= (w_{l,OPT}^C)^H a_{l,i}[n] = (\gamma_l^C)^* a_{l,i}^H[n] (R_{uu}^C[n]^{-1})^H a_{l,i}[n] \end{aligned} \quad (6.35)$$

Substituting (6.34) and (6.35) in (6.28), the output of the RAKE combiner is then

$$\begin{aligned} z_i^D[n] &= \sum_{l=1}^M z_{l,i}^D[n] (\hat{\alpha}_{l,i}[n])^* = \sum_{l=1}^M |\gamma_l^D|^2 \|a_{l,i}[n]\|^4 \beta_i^D b_i^D[n] + \sum_{l=1}^M \hat{\eta}_l'^D[n] \\ z_i^C[n] &= \sum_{l=1}^M z_{l,i}^C[n] (\hat{\alpha}_{l,i}[n])^* = \sum_{l=1}^M |\gamma_l^C|^2 \|a_{l,i}[n]\|^4 \beta_i^C b_i^C[n] + \sum_{l=1}^M \hat{\eta}_l'^C[n] \end{aligned} \quad (6.36)$$

where the noise and interference terms $\hat{\eta}_l^D[n]$ and $\hat{\eta}_l^C[n]$ are given by

$$\begin{aligned} \hat{\eta}_l'^D[n] &= |\gamma_l^D|^2 a_{l,i}^H[n] (R_{uu}^D[n]^{-1})^H \hat{\eta}_l^D[n] a_{l,i}[n] R_{uu}^D[n]^{-1} a_{l,i}[n] \\ \hat{\eta}_l'^C[n] &= |\gamma_l^C|^2 a_{l,i}^H[n] (R_{uu}^C[n]^{-1})^H \hat{\eta}_l^C[n] a_{l,i}[n] R_{uu}^C[n]^{-1} a_{l,i}[n] \end{aligned} \quad (6.37)$$

The output signal to noise plus interference ratio (SINR) then is given by

$$SINR_{OPT}^D = \frac{\beta_i^D E\{|b_i^D|^2\} \sum_{l=1}^M |\gamma_l^D|^2 \|a_{l,i}[n]\|^4}{E\left\{\left|\sum_{l=1}^M \hat{\eta}_l'^D[n]\right|^2\right\}} \quad (6.38)$$

$$SINR_{OPT}^C = \frac{\beta_i^C E\left\{\left|b_i^C\right|^2\right\} \sum_{l=1}^M\left|\gamma_l^C\right|^2\left\|a_{l,i}[n]\right\|^4}{E\left\{\left[\sum_{l=1}^M \hat{\eta}_l^C[n]\right]^2\right\}}$$

6.6 Summary

In this chapter, we developed the mathematical model of our proposed space-time processing system for W-CDMA. The formulation started with a model of the W-CDMA uplink transmitter. A simple characterization of the spatio-temporal channel suitable for the analytical purpose is presented. Using these two formulations we then extensively analyze a PSA coherent space-time RAKE receiver intended for the base station.

CHAPTER SEVEN

SIMULATION RESULTS AND DISCUSSION

FOR UPLINK-DOWNLINK SCENARIOS

7.1 Introduction for Uplink Scenario

In the previous chapter, we present a detailed mathematical description of our proposed PSA space-time beamformer-Rake receiver for the W-CDMA system. We formulate the W-CDMA transmitter model and the spatio-temporal channel model and use those to analyze the receiver. In doing so, we get a qualitative measure of the performance of a beamformer-Rake receiver in a frequency selective multipath channel with MAI. In this chapter, we quantify the performance by simulating the PSA beamformer-Rake receivers in the GBSB circular channel with the uplink W-CDMA signal standard. We consider the LMS, DMI and RLS based PSA beamforming techniques with varying number of antenna elements. We also consider MRC coherent RAKE receiver with different number of fingers. We compare the performance of these different PSA beamformer-Rake receivers with the conventional (1-D) RAKE receivers and the conventional PSA based beamformer. We simulate the receiver operation in channel conditions that show the performance trade-off between array processing and RAKE combining. Performances are compared in terms of three parameters: antenna elements, RAKE fingers and beamforming algorithms. Both the BER versus number of users and the BER versus E_b/N_0 performances are considered.

The chapter is organized as follows: In section 7.2, we present the simulation set up for the proposed system. We describe the transmitter specifications for the W-CDMA used in the simulation. In section 7.3, the multipath channel generation is discussed. Section 7.4 presents the block diagram of the receiver used in the simulation. Section 7.5 provides the parameters to create the simulation environment. In section 7.6, we present the simulation

results along with the relevant discussion. Finally we conclude the chapter with a brief summary in section 7.7.

7.2 Simulation Set Up for Uplink

7.2.1 Transmitter Specifications

The W-CDMA uplink physical channels have a frame/slot structure as described in chapter 5 [1]. The frame length is 10 ms and it comprises of 15 slots with duration of 0.667 ms each. The uncoded DPDCH and DPCCH bits are channel coded by a convolutional encoder and subsequently mapped into I and Q channels respectively. In the simulation, we assume that the channel coding is already performed so that the signals of interest are the encoded DPDCH and DPCCH bits. The encoded DPDCH bits are Binary Phase Shift Keying (BPSK) modulated and grouped into 80 symbols to form one DPDCH slot so that the resulting data symbol rate is 120ksps. Similarly, the encoded DPCCH bits are also BPSK modulated to form the antipodal signal. Each DPCCH slot has 8 pilot symbols time multiplexed with 2 TPC symbols resulting in a control symbol rate of 15 ksps. The uplink frame/slot parameters are listed in Table 7.1.

Table 7.1: Uplink WCDMA Frame-Slot parameters

Frame duration		10 ms
Frame rate		100 frames/sec
Slots/frame		15
Slot duration		0.667 ms
Slot rate		1500 slots/sec
Symbol/slot	DPDCH	80
	DPCCH	10
DPCCH slot field*	Pilot	8
	TPC	2
	TFCI	0
	FBI	0

* DPCCH slot fields are described in chapter 5

It is assumed that each uplink user has only one DPDCH even though the maximum possible DPDCH that can be assigned to a particular user is six. The spreading factor (SF) for each user's DPDCH is taken to be 32. The SF for the DPCCH is always set at 256. For spreading, orthogonal variable spreading factor (OVSF) codes are used which are explained in chapter 5. Each uplink user's DPDCH is spreaded by a length 32 OVSF code, $C_{32,9}$, where the 1st index is the level in the code tree and the 2nd index is the code number in that particular level. The spreading code for DPCCH is a length 256 sequence of all 1's. Both the DPDCH and DPCCH gain factors are set at 1. The spreaded I and Q channels are QPSK modulated and the resulting complex chip sequence has a rate of 3.84 Mcps. A user specific complex long scrambling code with a repetition period of 38400 chips (1 frame) is used to multiply the QPSK chip sequence. The scrambling code is generated uniquely for a specific code user and is described in details in chapter 5. Each scrambled chip samples are then upsampled by a factor of 4. Finally, to confine the spreaded wideband signal within the 5 MHz allocated bandwidth for uplink, a square-root raised cosine Nyquist transmitter filter with a roll off factor of 0.22 is applied. The resulting pulse-shaped signal is the transmitted baseband signal from an uplink user. The major transmitter parameters used in simulation are listed in Table 7.2.

Table 7.2: Uplink WCDMA transmitter parameters for simulation

Dedicated physical channels	DPDCH	1
	DPCCH	1
Data modulation	DPDCH	BPSK
	DPCCH	BPSK
Spreading factor	DPDCH	32
	DPCCH	256
Spreading code (OVSF) *	DPDCH	$C_{32,9}$
	DPCCH	$C_{256,1}$
Symbol rate	DPDCH	120 ksps
	DPCCH	15 ksps
Gain factor	DPDCH	1.0
	DPCCH	1.0
Spreading (chip) modulation		Dual Channel QPSK
Scrambling code		Uplink long scrambling code
Chip rate		3.84 Mcps
Oversampling factor		4 samples/chip
Pulse shaping		Root RC with roll-off 0.22
Carrier frequency		1.92 GHz

* OVSF codes $C_{SF,k}$ are described in chapter 5

7.3 Multipath Channel Generation for Uplink

7.3.1 Macrocelluar Environments

Macrocells correspond to large cells where base station has relatively high antenna. The propagation path length can be up to several miles. Typically users are considered to be within 10 km of the base station. Circular channel models are more appropriate in such environments, which depicts suburban and rural multipath propagation scenario. We considered three-sectored base station with a linear antenna array for each 120° sector is considered. The element spacing is set at 0.5λ where λ is the wavelength of the transmitted W-CDMA waveform with a carrier frequency of 1.92 GHz. As described in chapter 4, each user has a circular region of large reflectors surrounding it. The radius of the circle is again determined by the maximum multipath delay relative to the LOS path delay. In accordance with the ETSI's vehicular A channel, the maximum relative multipath delay for all the users are against to be 8 W-CDMA chip period (1 chip period $\approx 0.3 \mu\text{s}$). Therefore, in simulation the maximum relative multipath delay for all the users

are set at 8 chip periods. A large reflector in an elliptical region contributes one resolvable multipath from the corresponding user. Resolvable multipaths are considered to be those paths whose relative delays are greater than a chip period. The delays, amplitudes and AOA of these paths are calculated using the procedure described in chapter 4. The fractional multipath delays are rounded up to integer chip samples. Only the distance dependent path loss is assumed and no long term fading is considered. The path loss exponent is taken to be 3.5. Perfect power control assumption for all the uplink users is validated by fixing their LOS power to a fixed level. Small scale fading due to the local scatterers is incorporated by assuming that each resolvable path undergoes independent Rayleigh fading. Ideally the samples of the fading envelope should be generated at the W-CDMA chip rate of 3.84 Mcps. However to make the simulation faster, the fading is generated at the rate of DPDCH data symbols (120ksps). The velocity range is 60~70 mph (96~113 kmph) which corresponds to a maximum Doppler frequency range of 180~200 Hz. The reasoning for this is that highways for fast moving vehicles typically run in rural and suburban areas. . It is also assumed that the users are moving in a direction directly away from the base station so that the LOS path from each user experiences the maximum Doppler spread. The doppler spread of the other multipaths from a user depend on their AOA at the base station with respect to the LOS path. For perfect synchronization of the uplink user's LOS path, the distance of all the users from the base station should be kept as the same. A macrocellular scenario employing circular reflector region around each user is shown in Figure 7.1.

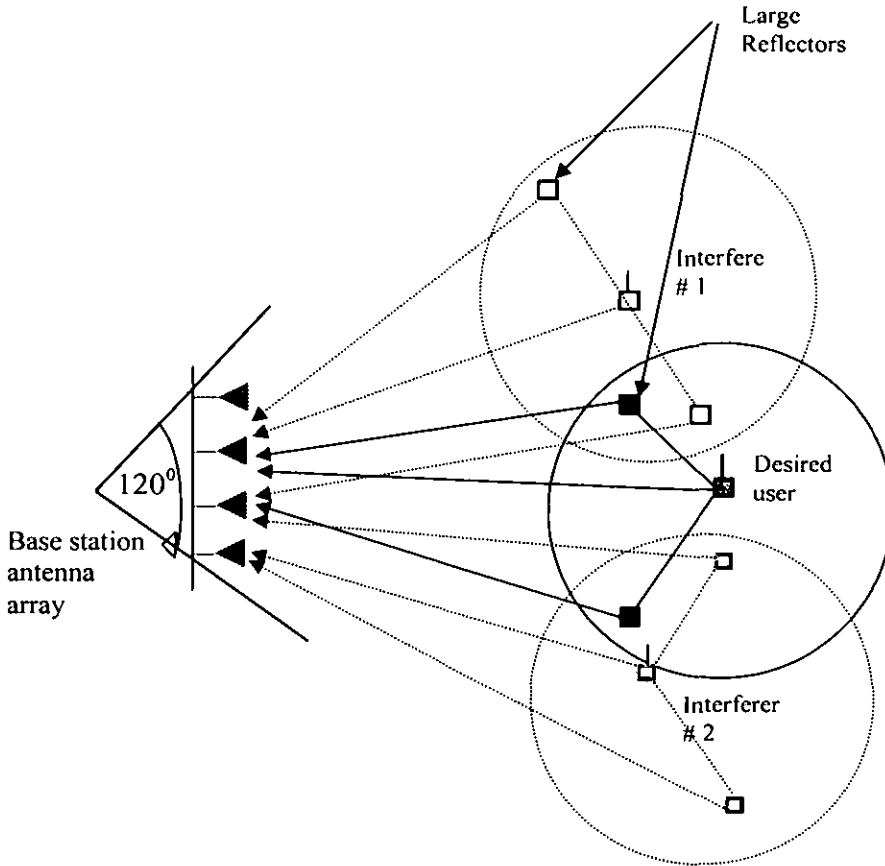


Figure 7.1: Multipath propagation model for macrocellular environment [1]

7.4 Receiver Operational Block for Uplink

The processing block diagram of a PSA beamformer-Rake receiver used for simulation is shown in Figure 7.2. The receiver operation is explained in details in chapter 6. The main assumption we make in simulating the receiver is perfect channel estimation [1]. That means the multipath channel delays, gains, phases and AOAs are assumed to be known in the receiver. Thus the synchronization and channel estimation blocks are not shown in Figure 7.2. Also all the control channel bits (both pilot and TPC) are assumed to be known in the receiver. In a practical system, the control channel signal level is usually estimated before applying it to any pilot symbol assisted operation such as channel estimation or beamforming. Thus, instead of using the known pilot bits directly as the

reference signal for beamforming, a modified version of the pilot bits are often employed. In the simulation, we did this modification by multiplying the pilot bits with the instantaneous complex channel gain, which is assumed to be known. Thus the reference signal for PSA beamforming is the product of known pilot bits and the instantaneous channel coefficient. Another practical issue in the receiver is that one complete DPCCH frame needs to be demodulated first to extract the information about the SF for DPDCH. This is due to the fact the TFCI bits, which extend over the whole frame, carry the information about variable data rate and the corresponding variable SF. Thus the data in DPDCH needs to be buffered for a full frame time before despreading. As mentioned in chapter 6, in our system beamformer weights calculated with one DPCCH slot is applied to the corresponding DPDCH slot. In this case, the data in DPDCH need to be buffered only for one slot. For simulation purposes, it does not make any difference in the performance of the receiver. Synchronization of frame, code (both scrambling and spreading) and symbol timing are assumed to be perfect.

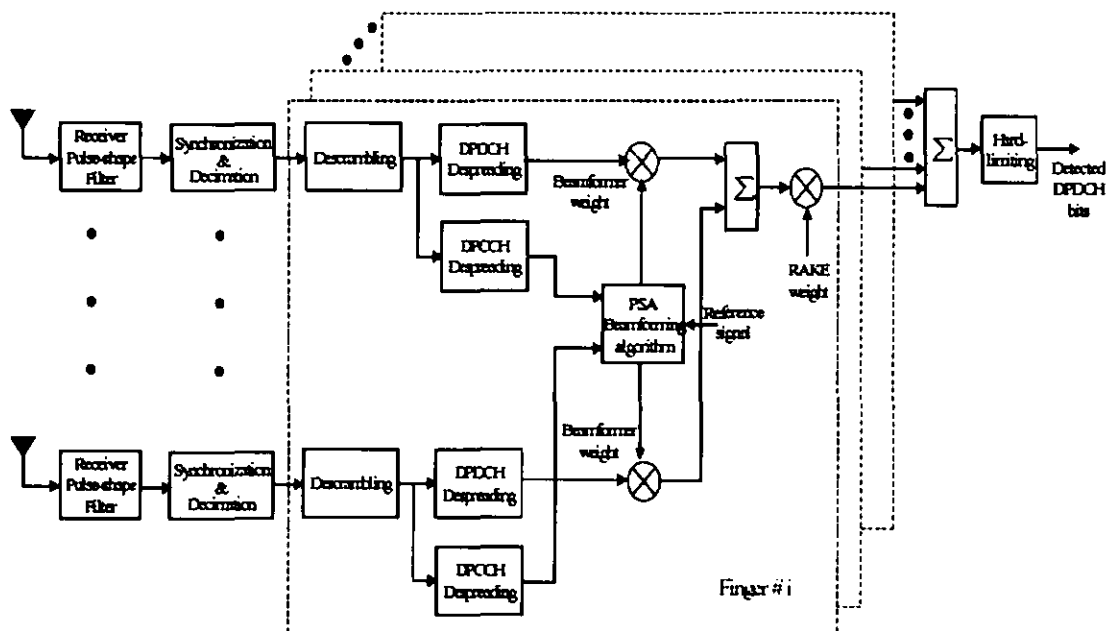


Figure 7.2: Block diagram of a PSA beamformer-Rake receiver used for simulation [1]

7.5 Simulation Environment for Uplink

In the simulation, the maximum number of users considered is 12, each having a SF of 32 (data rate=120 kbps). As the PSA beamformer-Rake receiver is a single user receiver, only one user is the desired one and all the others are interferers. The users are distributed uniformly in a 120° sector. The distances of all the users are kept at 8 km from the base station for macrocellular circular channel. Thus the receive timing of the user's LOS path are synchronous. Also, the received power of LOS components all the users are fixed at 1 W, thereby ensuring perfect power control. Each user has six resolvable multipaths (including the LOS) with different delays, gains and AOAs generated by the circular channel model. A Rayleigh fading simulator is used to incorporate the independent fading that each multipath experiences. For the circular channel the velocity of all the users are kept at 100 kmph (62 mph) which corresponds to a maximum Doppler frequency of 178 Hz. This is done to simulate an extreme case scenario where all the users are moving directly away from the base station. The beamformer-Rake receiver adopts a linear antenna array of 2, 4 and 6 elements and a RAKE receiver with 3, 4 and 6 fingers. The step size parameter, μ , for LMS algorithm is chosen as 0.001 and the weighting/forgetting factor, λ , for both DMI and RLS algorithm is taken to be 0.99. The initial antenna weight vectors for both the LMS and RLS algorithms are chosen to be a zero vector. For each Monte-Carlo simulation 50 different channel snapshots are generated and the performance results over all the iterations are averaged.

7.6 Simulation Results for Uplink

7.6.1 BER performance Versus Number of Users

The first set of performance curves that we present is the BER vs. number of users of the beamformer-Rake receivers as a function of antenna elements and RAKE fingers. As already mentioned, we consider three different PSA beamforming techniques, i.e., LMS, DMI and RLS algorithms in the simulation of the beamformer-Rake receiver. We consider 2, 4 and 6-element antenna arrays along with 3, 4 and 6-finger RAKE receivers.

For comparison we also plot the corresponding curves for single element (1-D) RAKE receivers and single finger (conventional) beamformer. It is assumed that the E_b/N_0 is fixed at 5dB. We compare the performance in both the macrocellular circular channel and the microcellular elliptical channel. From these performance curves, we intend to demonstrate the interference suppression capability of the beamformer in a beamformer-Rake receiver.

7.6.1.1 Macrocelluar Circular Channel Environment

7.6.1.1.1 LMS Beamforming

Figure 7.3 shows the BER performance of a beamformer-Rake receiver for varying number of users in a macrocelluar circular channel environment. The receiver uses a 2-element adaptive LMS beamformer for each finger of the RAKE receiver. The number of RAKE fingers can be 1, 3, 4 and 6. As can be seen, with the increase of RAKE fingers the performance of both the 1-D RAKE and 2-D RAKE improves. However, the performance improvement for the beamformer-Rake is more pronounced than the 1-D RAKE for the corresponding number of finger. For example, a 3-finger beamformer-Rake receiver can outperform both the 3 and 4-finger 1-D RAKE receiver for same number of users and similar channel condition. This performance enhancement comes at the expense of increasing the number of antenna elements by 1 and performing the extra spatial domain processing. Also, can be seen that the relative performance improvement between the 1-D and the beamformer-Rake receiver increases with the number of RAKE fingers. That is, the performance improvement between a 6-finger 1-D RAKE and a 6-finger beamformer-Rake is higher than that of between the 3 and 4-finger 1-D and beamformer-Rake receivers.

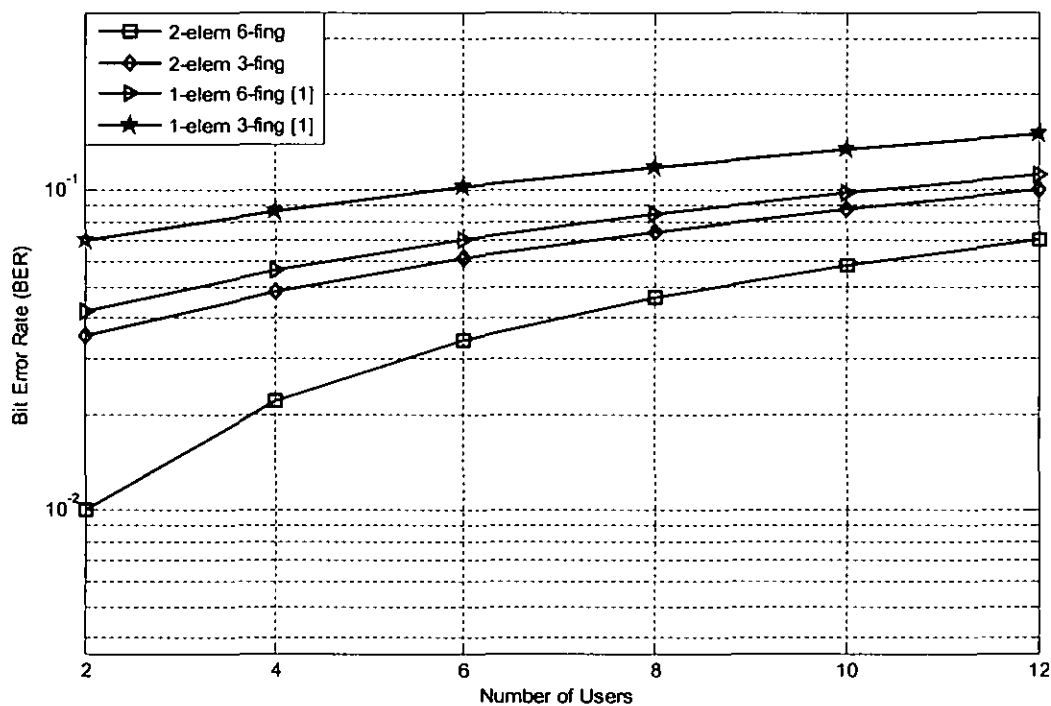


Figure 7.3: BER performance of a beamformer-Rake receiver with 2-element LMS beamformer

Another interesting observation from Figure 7.3 is that the 1-finger beamformer-Rake receiver, which is just a 2-element LMS beamformer, performs worse than all the 1-D RAKE receivers. The reason, which is already mentioned in chapter 4, is twofold. First the circular channel model offers less angular separation between the multipath components; meaning that the beamformers directed to different multipath components will not perform as well as they would have if the multipath components have more angular separation. Secondly, it was shown in chapter 4, that the relative power levels of the multipaths are close to each other in the power delay profile of the circular channel model, which obviously improves the performance of a RAKE receiver. This is also the reason, that the both the 1-D and beamformer-Rake receiver shows a substantial improvement in performance when the number of RAKE finger is increased. This is the so-called RAKE-array performance tradeoff with respect to the multipath channel characteristics. As, we will see later, the situation will be reversed in the microcellular

elliptical channel environment. The BER performance for a 4-element beamformer-Rake with LMS beamforming is shown in Figure 7.4.

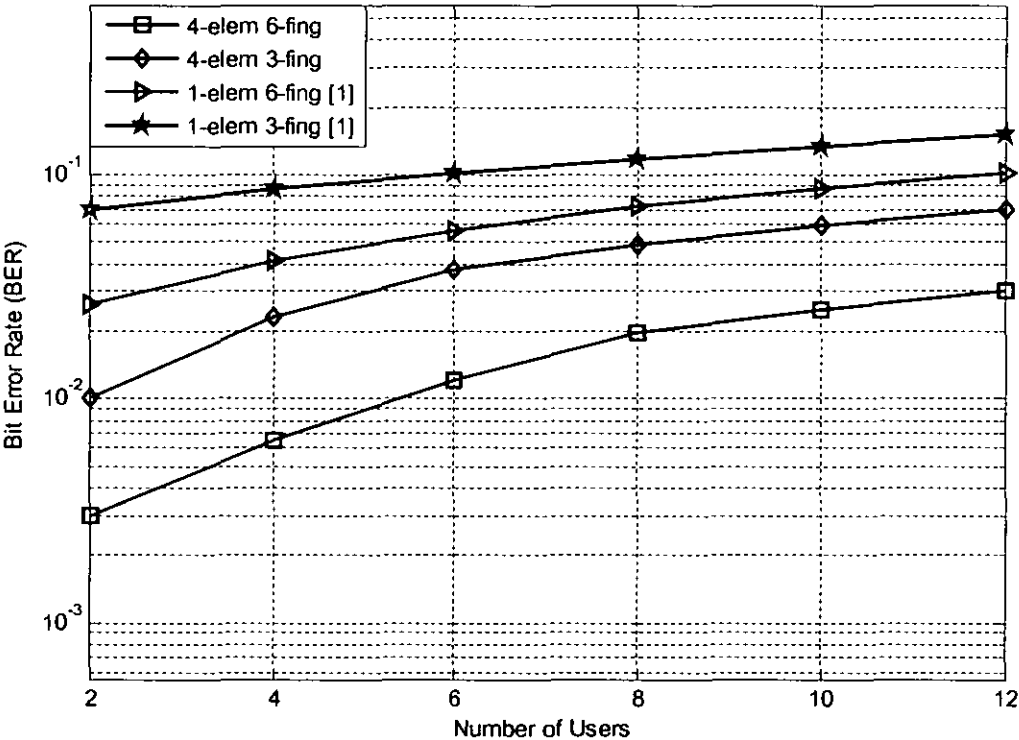


Figure 7.4: BER performance of a beamformer-Rake receiver with 4-element LMS beamformer

Again, the curves follow the same trend as those for the 2-element beamformer-Rake receiver, i.e., performance of both of them improves with the RAKE fingers and the relative performance improvement between the 1-D and the beamformer-Rake for the corresponding RAKE finger increases with the number of finger. As can be expected, the increase of antenna element from 2 to 4 improves performance over the 2-element case. Indeed, a 3-finger beamformer-Rake outperforms the 3, 4 and 6 finger 1-D RAKE receivers. With the increase of RAKE fingers substantial improvement in performance of the beamformer-Rake receiver can be achieved. Also it can be seen that the performance

of the single finger 4-element antenna array is better than that of the single finger 2-element array in Figure 7.4.

7.6.1.1.2 DMI Beamforming

The BER performance curves as a function of users for 2, 4 element beamformer-Rake receivers employing the DMI beamforming [1] are shown in Figure 7.5, 7.6 respectively.

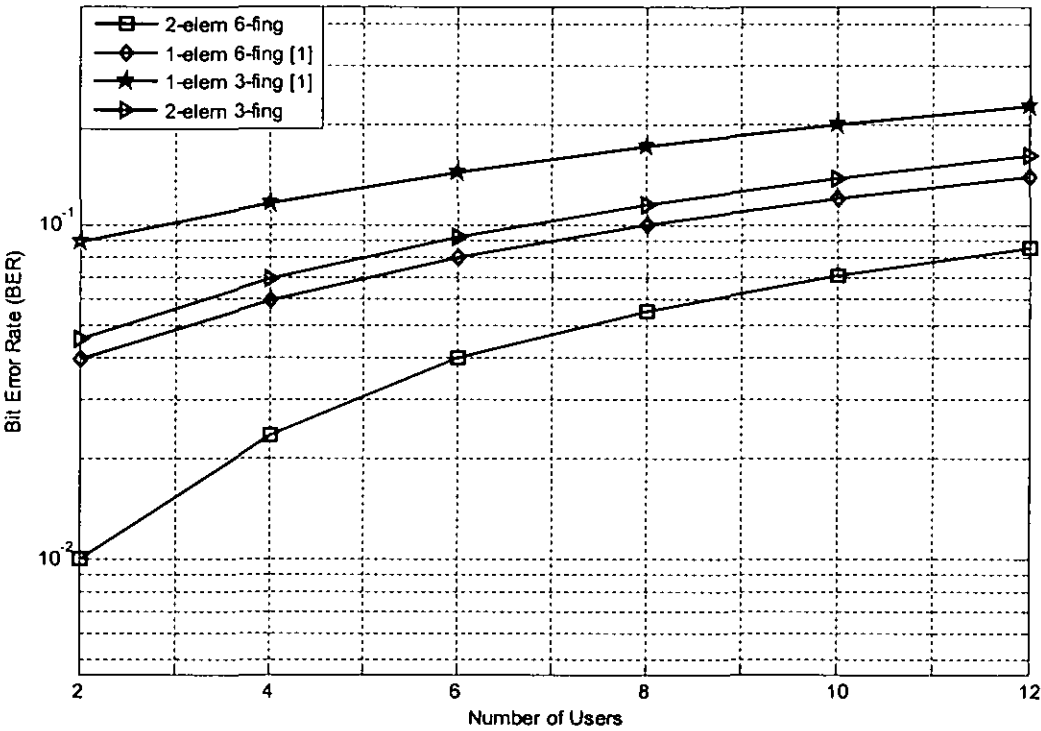


Figure 7.5: BER performance of a beamformer-Rake receiver with 2-element DMI beamformer

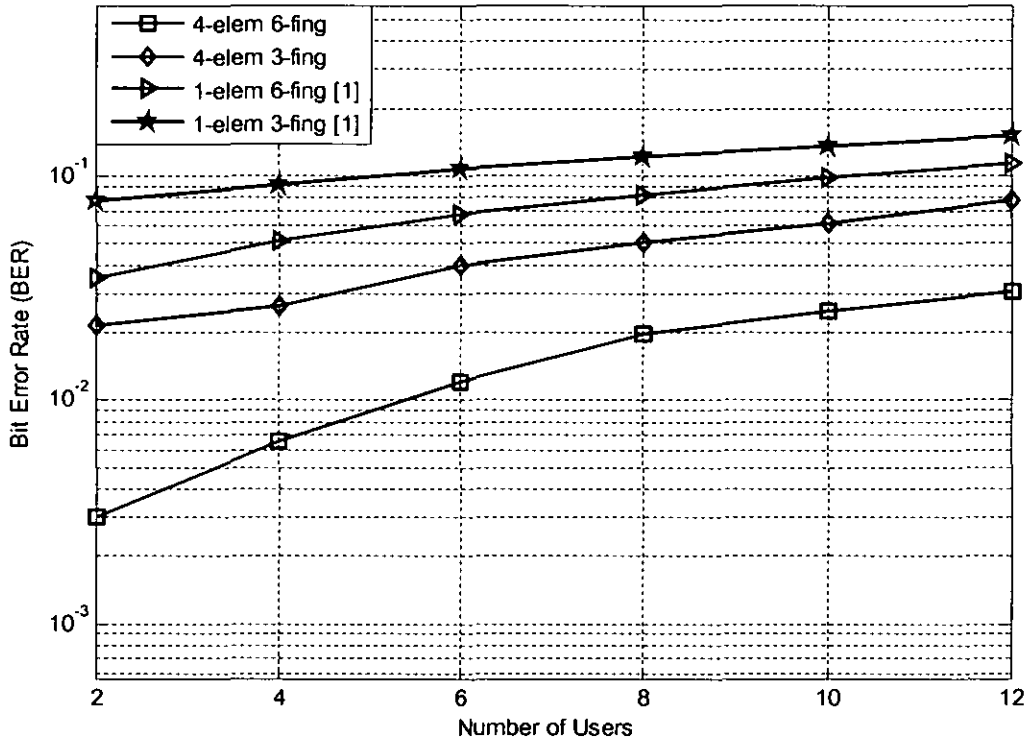


Figure 7.6: BER performance of a beamformer-Rake receiver with 4-element DMI beamformer

The behavior of the curves are very similar to those for beamformer-Rake receiver with LMS beamformer. The performance of the beamformer-Rake receiver improves with the increase of both the antenna elements and the RAKE fingers. As already explained for the case of LMS, due to the characteristics of the circular channel model, performance improvement with RAKE fingers is better than that with the antenna elements. In almost all the cases the beamformer-Rake receiver outperforms both the single element RAKE receiver and the single finger antenna array.

7.6.1.1.3 RLS Beamforming

The BER vs. user performance curves for a RLS based 2-D RAKE receiver with 2, 4element antenna array are shown in Figure 7.7, 7.8 respectively. Again the trends of the

curves are the same as those for the LMS and the DMI beamformer-Rake receivers, i.e., the performance improves with the increase in either the antenna elements and RAKE fingers. For the case of RLS we observe that the curves are not as smooth as those for LMS and DMI. The reason behind this is that in a rapidly time varying channel, as is the case in our simulation, it is very difficult to fix a suitable value for the forgetting factor λ . As mentioned in chapter 6, the most obvious choice of λ should be the channel coherence time, which we did not use in the simulation. Also it is more appropriate to choose different values of λ for different beamformer connected to different fingers of the RAKE receiver.

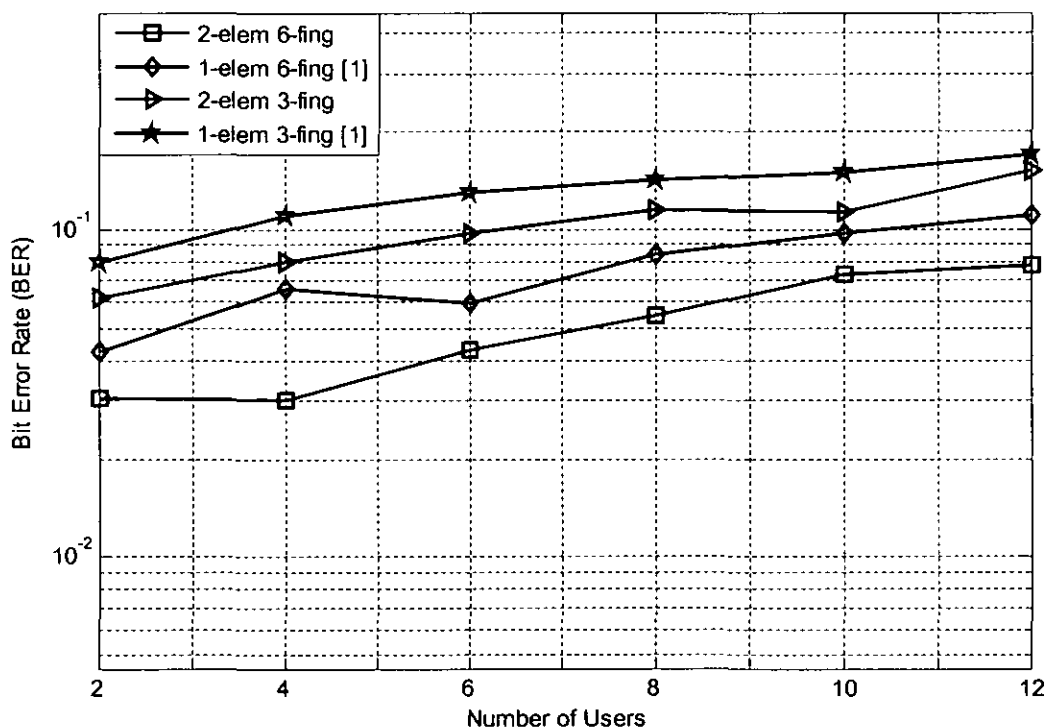


Figure 7.7: BER performance of a beamformer-Rake receiver with 2-element RLS beamformer

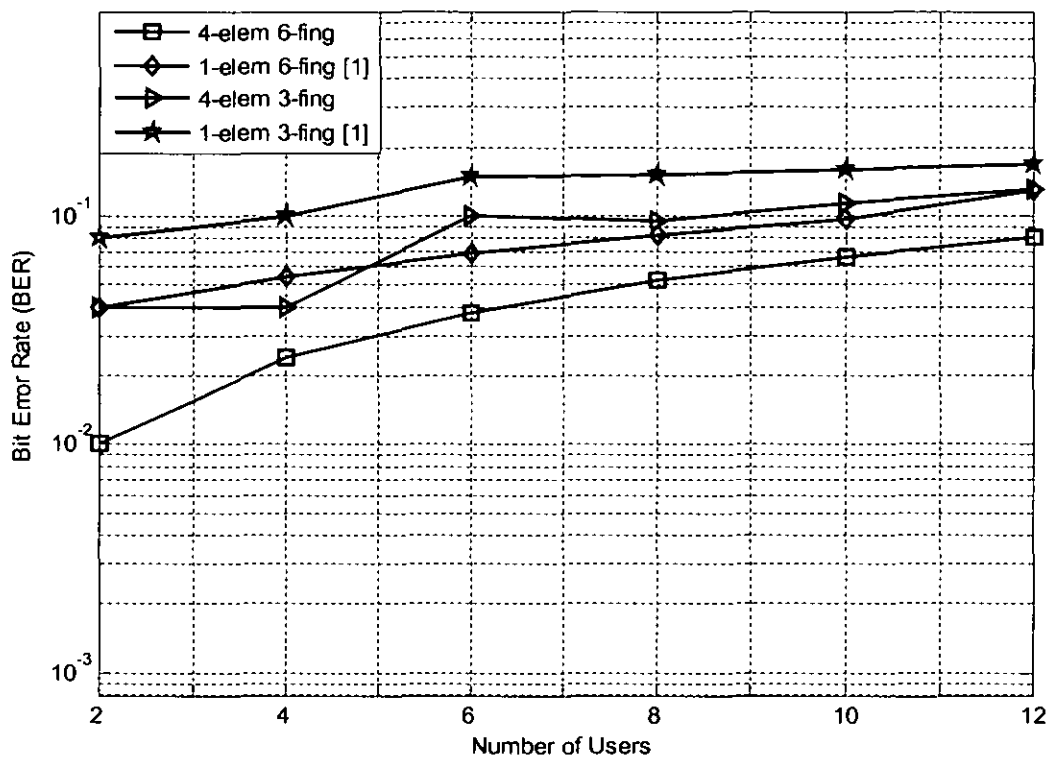


Figure 7.8: BER performance of a beamformer-Rake receiver with 4-element RLS beamformer

To summarize the performance of a beamformer-Rake receiver with the circular channel model, it can be definitely said that the processing in the spatial domain (in this case beamforming) improves the performance over that of a single element RAKE receiver. The degree of performance enhancement depends on the number of antenna elements and the number of RAKE fingers. It was shown that in most cases a 2-element beamformer-Rake is able to achieve performance close enough to a 1-D RAKE receiver with arbitrary number of fingers. Increasing the number of elements will of course give better performance but at the same time increases the computational burden. Also, it was seen that when the channel condition is similar to that modeled by a circular channel, increasing the number of antenna elements is not as effective as increasing the number of RAKE fingers, i.e., RAKE combining gives better performance than array processing.

7.6.2 BER Performance vs. E_b/N_0

The second set of results that we present is the BER performance curves as a function of E_b/N_0 for the beamformer-Rake receivers with varying number of antenna elements and RAKE fingers. For each set of antenna elements we considered two distinct cases. In the first case, the number of users is kept the same as the number of antenna elements i.e., the underloaded case while in the second case it is doubled, i.e., the overloaded case. Again the users are assumed to be uniformly distributed in a 120° sector. As in the case of BER vs. user plots, we compare the performance of the beamformer-Rake receiver with the conventional 1-D RAKE receiver and the conventional beamformer. Also, the performance comparison among different PSA beamforming techniques is provided.

7.6.2.1 Macrocellular Circular Channel Environment

7.6.2.1.1 LMS beamforming

Figure 7.9 shows the BER vs. E_b/N_0 plots for a beamformer-Rake receiver employing a 2-element LMS beamformer in the circular channel model and the 2-user scenario. As can be seen, the performance of the beamformer-Rake receivers are much better than both the 1-D RAKE receiver and the conventional 2-element LMS beamformer. For example, a 2-element, 3-finger, beamformer-Rake receiver can match the performance of a 6-finger 1-D RAKE receiver. Similar to the case in the BER vs. user plots, with the increase of RAKE fingers, the performance of both the 1-D RAKE and the beamformer-Rake receiver improves substantially for the circular channel model. Also it can be seen that the conventional 2-element LMS beamformer performs worse than both the 1-D and the 2-D RAKE receivers, the reason is given in section 7.6.1.1.1.

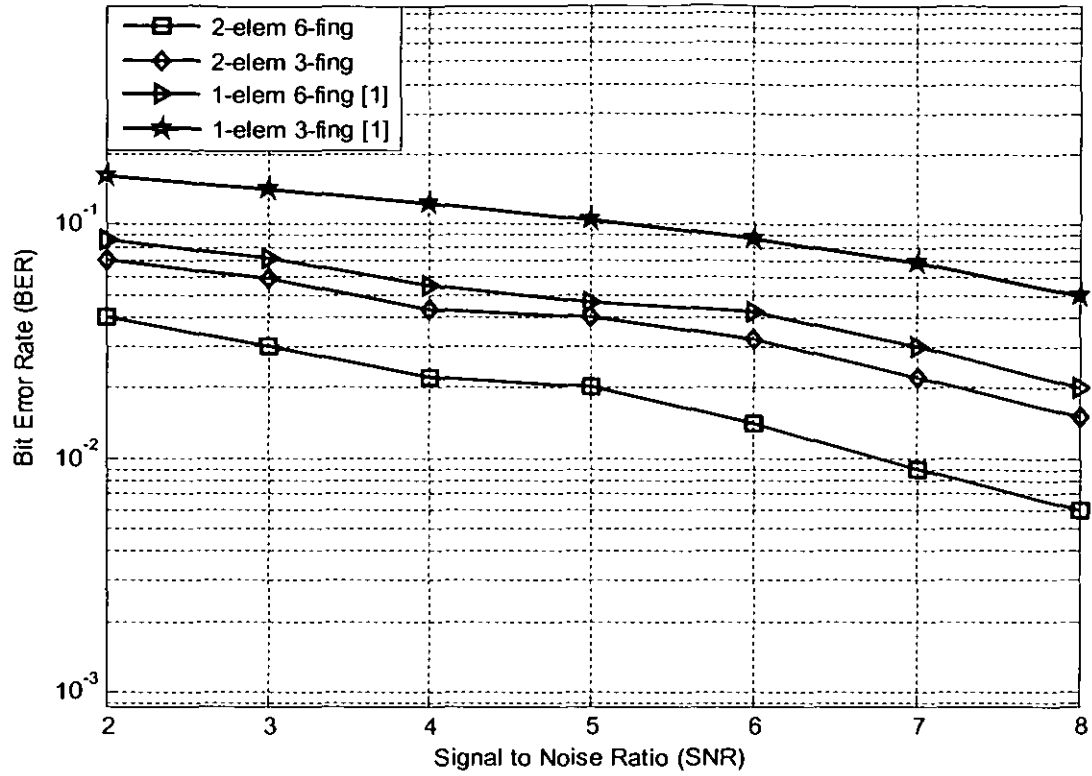


Figure 7.9: BER vs. E_b/N_0 for a 2-element LMS beamformer-Rake receiver with 2-user scenario

The BER performance curves for an overloaded 4-user scenario is shown in Figure 7.10.

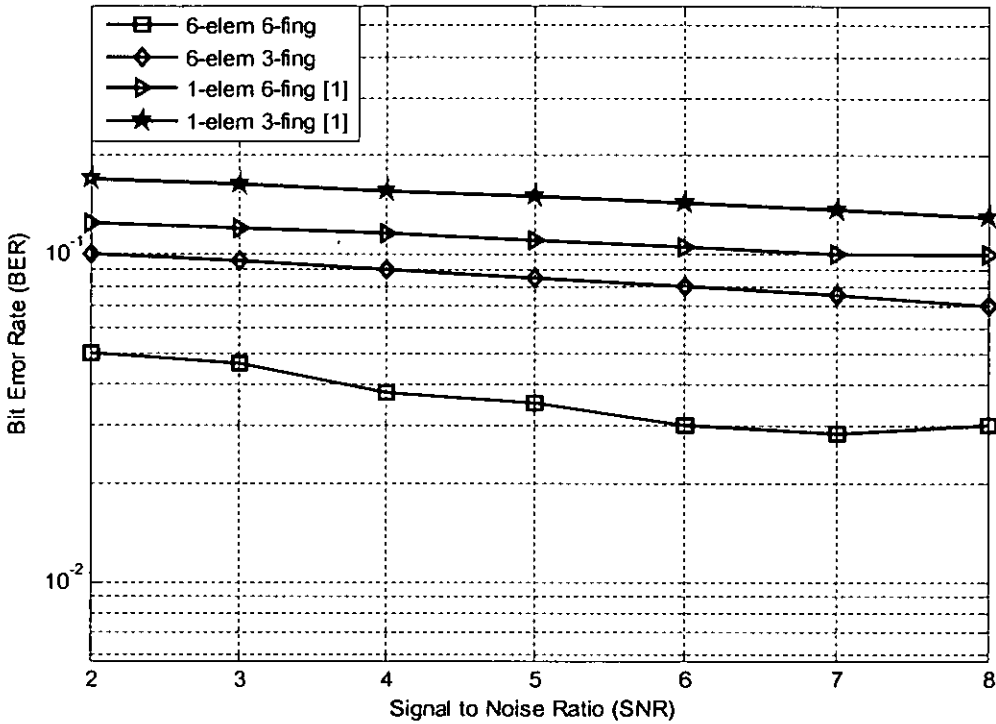


Figure 7.11: BER vs. E_b/N_0 for a 6-element LMS beamformer-Rake receiver with 6-user scenario

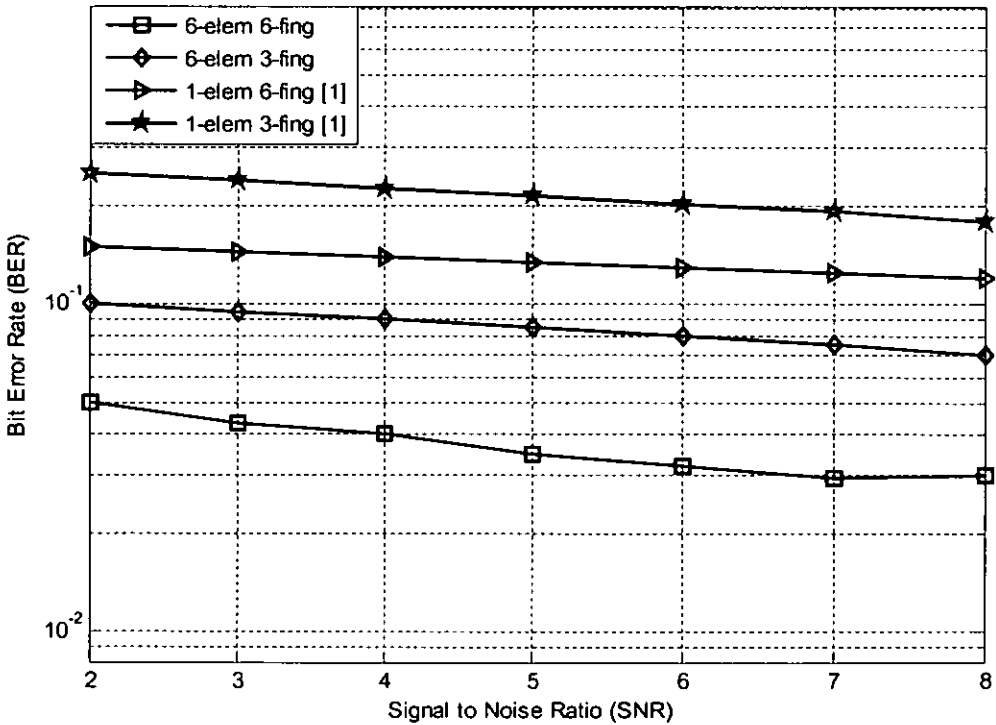


Figure 7.12: BER vs. E_b/N_0 for a 6-element LMS beamformer-Rake receiver with 12-user scenario

7.6.2.1.2 DMI Beamforming

Figure 7.13 through 7.15 show the BER performance curves as a function of E_b/N_0 for the DMI beamforming based beamformer-Rake receiver with 2, 4 and 6 antenna elements in both the underloading and the overloading scenarios. The curves have the same general trend as those for the LMS case.

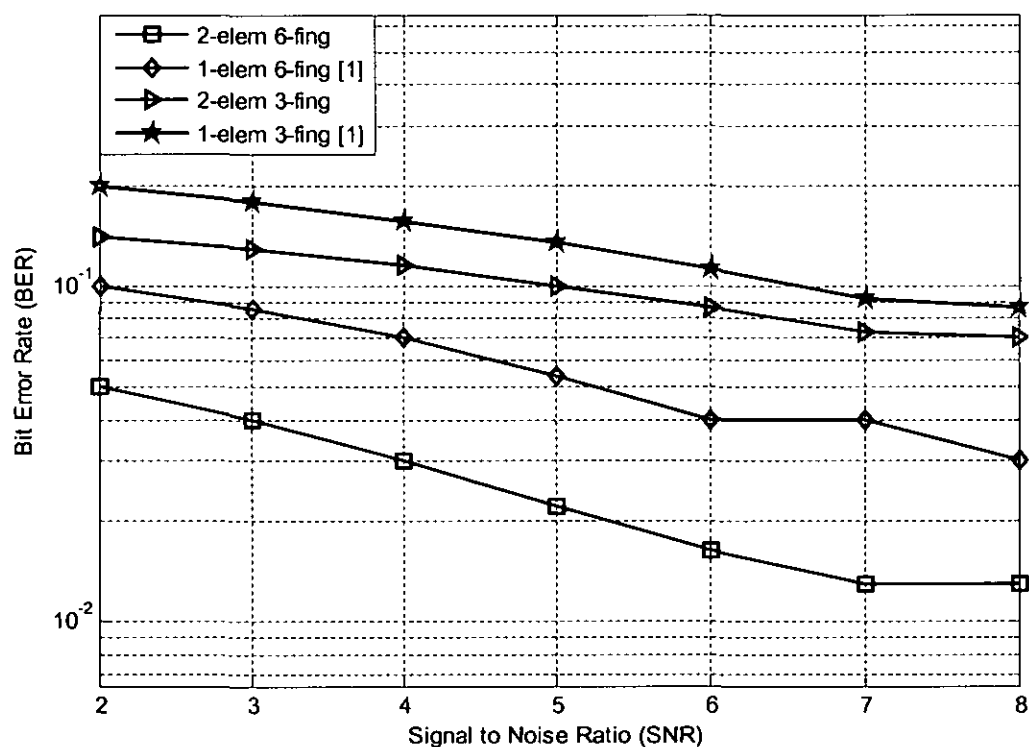


Figure 7.13: BER vs. E_b/N_0 for a 2-element DMI beamformer-Rake receiver with 2-user scenario

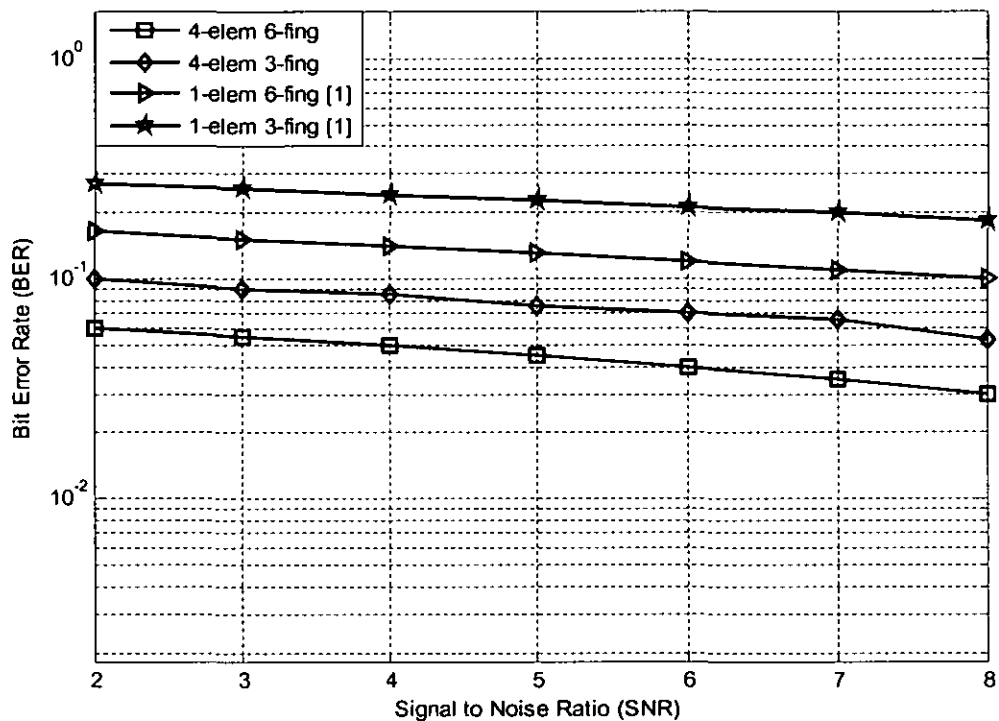


Figure 7.14: BER vs. E_b/N_0 for a 4-element DMI beamformer-Rake receiver with 8-user scenario

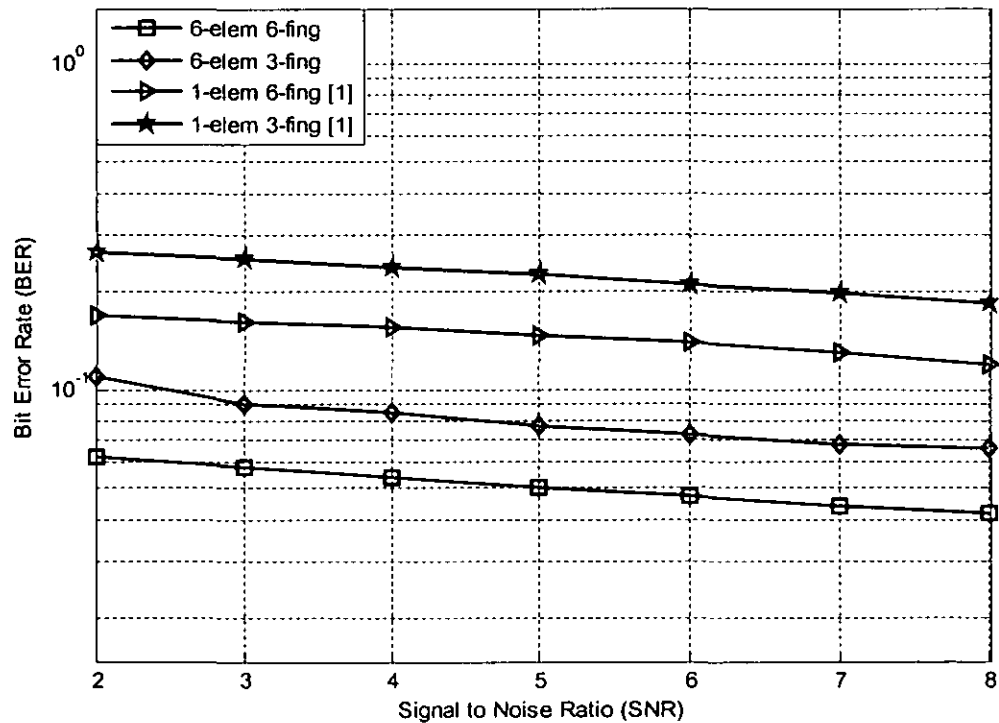


Figure 7.15: BER vs. E_b/N_0 for a 6-element DMI beamformer-Rake receiver with 12-user scenario

7.6.2.1.3 RLS beamforming

Figures 7.16 through 7.18 show the BER performance curves as a function of E_b/N_0 for the RLS beamforming based 2-D RAKE receiver with 2, 4 and 6 antenna elements in both the underloading and the overloading scenarios. The curves also have the same general trend as those for the LMS and DMI beamforming cases.

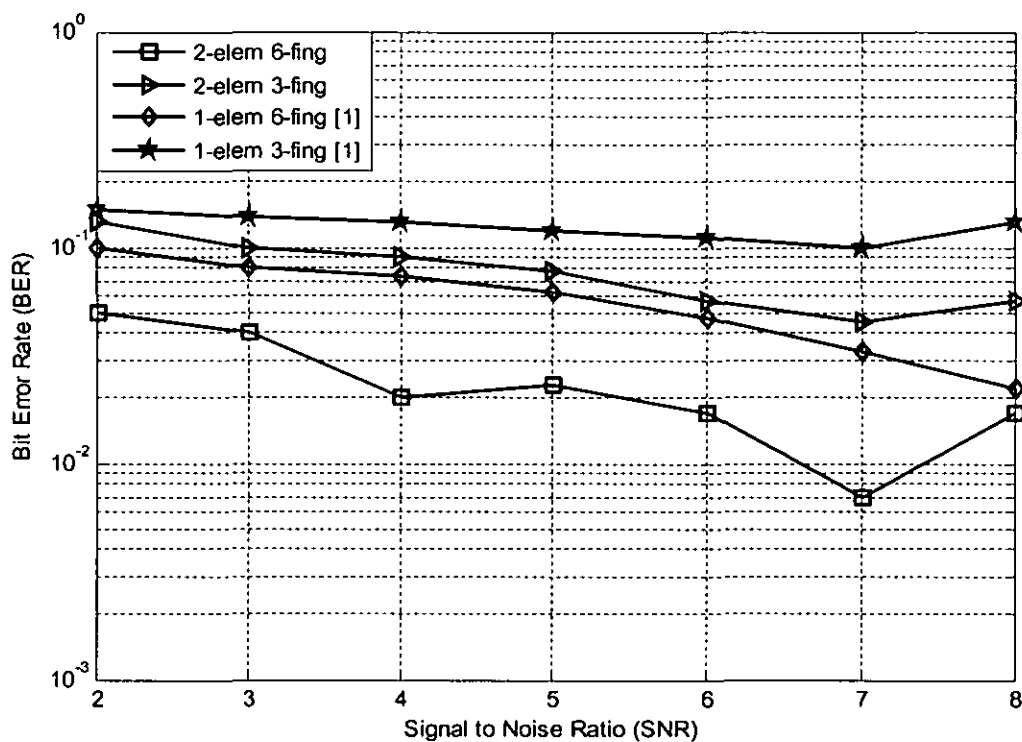


Figure 7.16: BER vs. E_b/N_0 for a 2-element RLS beamformer-Rake receiver with 2-user scenario

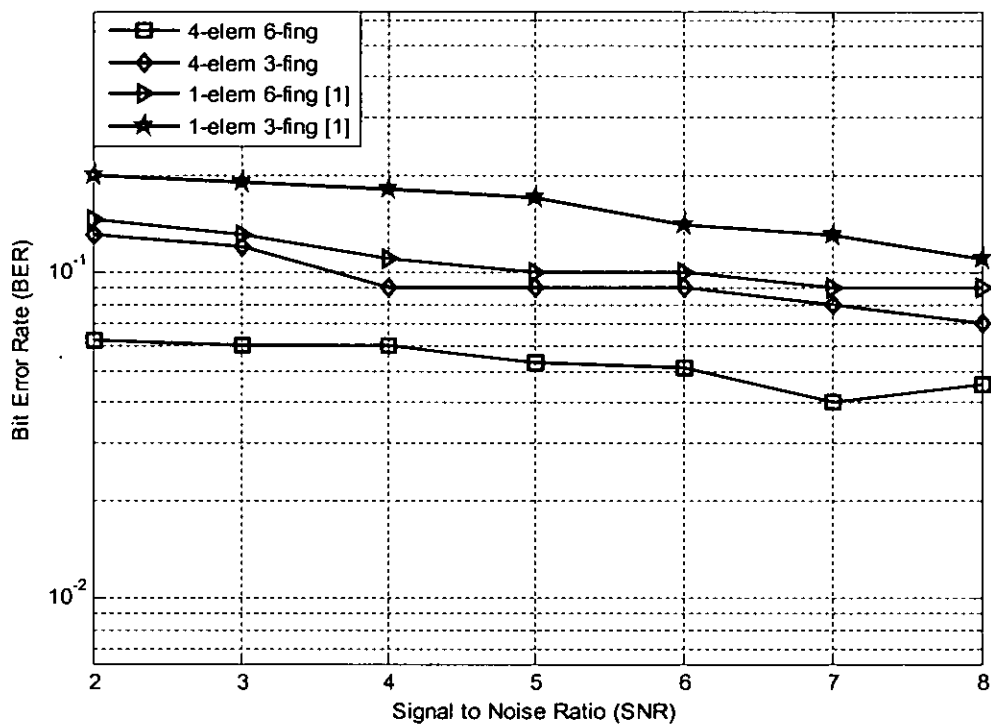


Figure 7.17: BER vs. E_b/N_0 for a 4-element RLS beamformer-Rake receiver with 8-user scenario

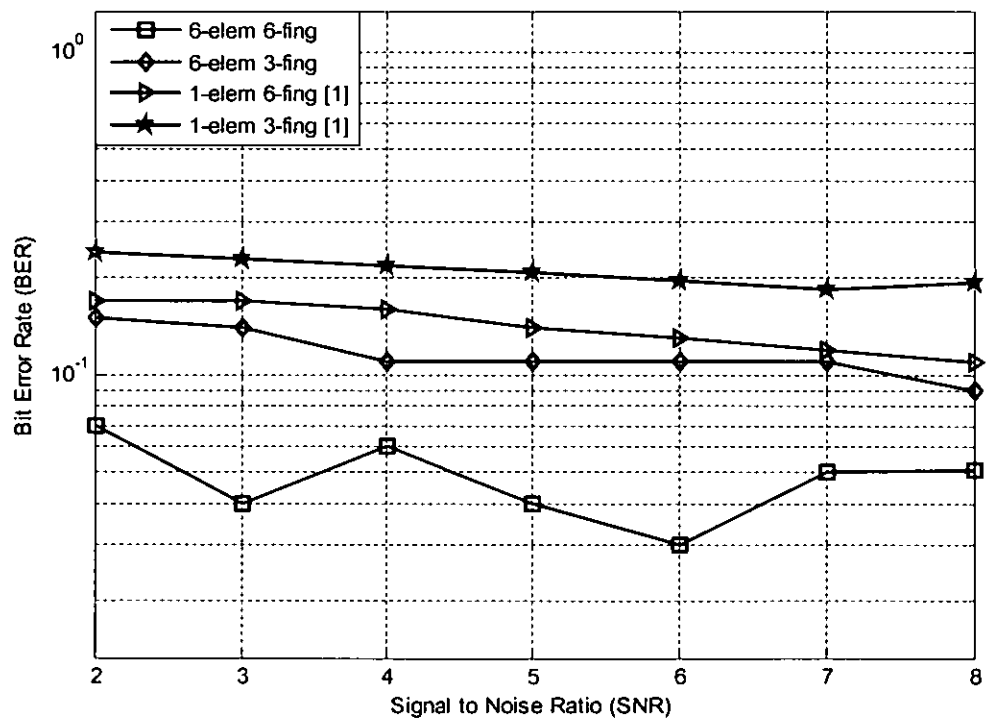


Figure 7.18: BER vs. E_b/N_0 for a 6-element RLS beamformer-Rake receiver with 12-user scenario

7.7 Performance of Adaptive Antennas for Downlink Scenario

7.7.1 Introduction

In this scenario, the simulation model employed in the study of the performance of the adaptive array antenna in downlink for WCDMA system and downlink power control. First of all, the topology used in this simulation has been defined. The simulation methodology, simulation scenario and the formulas used in the simulation also will be discussed. Next, the simulation program flowchart is explained. Finally, the principal parameters used in the performance evaluation, and the outputs of this simulation have been pointed out.

7.7.2 Topology

The topology of the system analyzed is of a macrocellular type, formed by seven hexagonal cells. Each cell is served by one base station, located in its centre and equipped with an adaptive array antenna. Mobile stations (MSs) are generated using uniform random distribution in the coverage area of the centre cell. The cells structure and the MSs distribution are shown in Figure 7.19

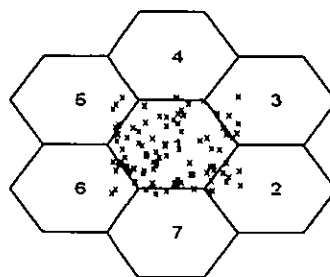


Figure 7.19: Cells layout and MSs Distribution

(x refers to MS)

7.7.3 Simulation Scenario

A computer software simulation has been developed purposely to evaluate the performance of adaptive array antenna downlink and power control in WCDMA system. The chosen simulation scenario consists of seven hexagonal cells, each with BS located in its centre. MS locations are generated using uniform random distribution in the coverage area of the centre cell.

Propagation path loss calculation is modeled based on one of the following four models with input parameters as indicated in the Tables 7.3 to 7.5.

$$L_{FSPL} = 32.4 + 20\log_{10}(f_c) + 20\log_{10}(d) \quad (7.1)$$

$$L_{ARIB} = 40(1 - 4 \times 10^{-3} h_t) \log_{10}(d) - 18\log_{10}(h_t) + 21\log_{10}(f_c) + 80 \quad (7.2)$$

$$L_{Lee} = 129.45 + 38.4\log_{10}(d) - 20\log_{10}(h_t + h_b) \quad (7.3)$$

$$L_{Hata} = 46.3 + 33.9\log_{10}(f_c) - 13.82\log_{10}(h_t + h_b) - ((1.1\log_{10}(f_c) - 0.7)h_m - (1.56\log_{10}(f_c) - 0.8)) + (44.9 - 6.55\log_{10}(h_t + h_b)) \log_{10}(d) \quad (7.4)$$

Where

f_c is the carrier frequency (in MHz)

d is the MS-BS separation distance (in km)

h_t is the base station antenna height (in meters) above rooftop

h_b is the rooftop height (in meters) and

h_m is the mobile station antenna height (in meters).

The fourth model, Hata model, has been used as the main model for downlink power control simulation and other models are used as references only. All models include MS-BS distance factor in the mean path loss calculation MS services consist of four choices that specify different kinds of data rate from 12.2 kbps to 384 kbps.

The simulation is consist of four stages, first one to calculate the average SINR and E_b/N_0 at MSs in different threshold separation angle of beamforming algorithm, this done to evaluate the best threshold separation angle for certain range of number of users, it repeats the generation of mobiles ten times and calculate the average SINR and E_b/N_0 at each cycle after that takes the average value of these ten values and repeats the same calculation after changing the threshold separation angle, in the last it plots the relation between the threshold separation angle and average received SINR and E_b/N_0 at MS, the second stage is to calculate the average SINR and E_b/N_0 at MSs in different number of users, it repeats the generation of mobiles ten times and calculate the average SINR and E_b/N_0 at each cycle after that takes the average value of these ten values and repeats the same calculation after changing the number of users, in the last it plots the relation between the number of users and average received SINR and E_b/N_0 at MS, the calculation done and plotted in various bit rates and cell radius, the third stage to compare between receive SINR and E_b/N_0 in adaptive array antenna and omindirectional antenna at same MSs distribution, the comparison done by changing number of users and E_b/N_0 for both antennas, the forth stage applying power control on downlink adaptive array antenna and calculate and plot EIRP, SINR and E_b/N_0 for each MS before and after power control, the initial transmitted power of the BSs is the average level value in the transmitted power levels without taking interference effect.

At every power control cycle, the data for every MS as MS received power, interference at MSs, SIR at MSs, BER , and E_b/N_0 will be computed.

7.7.3.1 Antenna Parameter

The overall gains in look direction of horizontal plane depend on antenna 3-dB beam width, β and its deviation from the main lobe, ϕ . By assuming that gain, G , and directivity, D , are nearly the same, the gain versus beam width relationship can be approximated as follow:

$$G = D = \begin{cases} \frac{32,400}{\phi\theta} & \text{For small } \phi \text{ and } \theta (\phi \text{ and } \theta < 40^\circ) \\ \frac{41,253}{\phi\theta} & \text{For large } \phi \text{ and } \theta (\phi \text{ and } \theta \geq 40^\circ) \end{cases} \quad (7.5)$$

Where ϕ and θ are the 3-dB beamwidth in two planes. The antenna pattern gain is modeled by a sinc^2 function [192].

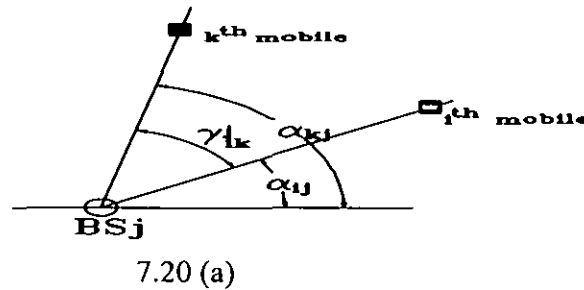
SINR calculation for downlink and uplink respectively can be modified from [193]:

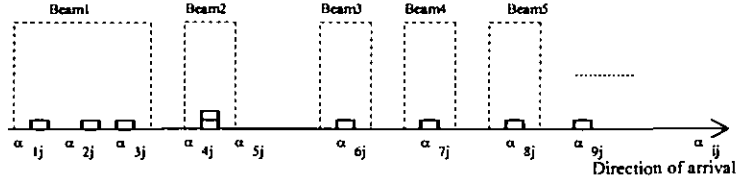
$$\text{SINR}(i)_{\text{downlink}} = \frac{G_p G_A P_{ki} / L_{ki}}{\sum_{k=1}^N I_{ik} + P_N} \quad (7.6)$$

Where G_p is processing gain, P_{ki} is the transmit power for BS # k to MS # i , L_{ki} is the path loss

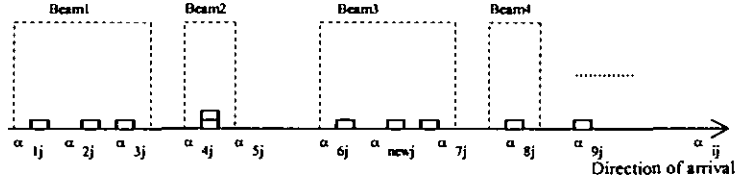
7.7.3.2 Adaptive Beamforming Technique

The beam formation at every base station is based on the mobiles' DOAs. Figure 7.20(a) shows the actual parameters used in the algorithm. Given the j^{th} base station and two mobiles, say the i^{th} and the k^{th} , the angles of arrival are denoted α_{ij} and α_{kj} respectively while the separation angle between the mobiles is γ_{ik}^j . By setting a threshold separation angle between adjacent mobiles, say γ , we are then in a position to narrow or widen antenna beamwidths after all directions of arrivals have been sorted.





7.20 (b)



7.20 (c)

Figure 7.20(a): Actual beam formation algorithm parameters, (b) Examples of beam formation and (c) Beam reformation to accommodate a new call.

Figure 7.20(b) shows an example of beam formation where

$$\begin{aligned} &(\alpha_{2j} - \alpha_{1j}) < \gamma \text{ and } (\alpha_{3j} - \alpha_{2j}) < \gamma, \\ &(\alpha_{4j} - \alpha_{3j}) > \gamma \text{ and } (\alpha_{5j} - \alpha_{4j}) < \gamma, \\ &(\alpha_{6j} - \alpha_{5j}) > \gamma, \\ &(\alpha_{7j} - \alpha_{6j}) > \gamma \text{ and} \\ &(\alpha_{8j} - \alpha_{7j}) > \gamma \end{aligned}$$

Henceforth, beam number 1 and 2 respectively will cater for a group of three and two mobiles, while beams numbers 3, 4 and 5 will cater each for a single mobile. The beams sizes are given by $(\alpha_{ij} - \alpha_{pj} + \gamma)$ where i and p represent the first and the last mobiles in the same beam respectively. If a new call arrived and served by the same BS_{*j*} such that,

$$\begin{aligned} &(\alpha_{2j} - \alpha_{1j}) < \gamma \text{ and } (\alpha_{3j} - \alpha_{2j}) < \gamma, \\ &(\alpha_{4j} - \alpha_{3j}) > \gamma \text{ and } (\alpha_{5j} - \alpha_{4j}) < \gamma, \\ &(\alpha_{6j} - \alpha_{5j}) > \gamma, (\alpha_{\text{newj}} - \alpha_{6j}) < \gamma, (\alpha_{7j} - \alpha_{6j}) > \gamma \text{ and} \\ &(\alpha_{8j} - \alpha_{7j}) > \gamma \end{aligned}$$

Then the new formation of beams are as shown in Figure 7.20(c). It can be seen that the number of beam is reduced from five to four and there are only two beams serving lone mobile instead of four.

7.7.3.3 Downlink Interference analysis

There are two types of interference intracell interference and intercell interferences both of them will be described.

7.7.3.3.1 Intracell interference

This interference occurs due to receiving the transmitted power to other users in the same cell, also there are two types of this interference.

7.7.3.3 .2 Intrabeam interference

This interference occurs because the interested user will receive the power of all other users in the same cell multiplied by its gain and the correlation factor, it is calculated based on formula below.

$$I_{\text{int ra_beam}} = \frac{(N - 1) \times P_t \times G_t(\theta) \times G_t(\phi) \times (1 - \alpha)}{L} \quad (7.7)$$

Where

N is the number of users in the same cell.

α is the orthogonal factor.

L is the losses.

7.7.3.3.2.1 Interbeam interference

This interference due to receiving the power of other users multiplied by the gain of interference beam and correlation factor, it is calculated based on formula below.

$$I_{inter_beam} = \sum_{i=1}^M \frac{(N-1) \times P_i \times G_{ii}(\theta) \times G_{ii}(\phi) \times (1-\alpha)}{L} \quad (7.8)$$

Where

M is the number of beams interfering with the user.

Interbeam interference depends on the interference gain, number of users in the same cell, orthogonal factor and separation angle in the beamforming algorithm; figure shows both types of intracell interference.

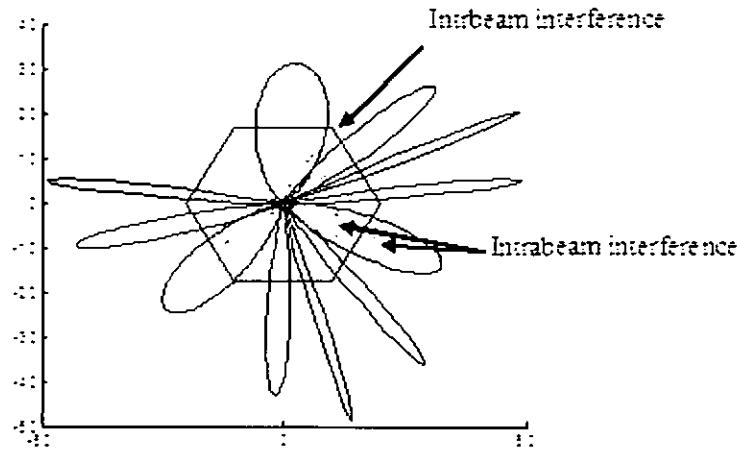


Figure 7.21: Intrabeam interference and interbeam interference

7.7.3.3.2 Intercell interference

This interference occur due to the interfering beams related to neighboring cell, to calculate this interference in the first we have to calculate the angle between the user and interfering base station after that we calculate the gain of all the beams related to that base station in this angle and after that we calculate the received power from the beams of that base station at the user.

$$I_{intercell} = \sum_{j=1}^B \sum_{i=1}^M \frac{(N-1) \times P_t \times G_{ii,j}(\theta) \times G_{ii,j}(\phi) \times (1-\alpha)}{L} \quad (7.9)$$

Where

B is the number of base stations interfering with the user.

M is the number of beams in the interfering base station.

7.7.4 Program Flowchart

This simulation program has been written in MATLAB 7 software. Figures 7.22, 7.23, 7.24, 7.25 show the flowcharts of the used simulation program.

At the beginning of the simulation, many essential parameters should be specified by the user such as propagation model selection, number of MSs, data rate selection, power control step size, and Eb/No threshold. Many other parameters are previously prescribed according to the standard of the WCDMA system.

Thereafter, 7 cells of hexagonal layout are generated; the mobile stations are generated using a uniform random distribution in the coverage area of the centre cell.

There are four stages, the first one to calculate the SINR and E_b/N_0 in the downlink adaptive array antenna by changing the separation angle in beamforming algorithm, second one to calculate SINR and E_b/N_0 in downlink for adaptive array antenna at various bit rates and cell radius, third one apply power control on downlink adaptive array antenna and calculate SINR and E_b/N_0 before and after power control, the last one to compare between adaptive array antenna and omnidirectional antenna in WCDMA downlink.

For power control stage the initial transmitted power setting for BS towards MS is set as the average level power.

The downlink power control is then started, the signal power, received at MSs from BS, will be calculated. For every MS, the ratio of its received signal power (S) to the total signals received powers for all other MSs and from other BSs will be calculated to yield downlink SINR, and from SINR we calculate E_b/N_0 .

The power control algorithm based on comparing the minimum received E_b/N_0 at MS with the threshold value to increase or decrease BS transmitted power by a specified step size.

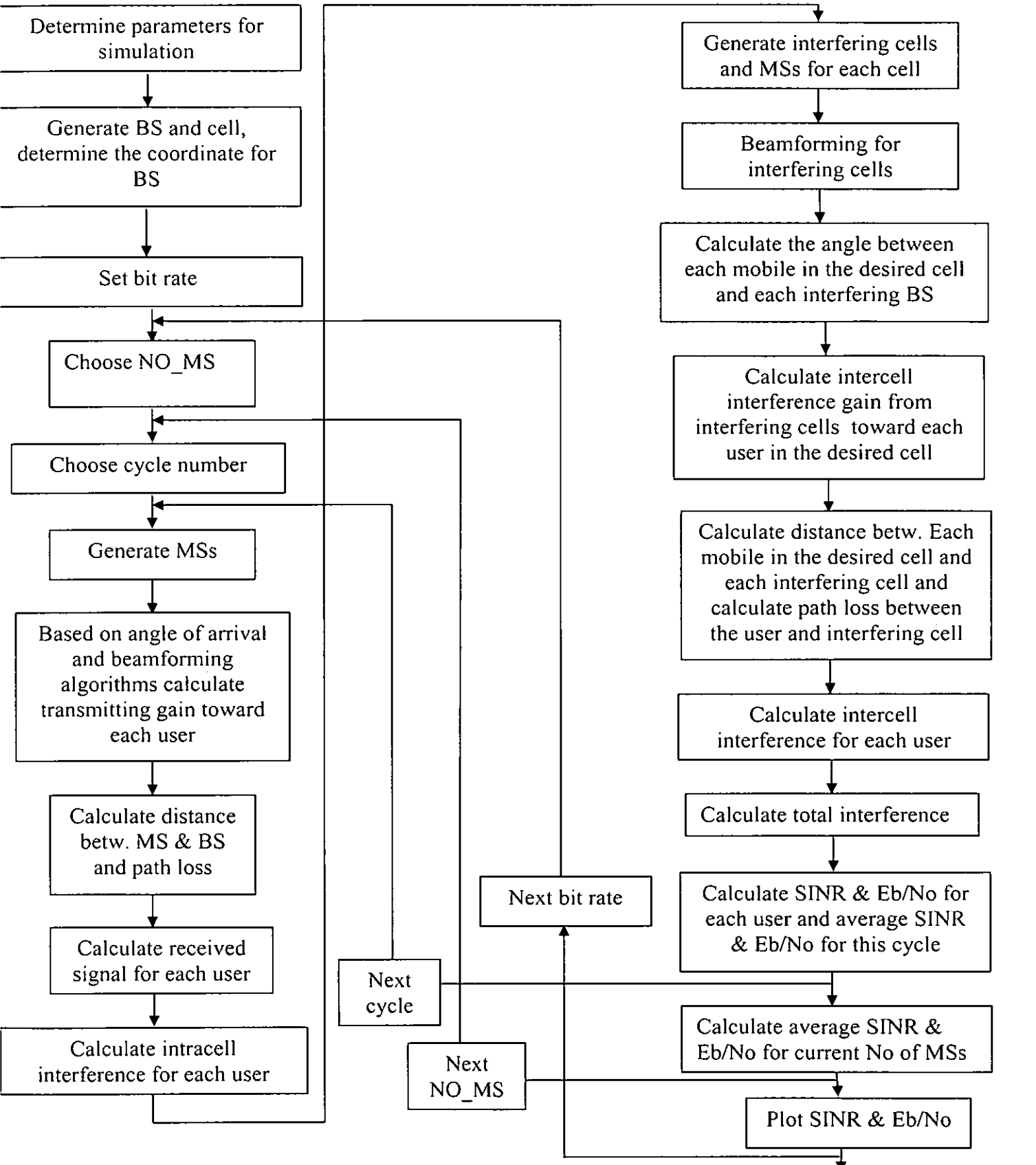


Figure 7.22: Adaptive array antennas in WCDMA downlink simulation algorithm
Calculating SINR and EbNo vs. No MSs algorithm

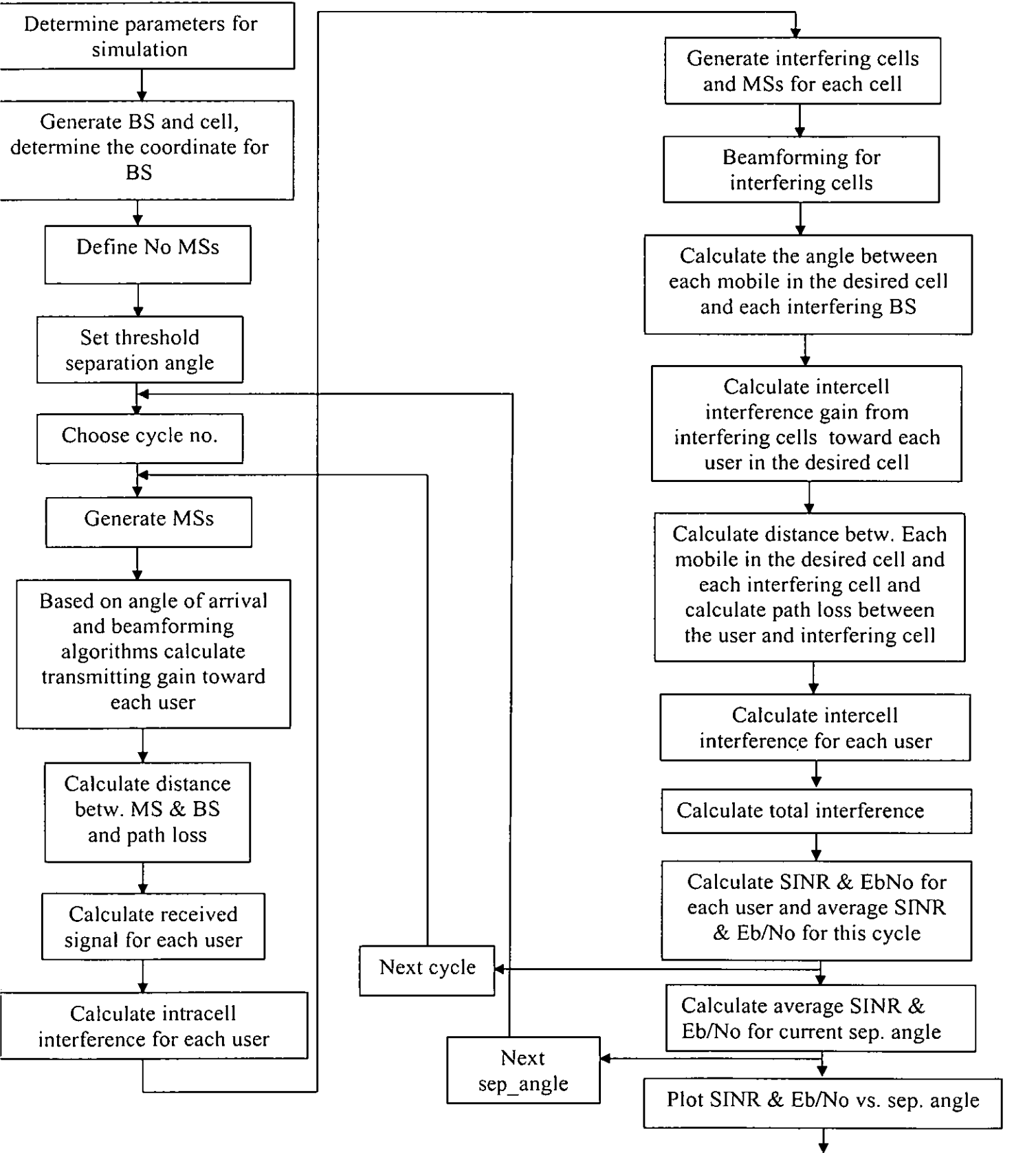


Figure 7.23: Adaptive array antennas in WCDMA downlink simulation algorithm
Calculating SINR and EbNo vs. separation angle algorithm

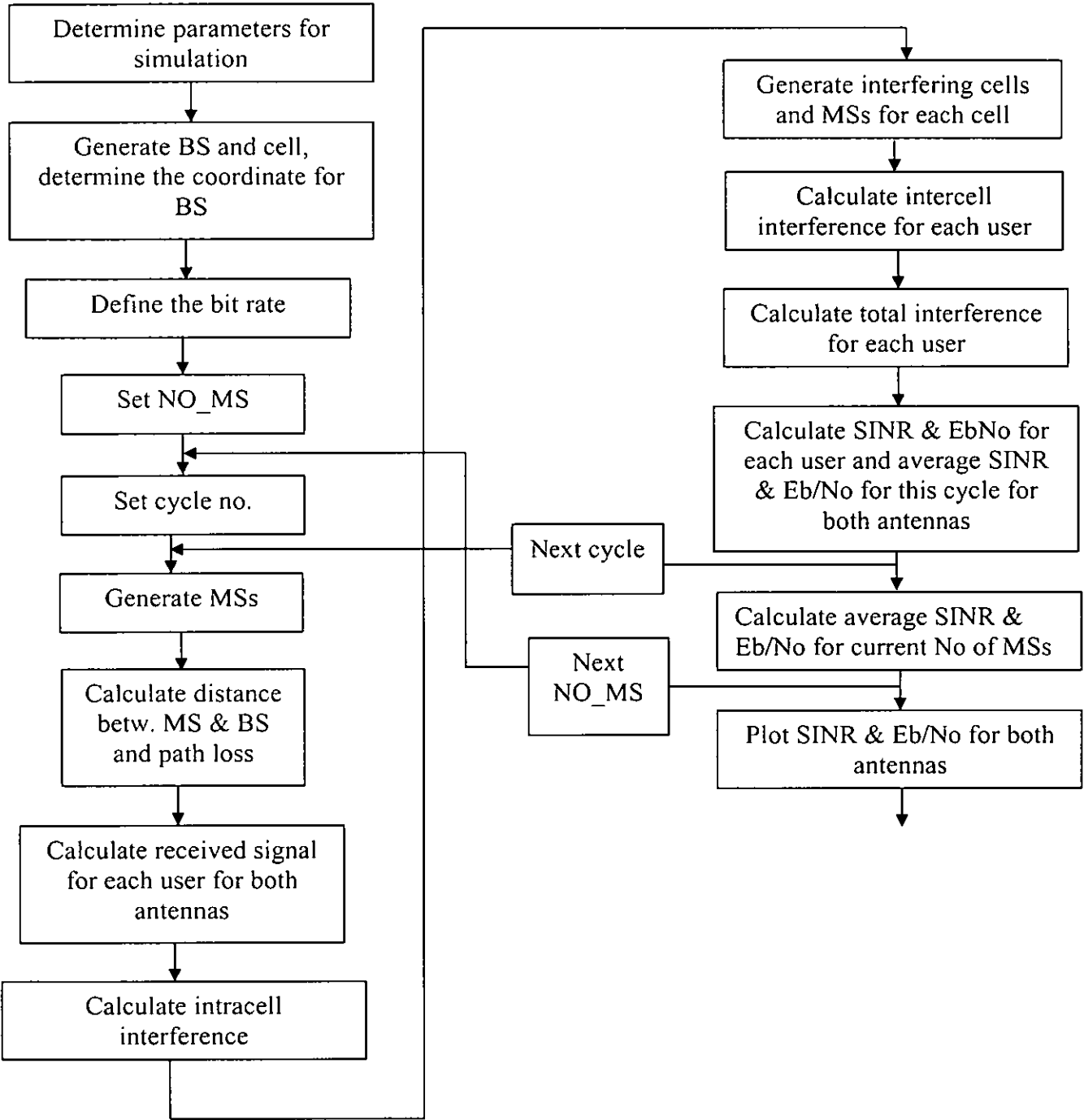


Figure 7.24: Comparisons between adaptive array antenna and omnidirectional antenna for downlink WCDMA system simulation algorithms

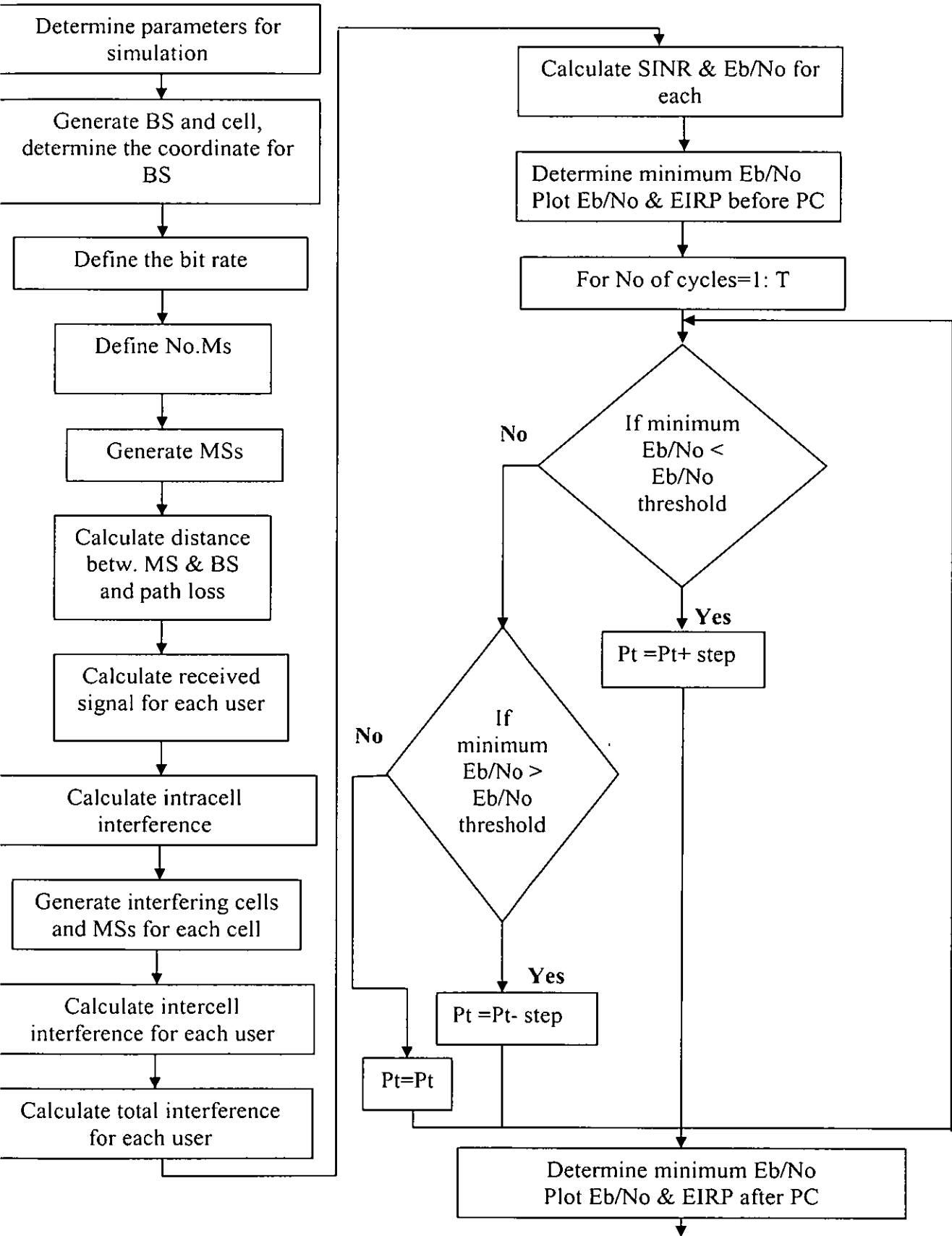


Figure 7.25: Adaptive array antenna power control for downlink WCDMA system simulation algorithms

7.7.5 Input Parameters

The major parts of the simulation input parameters are fixed and previously defined. The other part needs to be identified by the user. Table 7.3, 7.4, and 7.5 indicate a list of the input parameters that have been used in the simulation based on [194], [195].

Table 7.3: Simulation input parameters

Parameter	Value	Explanation
fc	2000	DL carrier frequency (MHz).
Chip_rate	3.84	Chip rate (Mcps).
BW	5	Channel bandwidth (MHz).
hbs	30	BS antenna height (m).
hm	2	MS antenna height (m).
X_init	0	X-coordinate of centre BS (m).
Y_init	0	Y-coordinate of centre BS (m).
ptx	5	BS transmit power towards each MS (dB) (=33dBm).
Gr	0	MS antenna gain (dB)
Noise_figure	5	Noise figure at BS and MS in dB
Xcorr	0.61	Code cross correlation
ptxmin	5	Minimum Bs transmitted power for PC stage
NO_BS	7	Number of base stations

The user needs to enter some parameters like those indicated in Table 7.4

Table 7.4: Simulation input parameters (user-defined)

Parameter	Description
Model (1,2,3, or 4)	Path loss model selection (FSPL, ARIB, Lee or Hata)
NO_MS	Number of mobile stations
Data rate (1, 2, 3, or 4)	Data rate selection (12.2 kbps, 64 kbps, 144 kbps, or 384 kbps).
step	Power control step size (0.5, 1.0, or 2.0 dB)
Cell_radius	The cell radius

From NO_MS we can find best threshold separation angle of this number of users for beamforming algorithm.

The selected data rate defines user data rate and E_b/N_0 threshold for power control (eb/no_threshold) which is illustrated in Table 7.5

Table 7.5: User data rates

	12.2 kbps	64 kbps	144 kbps	384 kbps
E_b/N_0	6 dB	4.5 dB	3 dB	3 dB
Data rate 1	100%	-	-	-
Data rate 2	-	100%	-	-
Data rate 3	-	-	100%	-
Data rate 4	-	-	-	100%

7.7.6 Simulation Output

The quantities in output to the simulator are the following ones:

- Average downlink SINR
- Average downlink E_b/N_0
- E_b/N_0 for each mobile in power control stage before and after power control.
- EIRP before and after power control

The next section gives an analysis for the data resulted of comparing SINR and E_b/N_0 at all MSs. It also gives an analysis for the data gathered by changing some of the prescribed input parameters as the number of users, separation angle, cell radius, and the user data rate to see their effect.

7.7.7 Simulation Results and Discussion for Downlink Scenario

7.7.7.1 Introduction

This chapter gives also the analysis and discussion of the simulation results of adaptive array antenna downlink performance, downlink power control in WCDMA system and comparison between adaptive array antenna and omnidirectional antenna which has been run. Every plotted data is the average value of the readings taken at the end of the cycles after repeating the simulation for 3 times. The results of the performance comparison between the two antennas are analysed. The performance of the adaptive array antenna will be analysed according to the particular parameter change such as user data rate with respect to the increasing number of MSs. The factors which have been observed are SIR , and E_b/N_0 .

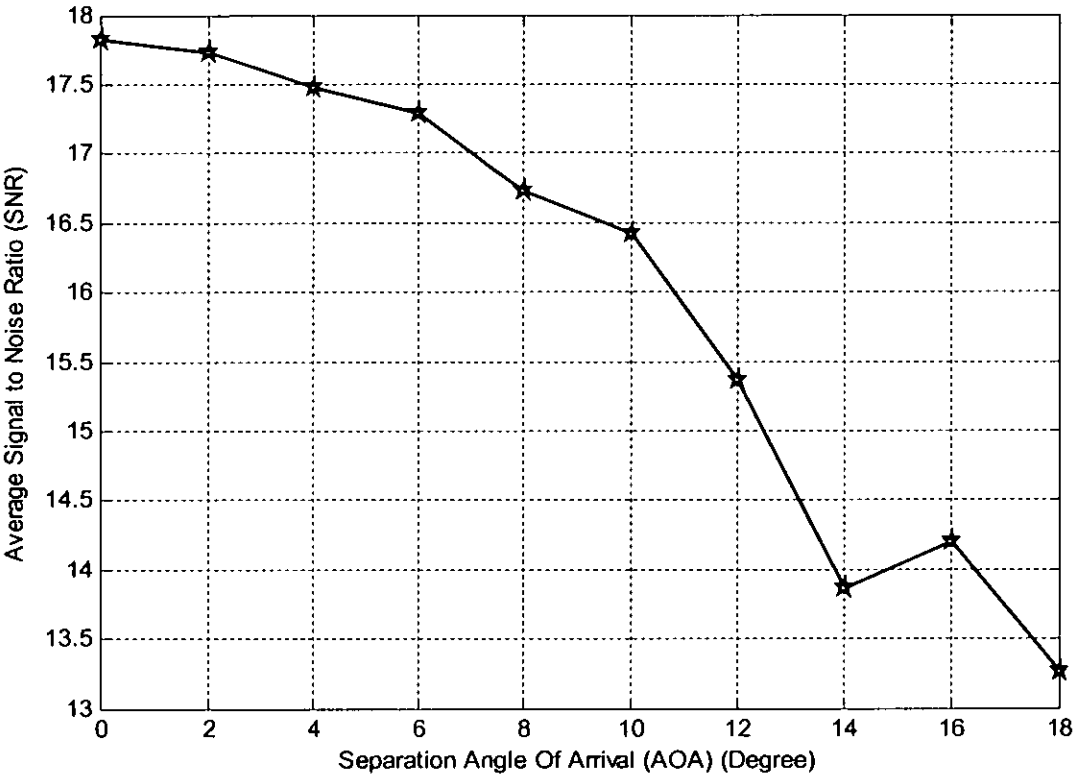
7.7.8 Performance of adaptive array antenna

The input parameters used during the simulation of the performance are shown in Table 7.6

Table 7.6: Input parameters for the simulation of adaptive array antenna performance in downlink WCDMA system performance comparison

Parameter	Value
Propagation path loss model	Hata model
Number of mobile stations	From 10 to 100
Data rate	(12.2, 64, 144, 384 kbps)

Figure 7.26 shows the relation between downlink average E_b/N_0 and threshold separation angle for beamforming algorithm in adaptive beam array antenna at number of users equal to one hundred.



Figures 7.26: Average SNR for adaptive array antenna in downlink WCDMA vs. Separation Angle of Arrival (AOA)

As we see from Figure 7.26 the best threshold separation angle for this number of users is zero, for downlink performance we will use beamforming algorithm with this threshold separation angle to evaluate average SINR and Eb/No in downlink WCDMA adaptive array antenna.

Figures 7.27 and 7.28 shows the SINR and Eb/No for adaptive array antenna in downlink WCDMA system, the simulation done with threshold separation angle for beamforming equal to zero, this threshold separation angle gives best SINR and Eb/No, threshold separation angle equal to zero that means all users with same angle of arrive will be formed in a one beam, simulation run for 10 cycles for each number of users and average result are shown in figures below.

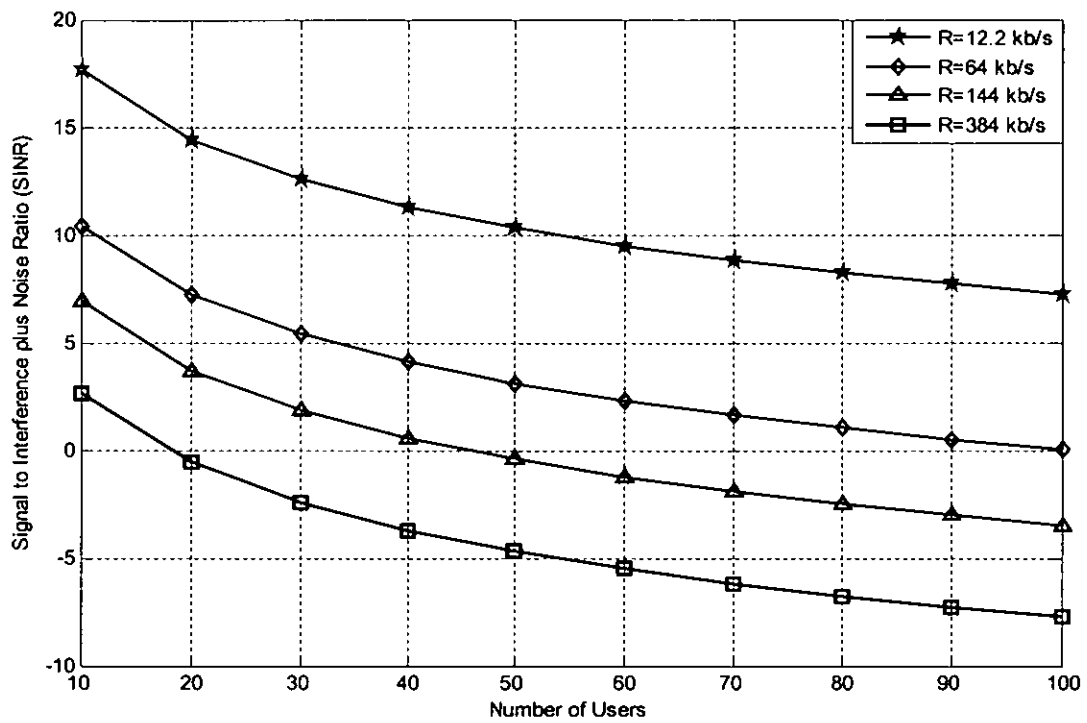


Figure 7.27: SINR vs. Number of users for adaptive array antenna in downlink WCDMA system

As we see from figure 7.27 the average downlink SINR in unit dB versus the number of MSs for data rates ranging from data rate 1 (12.2 kbps) to data rate 4 (384 kbps). From this figure, it can be clearly observed that the lower data rate yields higher downlink SINR as the number of MSs becomes lower.

Figure 7.28 shows the average E_b/N_0 in unit dB versus the number of users. From this figure it can be clearly observed that the E_b/N_0 threshold has been achieved for data rates 12.2 kb/s, 64 kb/s and 144 kb/s with one hundred users, but for data rate 384 kb/s the E_b/N_0 threshold achieved until number of users about 82 users, because E_b/N_0 threshold of 384 kb/s is 3 dB.

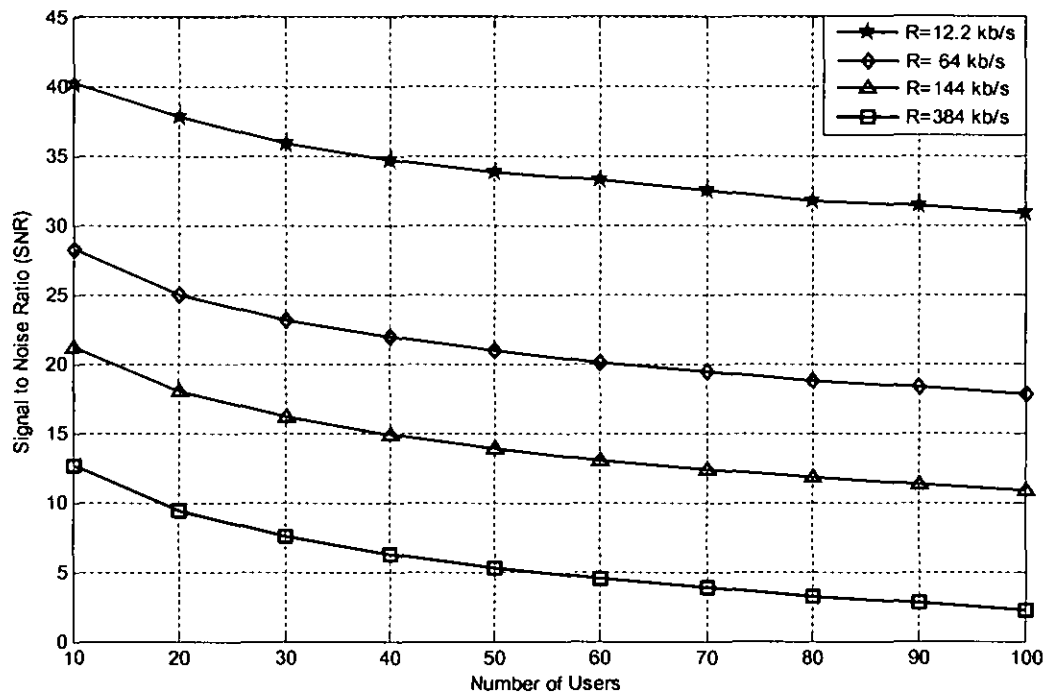


Figure 7.28: SNR vs. Number of users for adaptive array antenna in downlink WCDMA system

We can find the maximum number of users can be accommodated for each bit rate by knowing E_b/N_0 threshold for each bit rate, Table 7.7 below shows E_b/N_0 threshold for each bit rate.

Table 7.7: E_b/N_0 threshold for each bit rate

	12.2 kbps	64 kbps	144 kbps	384 kbps
E_b/N_0	6 dB	4.5 dB	3 dB	3 dB
Data rate 1	100%	-	-	-
Data rate 2	-	100%	-	-
Data rate 3	-	-	100%	-
Data rate 4	-	-	-	100%

Now we can evaluate the maximum number of users can be accommodated in which all users have a $E_b/N_0 > E_b/N_0$ threshold for each bit rate, The simulation results show that for 12.2 kb/s the number of users is quit high more than 10000 users, for 64 kb/s the number of users can be accommodated is 2100 users, for 144 kb/s the number of users is 573 users, and for 384 kb/s the number of users is 82 users.

7.7.9 Performance comparison between adaptive array antenna and omnidirectional antenna

Figure 7.29 shows comparison between adaptive array antenna using single beam for users with same angle of arrival and omnidirectional antenna in downlink WCDMA system by calculating average E_b/N_0 for both antennas with bit rates 64 kb/s in each number of users.

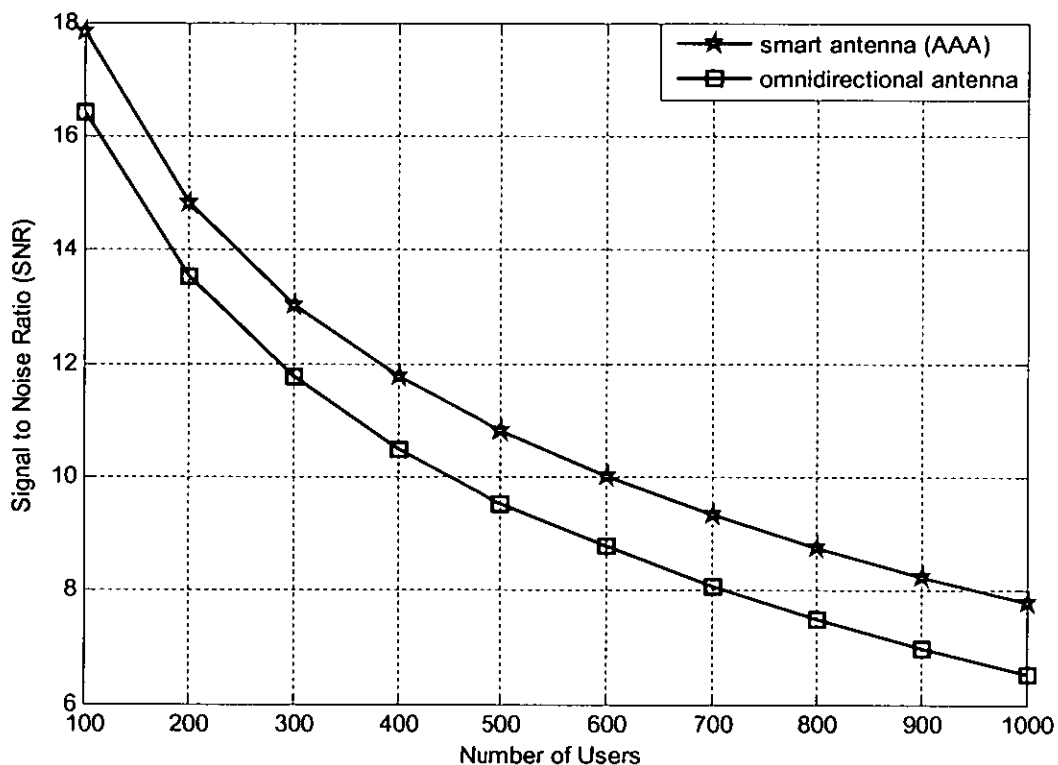


Figure 7.29: Average downlink SNR vs. Number of users for omnidirectional and Adaptive array antennas

As we see from the figure until 1000 users adaptive array antenna is better than omnidirectional antenna by about 2 dB.

7.7.10 Downlink power control of adaptive array antenna (AAA)

Figures 7.30 to 7.31 show the results of the simulation which have been run using the input parameters shown in Table 7.8

Table 7.8: Input parameters for the simulation of the user data rate effect

Parameter	Value
Propagation path loss model	Hata model
Number of mobile stations	50
Power control step size	2 dB
E_b/N_0 threshold	5 dB
Number of simulation cycles	50
Bit rate	64 kB/s

Figure 7.30 shows E_b/N_0 for each user when the threshold separation angle for beam forming algorithm is zero and figure 7.31 shows EIRP in this case.

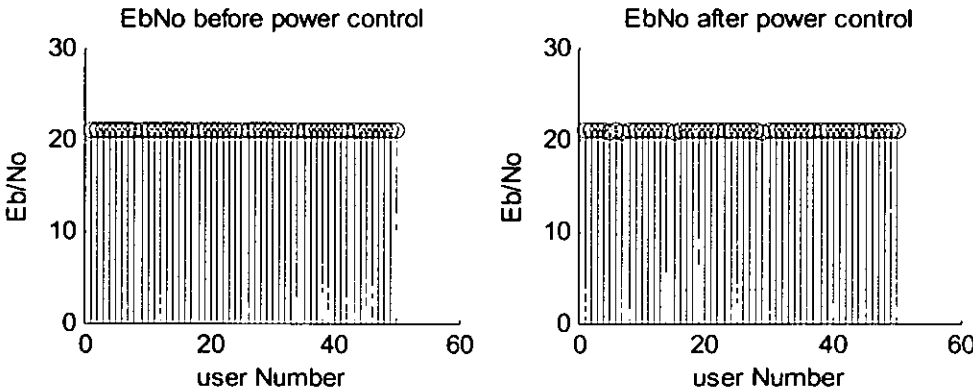


Figure 7.30: E_b/N_0 for each mobile before and after power control

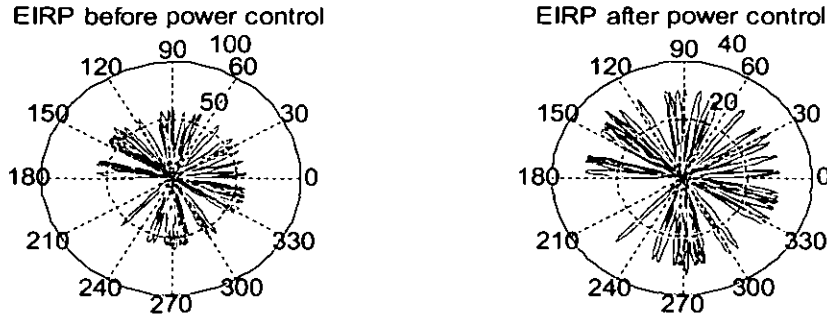


Figure 7.31: EIRP before and after power control

Figure 7.32 shows that the received E_b/N_0 at the user before and after power control same, and figure 7.26 shows that the base station EIRP has been reduced from around 50 to around 20, this means that the reducing of transmitted power is reducing the received signal and intracell interference by same factor, and the dominant interference in this case is intracell interference

Figure 7.32 shows E_b/N_0 for each user when the threshold separation angle for beam forming algorithm is five and figure 7.33 shows EIRP in this case.

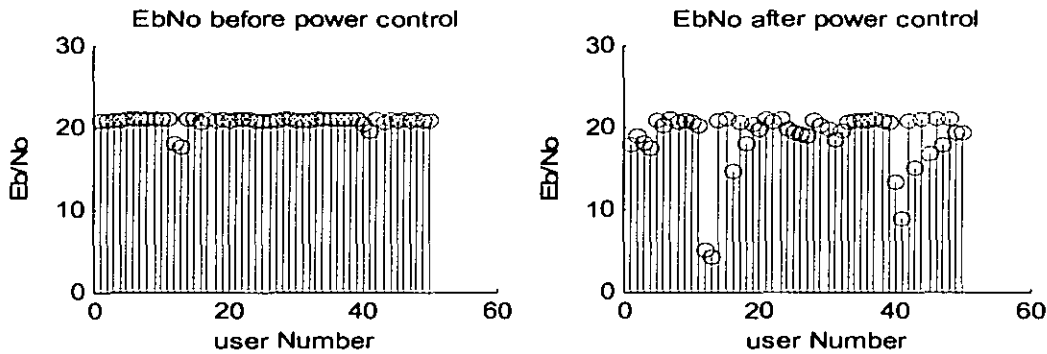


Figure 7.32: E_b/N_0 for each mobile before and after power control

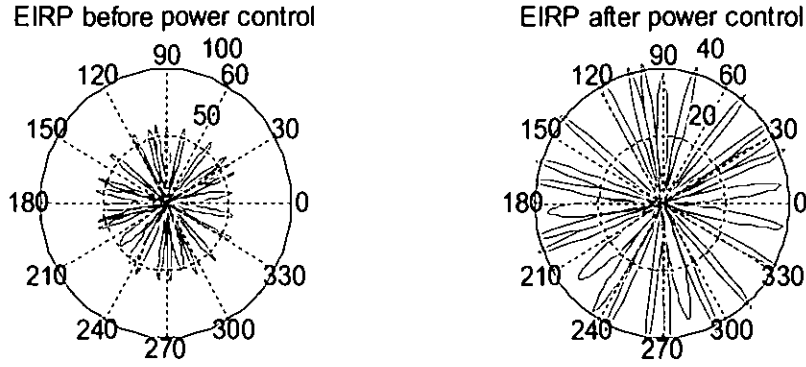


Figure 7.33: EIRP before and after power control

In figure 7.32 the minimum Eb/No reduced to threshold value, and some users Eb/No haven't effected by reducing the base station transmitted power because they are affected by intracell interference more than intercell interference and reducing the power will reduce both signal and interference by same factor that means Eb/No will be same before power control, in the figure 7.31 and 7.33 both cases reducing the transmitted power, if the system need to increase the transmitted power, power control will be effective if $(GP > (\text{number of users} - 1) * \text{correlation factor})$, This can be obtained from the analysis below.

$$P_r = \frac{P_t \times G_p \times (G(\theta) + G_{inter}(\theta))}{L} \quad (7.10)$$

$$I_{intra_cell} = \frac{P_t \times (N - 1) \times (1 - \alpha)}{L} \times (G(\theta) + G_{inter}(\theta)) \quad (7.11)$$

Power control to be effective in state of increasing $\Delta P_r > \Delta I$

$$\frac{\Delta P_t \times G_p \times G(\theta) + G_{inter}(\theta)}{L} > \frac{\Delta P_t \times (N - 1) \times (1 - \alpha)}{L} \times (G(\theta) + G_{inter}(\theta)) \quad (7.12)$$

From equation (7.12)

$$G_p > (N-1) * (1-\alpha)$$

Where

G_p is processing gain.

N is the number of users.

α is orthogonal factor and $(1-\alpha)$ is correlation factor.

That means power control is more effective at lower bit rate because as bit rate lower the processing gain is higher, and for each bit rate there is a limit of number of users to control the power.

For bit rate =12.2 kb/s

$$G_p = 314,$$

$$(N-1)*(1-\alpha) \text{ should be } < 314, (1-\alpha) = 0.6$$

This means $N < 525$ users.

For bit rate 64 kb/s

$$G_p = 60$$

$$N < 101.$$

But for 12.2 and 64 kb/s with applying single beam for users with same AOA (threshold separation angle =0) and with this number of users power need to be reduced because the signal level is higher than the interference level, this means the power control is not effect in term of capacity, it is benefit is reducing the transmitted power from the base station, it is needed in term of power not in term of capacity.

The capacity will not increased by power control, while transmitted power reduced, figure 7.34 show that the maximum number of users in which power control is effective for bit rate =144kb/s and this number equal to the maxim number of users can be accommodate with out power control, it is about 573 users.

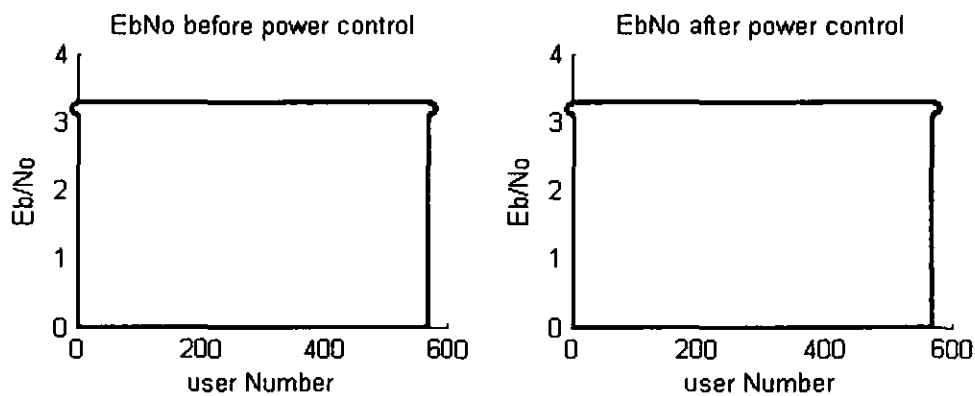


Figure 7.34: Eb/No for each user before and after power control for R=144 kb/s

The number of users with or without power control is same and for this number of users which threshold number the transmitted power before and after power control is same, but for number of users less than this number the transmitted power after power control is lower than the transmitted power before power control and lower than neighboring cells, figure 7.35 show EIRP before and after power control for bit rate 144 kb/s.

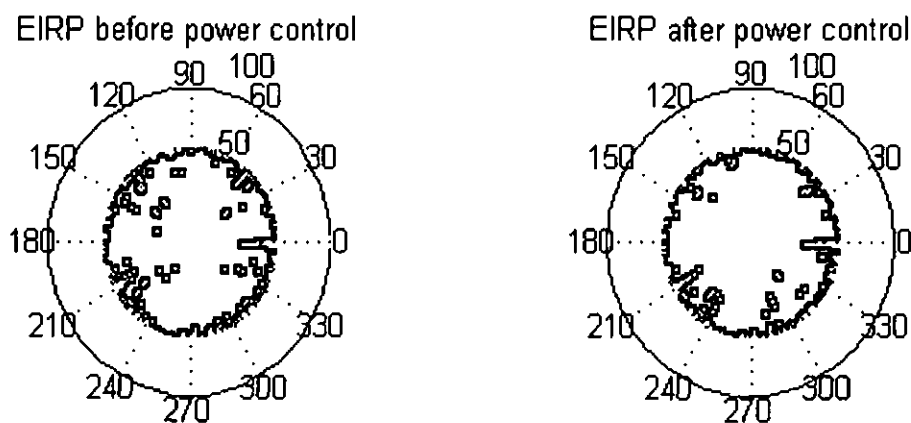


Figure 7.35: EIRP before and after power control for R=144 kb/s

Same thing for bit rate 384 kb/s, but the maximum number of users that can be accommodated is much lower than the number of users accommodated with bit rate 144kb/s, and also equal to the maximum number of users that can be accommodated with out power control, and equal to 82 users.

Figure 7.36 show E_b/N_0 before and after power control and figure 7.37 shows EIRP before and after power control.

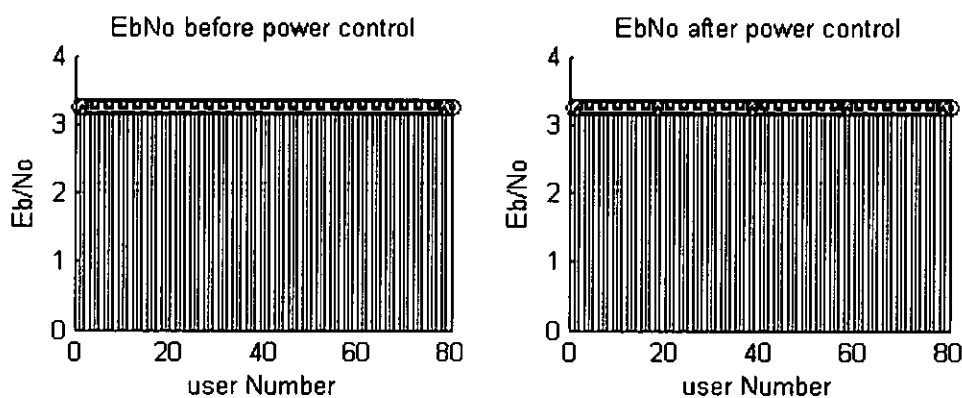


Figure 7.36: E_b/N_0 for each user before and after power control
for $R=384$ kb/s

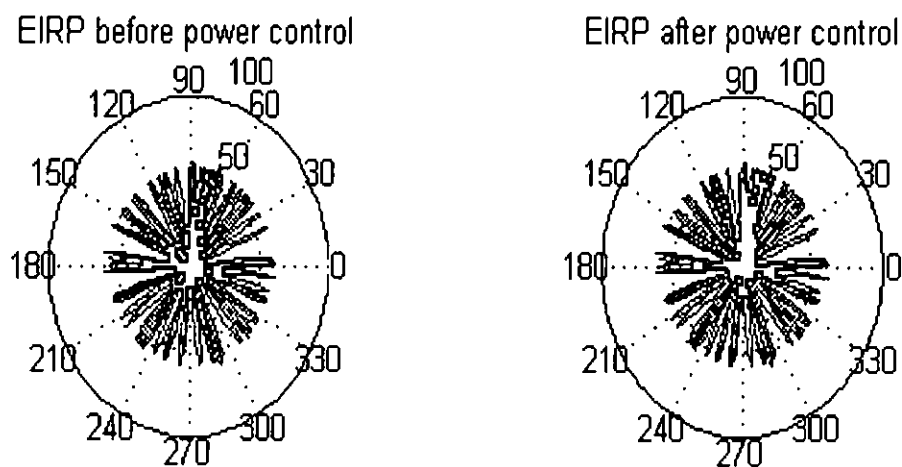


Figure 7.37: EIRP before and after power control for
 $R=384$ kb/s

7.7.11 Summary

In this chapter, we present the simulation results of different PSA beamformer-Rake receivers in the macrocellular circular channel. We provide the BER vs. user and the BER vs. E_b/N_0 performances of the LMS, DMI and RLS based beamformer-Rake receivers as a function of number of antenna elements and number of RAKE fingers. We compare the performance curves of the beamformer-Rake receiver with both the conventional 1-D RAKE receiver and the conventional beamformer. From the comparisons, we conclude that in almost all the cases, the beamformer-Rake receiver outperforms both the conventional 1-D RAKE and the conventional beamformer by a significant margin. We also see that, RAKE combining gives improved performance in the circular channel. Also we see that, all the PSA beamforming techniques employed in the beamformer-Rake receiver perform very similar in macrocellular circular channel. Also in this chapter, we develop, simulate and evaluate the SINR and E_b/N_0 (Signal to Noise Ratio) performances of an adaptive beamforming technique in WCDMA system for downlink scenario with and without power control algorithm. The performance is then compared with an omnidirectional antenna system. Simulation results shows that the best performance can be achieved when all mobiles with different distance from the base station have the same angle of arrival (AOA) in one beam. Furthermore, the maximum capacity for different data rate users that can be accommodated by the system was determined in this chapter.

CHAPTER EIGHT

CONCLUSIONS AND FUTURE WORK

8.1 Conclusion

In this thesis, we investigate the performance of three different PSA coherent beamformer-Rake receivers intended for the uplink of the W-CDMA system. First, we present a detailed mathematical analysis of these PSA beamformer-Rake receivers with the uplink W-CDMA signal format. Then we set up a computer simulation test bed to compare the performance of these receivers in GBSB statistical channel environment with multipath Rayleigh fading. The BER performance versus both the number of users and E_b/N_0 of all these receivers are compared with varying number of spatial and temporal processing parameters (e.g., number of antenna elements and RAKE fingers). It is shown that, in most of the cases, a combination of a beamformer with a small number of elements and a RAKE combiner is sufficient to outperform both the single element RAKE receiver and the single finger beamformer. It is also shown that, depending on the channel conditions; there is a performance tradeoff between the beamformer and the RAKE combiner of the beamformer-Rake receiver. The beamformer works well when the multipath AOA range is large, while the RAKE receiver shows better performance when many dominant multipaths are present in the channel. We compare the performance of the three PSA beamforming techniques used in the beamformer-Rake receiver, i.e., DMI, LMS and RLS adaptive beamforming. In most of the cases, the performance is very close to each other. We also derived the output SINR expression of a beamformer-Rake receiver using the generalized expression of an optimum beamformer. In this thesis, a detailed literature survey on different space-time processing techniques intended for CDMA is also provided.

In this thesis, we develop, simulate and evaluate the SINR and Eb/No performances of an adaptive beamforming technique in WCDMA system for downlink scenario with and without power control algorithm. The performance is then compared with an omnidirectional antenna system. Simulation results shows that the best performance can be achieved when all mobiles with different distance from the base station have the same angle of arrival (AOA) in one beam. Furthermore, the maximum capacity for different data rate users that can be accommodated by the system was determined in this chapter. Also it shown that, downlink power control is effective in term of reducing BS transmitting power, but it is not effective in term of increasing the capacity of adaptive array antenna system, it is effective if the signal level is higher than interference level and the transmitted power need to be reduced.

8.2 Future Work

Based on the work that we have done in this thesis, a number of interesting research direction can be pursued in the future. These are outlined below:

1. Since the W-CDMA has pilot symbols defined in the uplink, we only concentrated on the PSA based beamforming techniques. It will be interesting to compare the performance of the blind beamforming based beamformer-Rake receivers with the PSA beamformer-Rake receiver.
2. Even though these receivers are attractive in terms of performance, their complexity maybe too high to make them feasible for implementation in a base station. It will definitely be useful to show the complexity trade-offs of a beamformer-Rake receiver with the 1-D RAKE receiver and the conventional antenna array.
3. In Chapter 6, we derived the generalized optimum SINR expression for a beamformer-Rake receiver. However, we need to validate the expression and the

assumptions that we made through simulation. Also, that analysis may be extended to derive the BER expression for the beamformer-Rake receiver.

4. In the simulation, we assumed that all the users have the same SF and hence the same data rate. It will be interesting, to shows the interference suppression performance of the antenna array for variable data rate users, which the W-CDMA is intended to support. Also, we assume perfect power control but the performance of beamformer-Rake receiver for imperfect power control scenario should be interesting.
5. For vector channel models, we used the GBSB circular channel model. Even though they are more realistic than the simple parametric channel models, it would be even better if the performance is evaluated using measurement-based channel model.
6. All the beamformer-Rake receivers proposed for the W-CDMA are designed for the uplink. The downlink still remains to be explored even though space-time processing for the downlink is not very computationally practical.
7. Finally, Study the downlink power control for sectorized antenna system and compare its performance with non-sectorized antenna system or switched antenna system should be interesting.

REFERENCES

- [1] J. H. Reed, B. D. Woerner, C. I. Jacobs, W. H. Tranter and S. G. Wilson, "Space Time Processing for Third Generation CDMA Systems", Ph.D. Dissertation, Virginia Tech, Nov 2005.
- [2] J. Litva and T. K. Lo, *Digital Beamforming in Wireless Communications*. Boston, MA: Artech House, 1996.
- [3] T.S. Rappaport, *Wireless Communications: Principles and Practice*. Upper Saddle River, NJ: Prentice Hall PTR, 1996.
- [4] J. G. Proakis, *Digital Communications*. New York, NY: McGraw-Hill Inc., third ed., 1995.
- [5] M. W. Oliphant, "The Mobile Phone Meets the Internet", *IEEE Spectrum*, pp. 20-28, August 1999.
- [6] UMTS, *Spreading and Modulation*, 3G TS 25.213 V3.2.0 (2000-03).
- [7] UMTS, *Physical Channels and Mapping of Transport Channels onto Physical Channels (FDD)*, 3G TS 25.211 V3.2.0 (2000-03).
- [8] T. Ojanpera and R. Prasad, "An Overview of Air Interface Multiple Access for IMT-2000/UMTS," *IEEE Communications Magazine*, vol. 36, pp. 88-95, September 1998.
- [9] E. Dahlman, B. Gudmundson, M. Nilsson, and J. Skold, "UMTS/IMT-2000 Based on Wideband CDMA," *IEEE Communications Magazine*, vol. 36, pp. 70-80, September 1998.

- [10] E. Dahlman, P. Beming, Jens Knutsson, F. Ovesjo, Magnus Persson, and Christiaan Roobol, " WCDMA- The Radio Interface for Future Mobile Multimedia Communications," *IEEE Transactions on Vehicular Technology*, vol. 47, No. 4, pp. 1105-1118, November 1998.
- [11] M. W. Oliphant, "The Mobile Phone Meets the Internet," *IEEE Spectrum*, pp. 20-28, Aug. 1999.
- [12] J. C. Liberti, Jr. and T. S. Rappaport, *Analysis of CDMA Cellular Radio Systems Employing Adaptive Antennas*. PhD thesis, Virginia Polytechnic Institute and State University, Sept. 1995.
- [13] A. Naguib and A. Paulraj, "Performance of CDMA Cellular Networks with Base-Station Antenna Arrays," in *Proc. International Zurich Seminar on Digital Communications*, (Zurich, Switzerland), pp 87-100, Mar. 1994.
- [14] A. F. Naguib, A. Paulraj, and T. Kailath, "Capacity Improvement with Base-Station Antenna Array in Cellular CDMA," *IEEE Trans. Veh. Tech.*, vol. VT-43(3), pp. 691-698, Aug. 1994.
- [15] F. Adachi, K. Ohno, A Higashi, T. Dohi, and Y. Okumura, "Coherent multicode DSSSS mobile radio access," *IEICE Trans. Commun.*, vol. E79-B, no. 9, pp. 1316-1325, Sept 1996.
- [16] B. Widrow, P. E. Mantez, L. J. Griffiths and B. B. Goode , .Adaptive Antenna Systems,. *IEEE Proceedings*, vol. 55, No. 12, pp. 2143 -2159, Dec. 1967.
- [17] L. C. Van Atta, .Electromagnetic Reflections,. U.S. Patent 2908002, Oct. 6, 1959.
- [18] .Special Issues on Active and Adaptive Antenna Systems,. *IEEE Trans. Antennas and Propagation*, vol. AP-12, March 1964.

- [19] F. Bryn, .Optimum Signal Processing of Three-Dimensional Arrays Operating on Gaussian Signals and Noise, *Journal of Acoust. Soc. Am.*, vol. 34, pp. 289-297, March 1962.
- [20] H. Mermoz, .Adaptive Filtering and Optimal Utilization of an Antenna,. U.S. Navy Bureau of Ships (Translation 903 of Ph.D. thesis, Institute Polytechnique. Grenoble, France), Oct. 4, 1965.
- [21] S. W. W. Shor, .Adaptive Techniques to Discriminate Against Coherent Noise in Narrow-Band System,. *Journal of Acoust. Soc. Am.*, vol. 39, pp. 74-78, Jan. 1966.
- [22] R. B. Ertel, *Antenna Array Systems: Propagation and Performance*. Ph.D. Dissertation, VirginiaTech, July 1999.
- [23] V. C. Anderson and P. Rudnick, .Rejection of a coherent arrival at an array,. *J. Acoust. Soc.Amer.*, vol. 45, pp. 406.410, 1969.
- [24] V. C. Anderson, .DICANNE, a realizable adaptive process,. *J.Acoust. Soc. Amer.*, vol. 45, pp.398.405, 1969.
- [25] H. A. d.Assumpcao and G. E. Mountford, .An overview of signal processing for arrays of receivers,. *J. Inst. Eng. Aust.and IREE Aust.*, vol. 4, pp. 6.19, 1984.
- [26] L. C. Godara and A. Cantoni, .Uniqueness and linear independence of steering vectors in array space,. *J. Acoust. Soc. Amer.*,vol. 70, pp. 467.475, 1981.
- [27] Y.Bresler, V. U. Reddy, and T. Kailath, .Optimum beamforming for coherent signal and interferences,. *IEEE Trans. Acoust.,Speech, Signal Processing*, vol. 36, pp. 833.843, 1988.

- [28] I. Chiba, T. Takahashi, and Y. Karasawa, .Transmitting null beam forming with beam space adaptive array antennas,. in the Proceedings of IEEE 44th Vehicular Technology Conf.,Stockholm, Sweden, pp. 1498.1502,1994.
- [29] L. E. Brennan and I. S. Reed, .Theory of adaptive radar,. IEEE Trans. Aerosp. Electron. Syst.,vol. AES-9, pp. 237.252, 1973.
- [30] I. S. Reed, J. D. Mallett, and L. E. Brennan, .Rapid convergence rate in adaptive arrays,. IEEE Trans. Aerosp. Electron. Syst.,vol. AES-10, pp. 853.863, 1974.
- [31] A. M. Vural, .An overview of adaptive array processing for sonar application,. EASCON.75 Records, pp. 34A.34M.
- [32] S. P. Applebaum, .Adaptive arrays,. IEEE Transaction on Antennas and Propagation, vol. AP-24, pp. 585.598, 1976.
- [33] J. Capon, .High-resolution frequency-wave number spectrum analysis,. IEEE Proceedings, vol.57, pp. 1408.1418, 1969.
- [34] J. H. Winters, .Optimum combining in digital mobile radio with cochannel interference,. IEEE Journal on Select Areas of Communications, vol. SAC-2, pp. 528.539, 1984.
- [35] J. H. Winters, .Optimum combining for indoor radio systems with multiple users,. IEEE Transactions on Communications, vol. COM-35, pp.1222.1230, 1987.
- [36] B. Suard, A. F. Naguib, G. Xu, and A. Paulraj, .Performance of CDMA mobile communication systems using antenna arrays,.IEEE Int. Conf. Acoustics, Speech, and Signal Processing(ICASSP), Minneapolis, MN, 1993, pp. 153.156.

- [37] A. F. Naguib and A. Paulraj, .Performance of CDMA cellular networks with base-station antenna arrays,. In the Proceedings of IEEE Int. Zurich Seminar on Communications, 1994, pp.87.100.
- [38] B. Widrow, J. R. Glover, J. M. McCool, J. Kaunitz, C. S. Williams, R. H. Hearn, J. R. Zeidler, E.Dong, Jr., and R.C. Goodlin, .Adaptive noise canceling: Principles and applications,. IEEE Proceedings, vol. 63, pp. 1692.1716, 1975.
- [39] S. P. Applebaum and D. J. Chapman, .Adaptive arrays with main beam constraints,. IEEE Transaction on Antennas and Propagation, vol. AP-24, pp. 650.662, 1976.
- [40] B. Widrow, K. M. Duvall, R. P. Gooch, and W. C. Newman, .Signal cancellation phenomena in adaptive antennas: Causes and cures,. *IEEE Trans. Antennas Propagat.*, vol. AP-30, pp.469.478, 1982.
- [41] C. L. Zahm, .Application of adaptive arrays to suppress strong jammers in the presence of weak signals,. *IEEE Trans. Aerosp.Electron. Syst.*, vol. AES-9, pp. 260.271, 1973.
- [42] L. J. Griffiths, .A comparison of multidimensional Wiener and maximum-likelihood filters for antenna arrays,. In IEEE Proceedings, vol. 55, pp. 2045.2047, 1967.
- [43] A. Flieller, P. Larzabal, and H. Clergeot, .Applications of high resolution array processing techniques for mobile communication system,. In the Proceedings of IEEE Intelligent Vehicles Symposium. Paris, France, pp. 606.611,1994.
- [44] J. H. Winters, J. Salz, and R. D Gitlin, .The impact of antenna diversity on the capacity of wireless communication systems, .IEEE Transaction on Communications, vol. 42, pp. 1740.1751, 1994.

- [45] S. Anderson, M. Millnert, M. Viberg, and B. Wahlberg, .An adaptive array for mobile communication systems,. IEEE Transaction on Vehicular Technology, vol. 40, pp. 230.236,1991.
- [46] T. Gebauer and H. G. Gockler, .Channel-individual adaptive beamforming for mobile satellite communications,. IEEE Journal on Selected Areas of Commun, vol. 13, pp. 439.448, 1995.
- [47] J. F. Diouris, B. Feuvrie, and J. Saillard, .Adaptive multisensor receiver for mobile Communications,. Ann. Telecommun., vol.48, pp. 35.46, 1993.
- [48] P. W. Howells, .Explorations in fixed and adaptive resolution at GE and SURC,. IEEE Transaction on Antennas and Propagation, vol. AP-24, pp. 575.584, 1976.
- [49] L. J. Griffiths and C. W. Jim, .An alternative approach to linearly constrained adaptive beamforming,. IEEE Transaction on Antennas and Propagation, vol. AP-30, pp. 27.34, 1982.
- [50] C. W. Jim, .A comparison of two LMS constrained optimal array structures,. IEEE Proceedings, vol. 65, pp. 1730.1731, 1977.
- [51] B. D. Van Veen and R. A. Roberts, .Partially adaptive beamformer design via output power minimization,. IEEE Transaction on Acoust., Speech, Signal Processing, vol. ASSP-35, pp.1524.1532, 1987.
- [52] F. Qian and B. D. Van Veen, .Partially adaptive beamformer design subject to worst case performance constraints,. IEEE Transaction on Signal Processing, vol. 42, pp. 1218.1221, 1994.

- [53] A. Cantoni and L. C. Godara, .Performance of a post beamformer interference canceller in the presence of broadband directional signals,. J. Acoust. Soc. Amer., vol. 76,pp. 128.138,1984.
- [54] E. Brookner and J. M. Howell, .Adaptive-adaptive array processing,. IEEE Proceedings, 1986, vol. 74, pp. 602.604.
- [55] J. T. Mayhan, .Adaptive nulling with multiple beam antennas,. IEEE Transaction on Antennas and Propagation, vol. AP-26, pp. 267.273, 1978.
- [56] W. E. Rodgers and R. T. Compton Jr., .Adaptive array bandwidth with tapped delay line processing,. IEEE Trans. Aerosp. Electron. Syst., vol. AES-15, pp. 21.28, 1979.
- [57] E. W. Vook and R. T. Compton, Jr., .Bandwidth performance of linear arrays with tapped delay line processing,. IEEE Trans. Aerosp. Electron. Syst., vol. 28, pp. 901.908, 1992.
- [58] T. S. Durrani, N. L. M. Murukutla, and K. C. Sharman, .Constrained algorithm for multi-input adaptive lattices in array processing,. In The Proceedings of ICASSP, Atlanta, GA, 1981, pp.297.301.
- [59] G. R. L. Sohie and L. H. Sibul, .Stochastic convergence properties of the adaptive gradient lattice,. IEEE Trans. Acoust., Speech, Signal Processing, vol. ASSP-32, pp. 102.107, 1984.
- [60] M. H. Er and A. Cantoni, .Derivative constraints for broadband element space antenna array processors,. IEEE Trans. Acoust., Speech, Signal Processing, vol. ASSP-31, pp. 1378.1393,1983.
- [61] I. Thng, A. Cantoni, and Y. H. Leung, .Derivative constrained optimum broadband antenna arrays,. IEEE Trans. Signal Processing, vol. 41, pp. 2376.2388, 1993.

- [62] K. M. Buckley, .Spatial/spectral filtering with linearly constrained minimum variance beamformers,. IEEE Trans. Acoust., Speech, Signal Processing, vol. ASSP-35, pp. 249.266,1987.
- [63] M. H. Er, .On the limiting solution of quadratically constrained broadband beamformers,. IEEE Trans. Signal Processing, vol.41, pp. 418.419, 1993.
- [64] N. Ishii and R. Kohno, .Spatial and temporal equalization based on an adaptive tapped-delay linearray antenna,. IEICE Trans.Commun. vol. E78-B, pp. 1162.1169, Aug. 1995.
- [65] R. Kohno, H. Wang, and H. Imai, .Adaptive array antenna combined with tapped delay line using processing gain for spread spectrum CDMA systems,. Presented at the IEEE Int. Symp.Personal Indoor and Mobile Radio Communications (PIMRC), Boston, MA, 1992.
- [66] V. A. N. Barroso, M. J. Rendas, and J. P Gomes, .Impact of array processing techniques on the design of mobile communication systems,. In the Proceedings of IEEE 7th Mediterranean Electrotechnical, Antalya, Turkey, 1994, pp. 1291.1294.
- [67] M. I. Miller and D. R. Fuhrmann, .Maximum likelihood narrow-band direction finding and the EM algorithm,. IEEE Trans. Acoust., Speech, Signal Processing, vol. 38, pp. 1560.1577, 1990.
- [68] J. Makhoul, .Linear prediction: A tutorial review,. IEEE Proceedings, vol. 63, pp. 561.580,1975.
- [69] D. P. Skinner, S. M. Hedlicka, and A. D. Mathews, .Maximum entropy array processing,. J.Acoust. Soc. Amer., vol. 66, pp.488.493, 1979.

- [70] V. F. Pisarenko, .The retrieval of harmonics from a covariance function,. *Geophys. J. R. Astron.Soc.*, vol. 33, pp. 347.366,1973.
- [71] M. Wax, T. J. Shan, and T. Kailath, .Spatio-temporal spectral analysis by eigenstructure methods,. *IEEE Trans. Acoust., Speech, Signal Processing*, vol. ASSP-32, pp. 817.827, 1984.
- [72] V. U. Reddy, B. Egardt, and T. Kailath, .Least-squares type algorithm for adaptive Implementation of Pisarenko.s harmonic retrieval method,. *IEEE Trans. Acoust., Speech, Signal Processing*, vol. ASSP-30, pp. 399.405, 1982.
- [73] J. R. Yang and M. Kaveh, .Adaptive eigensubspace algorithms for direction or frequency estimation and tracking,. *IEEE Trans. Acoust., Speech, Signal Processing*, vol. ASSP-36, pp.241.251, 1988.
- [74] M. G. Larimore, .Adaptive convergence of spectral estimation based on Pisarenko harmonic retrieval,. *IEEE Trans. Acoust., Speech, Signal Processing*, vol. ASSP-31, pp. 955.962, 1983.
- [75] H. Ouibrahim, .Prony, Pisarenko and the matrix pencil: A unified presentation,. *IEEE Trans.Acoust., Speech, Signal Processing*, vol. ASSP-37, pp. 133.134, 1989.
- [76] B. Friedlander, .A signal subspace method for adaptive interference cancellation,. *IEEE Trans.Acoust., Speech, Signal Processing*, vol. 36, pp. 1835.1845, 1988.
- [77] H. Ouibrahim, D. D. Weiner, and T. K. Sarkar, .A generalized approach to direction finding, .*IEEE Trans. Acoust., Speech, Signal Processing*, vol. 36, pp. 610.613, 1988.
- [78] A. Paulraj and T. Kailath, .Eigenstructure methods for direction of arrival estimation in the presence of unknown noise field,.*IEEE Trans. Acoust., Speech, Signal Processing*, vol. ASSP-34, pp. 13.20, 1986.

- [79] R. O. Schmidt, .Multiple emitter location and signal parameter estimation,. IEEE Trans.Antennas Prop., vol. AP-34, pp. 276.280, 1986.
- [80] R. D. DeGroat, E. M. Dowling, and D. A. Linebarger, .The constrained MUSIC problem,. IEEE Trans. Signal Processing, vol. 41, pp. 1445.1449, 1993.
- [81] R. W. Klukas and M. Fattouche, .Radio signal direction finding in the urban radio environment,. In *Proc. Nat. Technical Meeting Institute of Navigation*, San Francisco, CA, 1993, pp. 151.160.
- [82] A. Barabell, .Improving the resolution of eigenstructured based direction finding algorithms,. In the Proceedings of ICASSP, Boston, MA, 1983, pp. 336.339.
- [83] J. T. Mayhan and L. Niro, .Spatial spectral estimation using multiple beam antennas,. IEEE Trans. Antennas Prop., vol. AP-35, pp. 897.906, 1987.
- [84] I. Karasalo, .A high-high-resolution post beamforming method based on semi definite linear optimization,. IEEE Trans. Acoust., Speech, Signal Processing, vol. 38, pp. 16.22, 1990.
- [85] S. S. Reddi, .Multiple source location. A digital approach,. IEEE Trans. Aerosp. Electron.Syst, vol. AES-15, pp. 95.105, 1979.
- [86] R. Kumaresan and D. W. Tufts, .Estimating the angles of arrival of multiple plane waves,. IEEE Trans. Aerosp. Elect. Systems, vol. AES-19, pp. 134.139, 1983.
- [87] K. M. Buckley and X. L. Xu, .Spatial spectrum estimation in a location sector,. IEEE Trans.Acoust., Speech, Signal Processing, vol. ASSP-38, pp. 1842.1852, 1990.

- [88] R. Roy and T. Kailath, .ESPRIT.Estimation of signal parameters via rotational invariance techniques,. IEEE Trans. Acoust., Speech, Signal Processing, vol. ASSP-37, pp. 984.995, 1989.
- [89] G. Xu, S. D. Silverstein, R. H. Roy, and T. Kailath, .Beamspace ESPRIT,. IEEE Trans. Signal Processing, vol. 42, pp. 349.356,1994.
- [90] R. Hamza and K. Buckley, .Resolution enhanced ESPRIT,. IEEE Trans. Signal Processing, vol.42, pp. 688.691, 1994.
- [91] A. Paulraj, R. Roy, and T. Kailath, .A subspace rotation approach to signal parameter estimation,. IEEE Proceedings, vol. 74, pp. 1044.1045, 1986.
- [92] A. J. Weiss and M. Gavish, .Direction finding using ESPRIT with interpolated arrays,. IEEE Trans. Signal Processing, vol. 39, pp. 1473.1478, 1991.
- [93] J. A. Gansman, M. D. Zoltowski, and J. V. Krogmeier, .Multidimensional multirate DOA estimation in beamspace,. IEEE Trans. Signal Processing, vol. 44, pp. 2780.2792, 1996.
- [94] A. L. Swindlehurst, B. Ottersten, R. Roy, and T. Kailath, .Multiple invariance ESPRIT,. IEEE Trans. Signal Processing, vol. 40, pp. 867.881, 1992.
- [95] N. Yuen and B. Friedlander, .Asymptotic performance analysis of ESPRIT, higher order ESPRIT, and virtual ESPRIT algorithms,. IEEE Trans. Signal Processing, vol. 44, pp. 2537.2550, 1996.
- [96] M. D. Zoltowski and D. Stavrinos, .Sensor array signal processing via a procrustes rotations based eigenanalysis of the ESPRIT data pencil,. IEEE Trans. Acoust., Speech, Signal Processing, vol. 37, pp. 832.861, 1989.

- [97] Y. Wang and J. R. Cruz, .Adaptive antenna arrays for cellular CDMA cellular communicationsystems,. in the Proceedings of IEEE ICASSP, Detroit, MI, pp. 1725.1728, 1995.
- [98] M. Viberg, B. Ottersten, and T. Kailath, .Detection and estimation in sensor arrays using weighted subspace fitting,. IEEE Trans. Signal Processing, vol. 39, pp. 2436.2449, 1991.
- [99] A. Klouche-Djedid and M. Fujita, .Adaptive array sensor processing applications for mobile telephone communications,. IEEE Trans. Veh. Technol., vol. 45, pp. 405.416, 1996.
- [100] B. D. Van Veen, .Adaptive convergence of linearly constrained beamformers based on the sample covariance matrix,. IEEE Trans. Signal Processing, vol. 39, pp.1470.1473, 1991.
- [101] L. J. Horowitz, H. Blatt, W. G. Brodsky, and K. D. Senne, .Controlling adaptive antenna arrays with the sample matrix inversion algorithm,. *IEEE Trans. Aerosp. Electron. Syst.*, vol. AES-15,pp. 840.847, 1979.
- [102] S. Haykin, *Adaptive Filter Theory*. Englewood Cliffs, NJ: Prentice Hall, 1991.
- [103] B. Widrow and J. M. McCool, .A comparison of adaptive algorithms based on the methods of steepest descent and random search,. IEEE Trans. Antennas Prop., vol. AP-24, pp. 615.637,1976.
- [104] W. A. Gardner, .Comments on convergence analysis of LMS filters with uncorrelated data,.IEEE Trans. Acoust., Speech, Signal Processing, vol. ASSP-34, pp. 378.379, 1986.

- [105] J. B. Foley and F. M. Boland, .A note on the convergence analysis of LMS adaptive filters with Gaussian data,. IEEE Trans. Acoust., Speech, Signal Processing, vol. 36, pp. 1087.1089, 1988.
- [106] V. Solo, .The limiting behavior of LMS,. IEEE Trans. Acoust., Speech, Signal Processing, vol.37, pp. 1909.1922, 1989.
- [107] A. Feuer and E. Weinstein, .Convergence analysis of LMS filters with uncorrelated Gaussian data,. IEEE Trans. Acoust., Speech, Signal Processing, vol. ASSP-33, pp. 222.229, 1985.
- [108] S. Jaggi and A. B. Martinez, .Upper and lower bounds of the misadjustment in the LMS algorithm,. IEEE Trans. Acoust., Speech, Signal Processing, vol. 38, pp. 164.166, 1990.
- [109] F. B. Boland and J. B. Foley, .Stochastic convergence of the LMS algorithm in adaptive systems,. Signal Process. vol. 13, pp. 339.352, 1987.
- [110] R. Y. Chen and C. L. Wang, .On the optimum step size for the adaptive sign and LMS algorithms,. IEEE Trans. Circuits Syst., vol. 37, pp. 836.840, 1990.
- [111] V. J. Mathews and S. H. Cho, .Improved convergence analysis of stochastic gradient adaptive filters using the sign algorithm,. IEEE Trans. Acoust., Speech, Signal Processing, vol. ASSP-35, pp. 450.454, 1987.
- [112] R. Nitzberg, .Application of the normalized LMS algorithm to MSLC,. IEEE Trans. Aerosp.Electron. Syst., vol. AES-21, pp. 79.91, 1985.
- [113] N. J. Bershad, .Analysis of the normalized LMS algorithm with Gaussian inputs,. IEEE Trans.Acoust., Speech, Signal Processing, vol. ASSP-34, pp. 793.806, 1986.

- [114] D. T. M. Slock, .On the convergence behavior of the LMS and the normalized LMS Algorithm,. IEEE Trans. Signal Processing, vol. 41, pp. 2811.2825, 1993.
- [115] M. Rupp, .The behavior of LMS and NLMS algorithms in the presence of spherically invariant processes,. IEEE Trans. Signal Processing, vol. 41, pp. 1149.1160, 1993.
- [116] O. L. Frost III, .An algorithm for linearly constrained adaptive array processing,. IEEE Proceedings, vol. 60, pp. 926.935, 1972.
- [117] A. Cantoni, .Application of orthogonal perturbation sequences to adaptive beamforming,.IEEE Trans. Antennas Prop., vol. AP-28, pp. 191.202, 1980.
- [118] L. C. Godara, .Improved LMS algorithm for adaptive beamforming,. IEEE Trans. Antennas Prop., vol. 38, pp. 1631.1635, 1990.
- [119] G. Raleigh, and A. Paulraj, .Time varying vector channel estimation for adaptive spatial equalization,. In the Proceedings of the IEEE Global Telecommunications Conference, pp.218-224, 1995.
- [120] P. Fabre and C. Gueguen, .Improvement of the fast recursive least-squares algorithms via normalization: A comparative study,. IEEE Trans. Acoust., Speech, Signal Processing, vol.ASSP-34, pp. 296.308, 1986.
- [121] E. Eleftheriou and D. D. Falconer, .Tracking properties and steady state performance of RLS adaptive filter algorithms,. IEEE Trans. Acoust., Speech, Signal Processing, vol. ASSP-34,pp.1097.1110, 1986.
- [122] M. S. Mueller, .Least squares algorithms for adaptive equalizers,. Bell Syst. Tech. J., pp.1905.1925, 1981.

- [123] J. M. Cioffi and T. Kailath, .Fast recursive-least-square, transversal filters for adaptive filtering,. IEEE Trans. Acoust., Speech, Signal Processing, vol. ASSP-32, pp. 998.1005, 1984.
- [124] R. A. Wiggins and E. A. Robinson, .Recursive solution to the multichannel filtering problem,.J. Geophys. Res., vol. 70, pp. 1885.1891, 1965.
- [125] G. V. Moustakids and S. Theodoridis, .Fast Newton transversal filters. A new class of adaptive estimation algorithms,. IEEE Trans. Signal Processing, vol. 39, pp. 2184.2193, 1991.
- [126] S. Qiao, .Fast adaptive RLS algorithms: A generalized inverse approach and analysis,. IEEE Trans. Signal Processing, vol. 39, pp. 1455.1459, 1991.
- [127] D. T. M. Slock and T. Kailath, .Numerically stable fast transversal filters for recursive least squares adaptive filtering,. IEEE Trans. Signal Processing, vol. 39, pp. 92.114, 1991.
- [128] J. Fernandez, I. R. Corden, and M. Barrett, .Adaptive array algorithms for optimal combining in digital mobile communication systems,. in the Proceedings of Inst. Elect. Eng. 8th Int. Conf.Antennas and Propagation, Edinburgh, Scotland, 1993, pp. 983.986.
- [129] Y. Wang and J. R. Cruz, .Adaptive antenna arrays for the reverse link of CDMA cellular communication systems,. Electron. Lett., vol. 30, pp. 1017.1018, 1994.
- [130] D. N. Godard, .Self-recovering equalization and carrier tracking in two-dimensional data communication systems,. IEEE Trans. Commun., vol. COM-28, pp. 1867.1875, 1980.

- [131] J. R. Treichler and B. G. Agee, .A new approach to multipath correction of constant modulus signals,. IEEE Trans. Acoust., Speech, Signal Processing, vol. ASSP-31, pp. 459.472, 1983.
- [132] R. Gooch, and J. Lundell, .The CMA array: An adaptive beamformer for constant modulus signal,. In the Proceedings of Int. Conf. on Acoust, Speech, Signal Processing,, pp. 2523.2526, April 1986.
- [133] B. G. Agee, .The Least Squares CMA: A new technique for rapid correction of constant modulus signals,. in the Proceedings of Int. Conf. on Acoust., Speech, Signal Processing,, pp.953.956, April 1986.
- [134] B. G. Agee, .Maximum likelihood approaches to blind adaptive signal extraction using narrowband arrays,. in the Proceedings of the Asilomar Conf. on Signals, Systems, and Computers, pp. 716-720, Nov. 1991.
- [135] T. E. Biedka, *A General Framework for the Analysis and Development of Blind Adaptive Algorithms*. Ph.D. dissertation, Virginia Tech, Oct 2001.
- [136] G. H. Golub and C.F. Van Loan, *Matrix Computations*, Baltimore, MD, John Hopkins University Press, 1989.
- [137] S. Kwon, I. Oh, and S. Choi, .Adaptive Beamforming from the Generalized Eigenvalue Problem with a Linear Complexity for a Wideband CDMA Channel ., In the Proceedings of the IEEE Vehicular Technology Conference 1999/Fall, pp.1890-1894.
- [138] D.Shim, F.Alam, and B.D. Woerner, .Performance Analysis of a Smart Antenna System with Blind Algorithm., In the Proceedings of the 11th Virginia Tech Symposium on Wireless Personal Communications, June 2001, USA.

- [139] F. Alam, D. Shim, and B.D. Woerner, .A New Low-Complexity Beamformer-Rake Receiver for WCDMA., in the proceedings of IEEE International Conference on Communications, ICC2002, vol. 1, pp. 160-164, New York, USA, April 2002.
- [140] S. Choi and D. Yun , .Design of an adaptive antenna array for tracking the source of maximum power and its application to CDMA mobile communications. IEEE Transactions on Antenna and Propagations, vol. 45, No. 9, pp. 1393 -1404, Sept. 1997.
- [141] S. Choi, T. K. Sarkar, and J. Choi, .Adaptive antenna array for direction of arrival estimation utilizing the conjugate gradient method., Signal Processing, vol. 45, pp. 313.327, 1995.
- [142] S. Choi and D. Shim, et al, .A New Blind Adaptive Beamforming Procedure Based on Conjugate Gradient Method for CDMA Mobile Communications., ETRI Journal, Vol. 22, No.2, pp 133-148, June, 1998.
- [143] S. Choi and D. Shim, .A novel adaptive beamforming algorithm for a smart antenna system in a CDMA mobile communication environment. IEEE Transactions on Vehicular, vol. 49, No. 5, pp. 1793 -1806, Sept. 2000.
- [144] S. Choi, S. Ahn and T. K. Sarkar, .A Linearized Power Method for Adaptive Beamforming in a Multipath Fading CDMA Environment., Microwave and Optical Technology Letter, Dec.2001.
- [145] S. Kim, S. Lee, Y. Yang, and Y. Kim, .A New Efficient Blind Beamforming Algorithm in WCDMA Systems. to appear in IEEE Signal Processing Magazine.
- [146] F. Alam, D. Shim, and B. D. Woerner , .A New Adaptive Algorithm for MSNR Beamforming in WCDMA System,. Submitted to the IEEE Vehicular Technology Conference, Spring 2003, Korea, April 2003.

- [147] B. H. Khalaj, A. Paulraj, and T. Kailath, .2D RAKE receivers for CDMA cellular systems,. In the Proceedings of IEEE Globecom, pp. 400-404, 1994.
- [148] A. F. Naguib, A. Paulraj, and T. Kailath, .Capacity improvement with base-station antenna arrays in cellular CDMA,. IEEE Trans. on Veh. Technol., vol. 43, no. 3, pp. 691-698, August 1994.
- [149] A. F. Naguib and A. Paulraj, .Effects of multipath and base-station antenna arrays on uplink capacity of cellular CDMA,. in the Proceedings of IEEE Globecom, pp. 395-399, 1994.
- [150] Y. M. Vasavada, T. E. Biedka, J. H. Reed, .Code Gated Algorithm: A Blind Adaptive Antenna Array Beamforming Scheme for Wideband CDMA", In the Proceedings of the Thirty-fourth Asilomar conference on Signals, Systems and Computers, November 2000, CA, USA.
- [151] S. Tanaka, M. Sawasashi, and F. Adachi, .Pilot symbol-assisted decision-directed coherent adaptive array diversity for DS-SS mobile radio reverse link,. *IEICE Trans. Commun.*, vol.E80-A, pp.2445-2454, Dec. 1997.
- [152] M. Dell'Anna, A.H. Aghvami, .Performance of optimum and suboptimum combining at the antenna array of a W-SS system,. IEEE Journal on Selected Areas in Communications, vol.17, Issue: 12, pp. 2123-2137, Dec. 1999.
- [153] J. C. Liberti, *Analysis of SS Cellular Radio Systems Employing Adaptive Antennas*. Ph.D.Dissertation, Virginia Tech, July 1999.
- [154] J.C. Liberti, and T.S. Rappaport, .A geometrically based model for line-of-sight multipath radio channels. In the Proceedings of the IEEE Vehicular Technology Conference 1996/Spring, pp.844-848.

- [155] W. C. Jakes, ed., *Microwave Mobile Communications*. New York: IEEE Press. 1974.
- [156] P. Petrus, Novel adaptive array algorithms and their impact on cellular system capacity. Ph.D.Dissertation, Virginia Tech, July 1997.
- [157] P. Petrus, J. H. Reed, and T.S. Rappaport, .Geometrically based statistical channel model for macrocellular mobile environments., In the Proceedings of the IEEE GLOBECOM, pp.1197-1201, 1996.
- [158] P. Petrus, J. H. Reed, and T.S. Rappaport, .Effects of directional antennas at the base station on the Doppler spectrum., IEEE Communications Letters, vol. 1, No:2, pp. 40-42, March 1997.
- [159] P. Zetterberg, .A downlink beam steering technique for GSM/DCS1800/PCS1900: Report version,. tech. rep., Royal Institute of Technology, 1996.
- [160] P. Zetterberg, P. Leth-Esperson, And P. Mogensen, .Propagation, beamsteering and uplink combining algorithms for cellular systems,. ACTS Mobile Communications Summit, Royal Institute of Technology, Nov. 1996.
- [161] P. Mogensen, P. Zetterberg, H. Dam, P. L. Espensen, S. L. Larsen, and K. Olsen, .Algorithms and antenna array recommendations,. Tech Rep. A020/AUC/A12/DR/P/1/xx-D2.1.2, Tsunami (II), September 1996.
- [162] S. P. Stapleton, X. Carbo, and T. McKeen, .Spatial channel simulator for phased arrays,. In the Proceedings of the IEEE Vehicular Technology Conference 1996, pp.1890-1894.
- [163] O. Norklit, and J. B. Anderson, .Mobile radio environment and adaptive arrays,. In the proceedings of PIMRC, pp. 725-728, 1994.

- [164] G. G. Raleigh, S. N. Diggavi, A. F. Naguib, and A. Paulraj, .Characterization of fast fading vector channels for multi-antenna communication systems,. n the Proceedings of the Asilomar Conf. on Signals, Systems, and Computers, pp. 853-857, 1994.
- [165] Q. Spencer, M. Rice, B. Jeffs, and M. Jensen, .A statistical model for angle of arrival in indoor multipath propagation,. In the Proceedings of the IEEE Vehicular Technology Conference 1997.
- [166] Q. Spencer, M. Rice, B. Jeffs, and M. Jensen, .Indoor wideband time/angle of arrival multipath propagation results,. In the Proceedings of the IEEE Vehicular Technology Conference 1997.
- [167] R. Michael Buehrer, Achilles G. Kogiantis, Shang-chieh Liu, Jiann-an Tsai, and DirkUptegrove, .Intelligent Antennas for Wireless Communications-Uplink,. Bell Labs Technical Journal, pp. 73-103, July-September 1999.
- [168] F.Alam, R. Boyle, R. Gozali, and R. Mostafa, .Space Time Processing Approaches for Third Generation Wireless Systems ., Tutorial conducted in 11th Annual MPRG/Virginia Tec Wireless Personal Symposium, Blacksburg, Virginia, USA, June 6-8, 2001.
- [169] J.Chenug, M.Beach, and J.McGeehan,"Network planning for third generation mobile radio systems," IEEE Commun .Mag, vol.32, pp.54-59 November 1994.
- [170] Z. Rong, *Simulation of Adaptive Array Algorithms for CDMA Systems*. M.S. Thesis, VirginiaTech, Sept 1996.
- [171] S.U. Pauli, *Array Signal Processing*. Springer-Verlag, New York, 1989.
- [172] W. L. Stutzman and G.A. Thiele, *Antenna Theory and Design*. John Wiley & Sons, New York, 1981.

- [173] F.Alam, D.Shim, and B.D. Woerner, .Comparison of Low Complexity Algorithms for MSNRBeamforming, submitted to VTC Spring, May 2002, Birmingham, Alabama, USA.
- [174] D. H. Johnson, and D. E. Dudgeon, *Array Signal Processing: Concepts and Techniques*. Englewood Cliffs, NJ: Prentice Hall PTR, 1993.
- [175] Haykin, S.1996.Adaptive filter theory .New Jersey: Prentice Hall.
- [176] F.Alam, K. A. Zahid, B.D. Woerner and J.H. Reed, .Performance Comparison between Pilot Symbol Assisted and Blind Beamformer-Rake Receivers at the Reverse Link of Third Generation CDMA System., In the Proceedings of IEEE Vehicular Technology Conference, October 2001, New Jersey, USA.
- [177] F.Alam, *Space Time Processing for Third Generation CDMA Systems*. Preliminary Report, Virginia Tech, Nov. 2001.
- [178] R. L. Burden, and J. D. Faires, *Numerical Analysis*. Brooks/Cole, Pacific Grove, California, 7thed., 2001.
- [179] Manolakis, D.G., Ingle, V.K. & Kogon, S.M., 2002.Statistical and adaptive signal processing .New York: The McGraw-Hill.
- [180] R. Ertel, P. Cardieri, K. Sowerby, T. Rappaport, and J. Reed, "Overview of spatial channel models for antenna array communication systems," *IEEE Personal Communications Magazine*, pp. 10-22, Feb. 1998.
- [181] A. A. M. Saleh, and R. A. Valenzuela, "A Statistical model for Indoor Multipath Propagation," *IEEE J. Select. Areas Commun.*,vol. JSAC-5, No.2, pp. 128-137, Feb. 1987.

- [182] Q. Spencer, M. Rice, B. Jeffs, and M. Jensen, "A statistical model for angle of arrival in indoor multipath propagation," in *Proc., IEEE Veh. Tech. Conf.*, 1997.
- [183] R. B. Ertel and J. H. Reed, *Antenna Array Systems: Propagation and Performance*. PhD thesis, Virginia Polytechnic Institute and State University, July 1999.
- [184] P. Petrus, J. H. Reed, and T. S. Rappaport, "Geometrically based statistical channel model for macrocellular mobile environments," in *Proc., IEEE Veh. Tech. Conf.*, pp. 844-848, Apr. 1996.
- [185] F. Alam, *Simulation of Third Generation CDMA Systems*. M.S. Thesis, Virginia Tech, Dec. 1999.
- [186] Kevin Laird, Nick Whinnet, and Soodesh Buljore, "A Peak-To-Average Power Reduction Method for Third Generation CDMA Reverse Links," in *Proc., IEEE Vehicular Technology Conference*, 1999.
- [187] UMTS, "Multiplexing and Channel Coding," 3G TS 25.212 V3.2.0 (2000-03).
- [188] Monica Dell'Anna and A. Hamid Aghvami, "Performance of Optimum and Suboptimum Combining at the Antenna Array of a W-CDMA System," *IEEE J. Select. Areas Commun.*, Vol. 17, No. 12, pp. 2123-2137, Dec. 1999.
- [189] A. F. Naguib and A. Paulraj, "Performance of Cellular CDMA with M-ary Orthogonal Modulation and Cell Site Antenna Arrays," *IEEE J. Select. Areas Commun.*, vol. 14-(9), pp. 1770-1783, Dec. 1996.
- [190] R. A. Monzingo and T. W. Miller, *Introduction to Adaptive Arrays*. New York: John Wiley & Sons, 1980.
- [191] S. Haykin, *Adaptive Filter Theory*. Englewood Cliffs, NJ: Prentice Hall, 1991.

- [192] Andreson, J.B., T.S., Rappaport and S.Yoshida, 1995. Propagation measurements for wireless communication channels. *IEEE Communi.Mag.*, 33: 42-44.
- [193] S. A. Ghorashi, E. Homayounvala, F. Said, A. H. Aghvami," Dynamic simulator for studying WCDMA based hierarchical cell structures," *12th IEEE International Symposium on Personal, Indoor and Mobile Radio Communications 2001 (PIMRC)*, San Diego, USA. 2001.
- [194] ARIB. 1998., Evaluation Methodology for IMT-200 Radio Transmission Technologies. Version-1.
- [195] Holma, H.& Toskala, A. 2000 .WCDMA for UMTS, Radio Access for Third Generation Mobile Communications .John Wiley & Sons, LTD.

PUBLICATIONS

1. **Ahmed. M. Ahmed. Jad Elrab** and Nidal. S. Kamel, "Performance Analysis of Non-blind Adaptive Beamforming Techniques for (3G) WCDMA Uplink", International conference on computer and communication Engineering 2008 (ICCCE08), 13th-15th May 2008, Istana Hotel-Kuala Lumpur, Malaysia.
2. **Ahmed. M. Ahmed. Jad Elrab** and Nidal. S. Kamel, "Comparative Study of Pilot Symbol Assisted (PSA) Beamforming Techniques for (3G) WCDMA reverse link", International conference on computer and communication Engineering 2008 (ICCCE08), 13th-15th May 2008, Istana Hotel-Kuala Lumpur, Malaysia.